Balancing Glare and Circadian Stimulus with Shading Device Simulation

Ka Kit Chiu

A thesis submitted in partial fulfillment

of the requirements for the degree of

Master of Science in Architecture

University of Washington

2024

Committee:

Mehlika Inanici

Christopher Meek

Program Authorized to Offer Degree:

Architecture

University of Washington

Abstract

Balancing Glare and Circadian Stimulus with Shade Fabric Simulation

Ka Kit Chiu

Chair of the Supervisory Committee:

Professor Mehlika Inanici

Department of Architecture

Daylight utilization in the built environment is highly valued for its dual benefits: energy conservation and enhancing human health. Yet, achieving visual comfort is challenging due to the uneven distribution of light levels, particularly in buildings with deep spaces. When encountering glare issues near windows, shading devices used to mitigate glare often compromise daylight exposure and its circadian stimulus elsewhere, impacting the healthy sleep-wake cycles known as circadian rhythms. Recent research has underscored the significance of photoreceptors in the eyes and skin, which govern circadian rhythms across species. Among these, intrinsically photosensitive retinal ganglion cells (ipRGCs) are pivotal in reacting to specific light spectrums, thereby becoming a focal point in daylighting design strategies. Considering that humans spend approximately 90% of their lifetime indoors, the quality of circadian lighting is paramount for wellbeing. Addressing the conflict between glare reduction and circadian health, this study identifies a theoretical balance. 2657 lux of vertical illuminance

at the eye typically precedes glare, while the WELL v2 standard specifies a minimum of 150-275 equivalent melanopic lux (EML) for adequate circadian entrainment. Moreover, human visual and non-visual responses peak at green and blue wavelengths respectively. This difference in spectral sensitivities provides a clue to the equilibrium between visual comfort and circadian stimulus. This research proposes a simulation-based approach to design shade fabric configurations that achieve a balance between visual comfort and circadian health. The goal is to effectively calibrate light intensity and color spectrum, thereby harmonizing the daylight entering through windows. Such an equilibrium can furnish spaces with holistic daylighting solutions that address the interplay between energy efficiency, visual comfort, and circadian stimulus, thus promoting occupant health and productivity.

Acknowledgements

I would like to express my deepest gratitude to my thesis supervisor, Dr. Mehlika Inanici, for her unwavering guidance, support, and invaluable insight throughout my MS degree journey and this thesis. It is a pleasure and I feel tremendously lucky to have her as my thesis committee chair and mentor. With her profound knowledge in the field of lighting research, she could always resolve any technical question and challenges I encountered with enthusiasm, care, precision, depth, and clarity. Conversations with her have always been enlightening and they have continuously sparked my curiosity and passion toward not just about this academic research but, more importantly, devolving oneself into discovering problems and contributing to the world as a scholar. Her expertise and encouragement have been instrumental in shaping multiple facets of this research as well as my career growth.

Also, I would like to extend my sincere thanks to my thesis committee member, Prof. Christopher Meek, for his supportive efforts and professional input regarding graphics, presentation materials, and safeguarding the details. His contributions have significantly enhanced the quality and clarity of this work.

I would also like to thank my good friend and senior schoolmate, Md Shariful Alam, who has been a wonderful source of inspiration, and support throughout the journey in UW.

Lastly, no words can ever depict my gratitude to my parents and siblings for their unconditional support, understanding, encouragement, and love; allowing me to pursue this accomplishment, and stay motivated to pursue my passions and dreams.

Table of Contents

List of Figures

Chapter 1 — Introduction:

The judicious integration of natural light into architectural spaces is a quintessential aspect of sustainable building design, offering substantial benefits in terms of energy conservation and enhancement of human wellbeing. The utilization of daylight as a primary light source not only reduces reliance on electric lighting, which contributes to energy efficiency, but also plays a vital role in maintaining the circadian health of occupants. Circadian rhythms, the physiological processes with a cycle between 23.7 to 25.1 hours, are profoundly influenced by light, particularly its intensity and spectral quality (Lockley 2009). Recent research underscores the discovery of intrinsically photosensitive retinal ganglion cells (ipRGCs), in the human eye, which are particularly responsive to blue light and directly influence the regulation of circadian rhythms (Brainard et al., 2001 and Thapan et al., 2001). These findings have propelled the consideration of circadian lighting quality as a fundamental component in the design of indoor environments where individuals spend 90% of their lifetime (Klepeis 2001). Despite the advantages, the challenge persists in balancing the ingress of natural light with the avoidance of glare, "condition of vision in which there is discomfort or a reduction in the ability to see details or objects, caused by an unsuitable distribution or range of luminance, or by extreme contrasts" (CIE 2019a). Commonly, this is mitigated through the use of shade fabrics (SF) or venetian blinds (VB), which, while effective at reducing glare, can inadvertently reduce the light penetration to deeper floor space, as well as diminish the quality of and quantity of daylight, thereby impeding the circadian stimulus hence disrupting occupants' circadian health.

To address this paradox, it is posited that an optimal threshold of light intensity exists which can sustain circadian health without inducing glare. The WELL v2 standard suggests a minimum of 275 equivalent melanopic lux (EML) is necessary for circadian entrainment,

providing a benchmark for designers (IWBI WELL v2). Whereas, 2657 lux as the threshold for discomfort glare which can be computed reversely by the daylight glare probability formula, developed by Wienold and Christoffersen (2006), after plugging-in the “imperceptible” value. Furthermore, human eyes have a different sensitivity to the different spectrum of light for photopic, melanopic, and neuropic responses, which is pivotal for both visual and circadian functions, necessitating a fine-tuned control over the spectral composition of daylighting within built environments.

1.1 — Goals and Objectives

Inspired by the gap between EML and Glare threshold, this research endeavors to explore the theoretical and practical avenues to achieve an equilibrium between visual comfort and circadian health, with comparative analysis on SF and further investigations for ideal SF properties within the building envelope to modulate the ingress of natural light. The objective is to devise holistic solutions that harmonize the competing demands of minimizing glare while maximizing the circadian stimulus, thereby fostering environments that support both the visual and circadian needs of occupants.

1.2 — Overview of Thesis

Chapter 2 is a literature review of current research in daylighting, electric, glare, circadian rhythm, shade fabrics, and simulation tools. Chapter 3 describes the methodology in which LARK 3.0 is used to simulate the lighting conditions under a variety of parameters. Chapter 4 discusses the simulation results and makes comparative analysis between commercial typical shades products, proposed spectrally selective shade fabric alternatives. Finally, Chapter 5 covers a summary of results, the conclusions, contributions, and future work.

Chapter 2 — Background

Since the invention of electric light in the 19th century, its vast deployment has dramatically prolonged the hours of day people stay indoors. Nowadays, the majority of the modern population spends about 90% of their lives indoors (Klepeis 2001). This increased reliance on electric light, often prioritizing quantity over quality cannot fully replicate the beneficial effects of daylight (Rea et al., 2010), has led to a decrease in daylight exposure and disrupted circadian rhythms (Brown et al., 2022). With the building technology advancement, modern buildings designed for high efficiency often feature deeper floor plates further limiting access to natural light (Klepeis et al., 2001). Despite the detrimental effects of limited daylight, its importance for both illumination and human wellbeing is increasingly recognized (Jaewook et al., 2020). Fortunately, advancements in building envelope technologies and fenestration systems offer new opportunities for daylighting design (Lee & Selkowitz, 1997). While attempts have been made to address this issue through specialized lighting solutions (Boyce, 2021), they come at the cost of increased energy consumption and contradict the sustainability goals of the building industry (International Energy Agency, 2018).

To allow daylighting in deeper spaces, large glazes are often used and hence presents a unique challenge: balancing the need for circadian stimulus with the potential for glare. Traditional solutions often involve shade fabrics combined with glazing, which address glare but inevitably reduce beneficial daylight exposure (Wienold & Christoffersen, 2006). This approach, while mitigating glare, inadvertently defeats the purpose of maximizing daylight for circadian entertainment. WELL v2 L03 guidelines provide valuable insights, suggesting a minimum of 275 Equivalent Melanopic Lumens (EML) for circadian stimulus over four hours, and 1100EML for one hour (IWBI, 2020). Additionally, Wienold and Christofferson's Daylight Glare Probability

(DGP) equation defined 2657 lux as imperceptible threshold before glare to human sensation (2006). The ideal lighting condition between 275 EML to maximum light level of 2657 lux before glare suggests promising opportunities for balancing glare and daylighting in deep spaces to promote healthy circadian entrainment.

2.1 — Physical World

To simulate the lighting condition of a space, it is important to first understand how light operates and how it interacts with materials differently in the physical world. Light, the very essence of our visual perception, is a complex phenomenon that underpins our interaction with the physical world. In radiometry, it is a form of electromagnetic radiation that is visible to the human eye, and it plays a pivotal role in how we experience our environment (CIE 1987). In geometrical optics, there are four fundamental principles: transmission as light passes through the material directly; absorption as light is absorbed by the material; reflection as light reflected by the materials; and refraction as light is bended by the material (Fig.2.1).

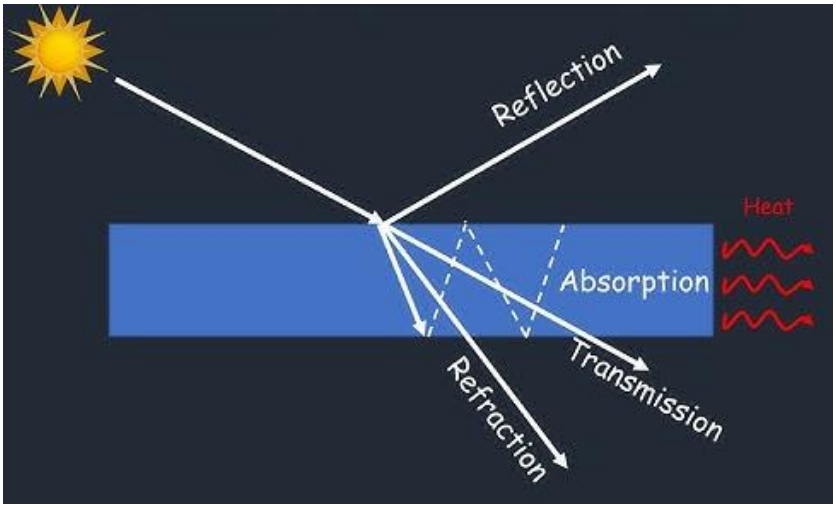

Fig.2.1: Four basic light interactions with object (Anderson 2015)

Unlike radiometry that measures light in all electromagnetic wavelengths, photometry is a subset that only applies to the visible electromagnetic spectrum (380-780 nm) and focuses on measuring the perceived brightness of light to the human eye (Wyszecki and Stiles, 2000). It takes into account the varying sensitivities of the eye to different wavelengths of light and is therefore weighted by the luminous efficiency function, which models the average visual sensitivity of the human eye under different lighting conditions (Wyszecki and Stiles, 2000). Photometric measurements include various quantities such as illuminance, luminance, luminous intensity, luminous flux (CIE, 1987). Instruments (Fig 2.2) used in photometry, like photometers, lux meters, and luminance meters, are designed to respond to light in a way that mimics the response of the human eye, often using filters and sensor combinations to achieve this. (CIE, 2010).

Fig 2.2: Photometer (L) and Luminance meter (R)

As shown in Fig 2.3, illuminance is the amount of light falling on a surface, measured in lux(lx) (CIE, 1987). Luminance is the intensity of light emitted from a surface in a specific direction, measured in candela per square meter (cd/m²) (CIE, 1987). Luminous intensity is the luminous flux emitted per unit solid angle, measured in candelas (cd)(CIE, 1987). Luminous flux is the total amount of visible light emitted by a source, measured in lumens(lm) (CIE, 1987).

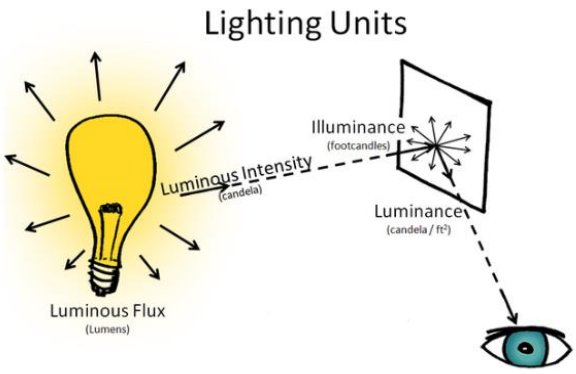

Fig 2.3: Diagram of light perception (J.C. Walker, 2010)

2.1.1 — Daylighting and Sky Spectra

Daylight, the Earth's primary natural light source, serves as the foundation for human vision and influences various biological processes. Spectral Power Distribution (SPD) is a measure that describes the power per unit area per unit wavelength of an optical radiation source, such as the sun. It represents how much power is emitted by the source at each wavelength in the visual spectrum ranging from 380 to 780 nm (Wyszecki and Stiles 2000). This spectrum is impacted by the Earth's rotation and orbital path, resulting in diverse lighting conditions that fluctuate from dawn to dusk and through seasons (CIE 1987). Atmospheric interaction further modulates this spectral distribution, with weather patterns and climatic factors infusing variability into the quality of light received at ground level (Iqbal 1983). In the context of daylight as shown in Fig 2.4, the SPD is highly dynamic and based on multiple factors, including the time of day, sky condition, orientation, and position under the sun (Jung and Inanici, 2019).

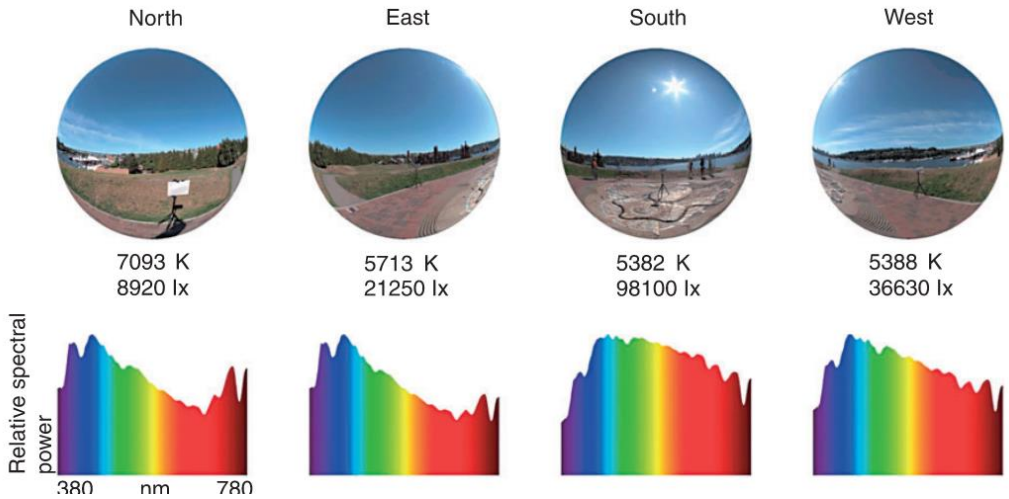

Fig 2.4: SPD of eye-level HDR image in Seattle (Jung, Inanici 2019)

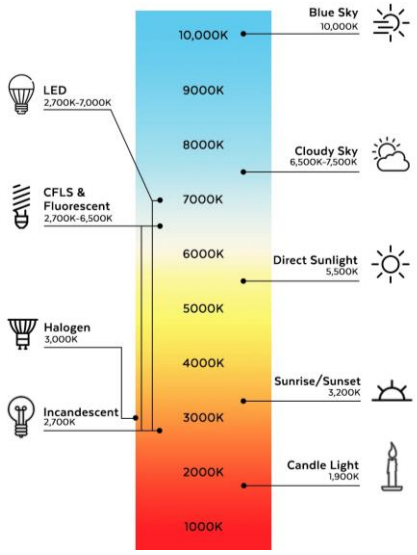

Fig 2.5: CCT scale (DelMar.com)

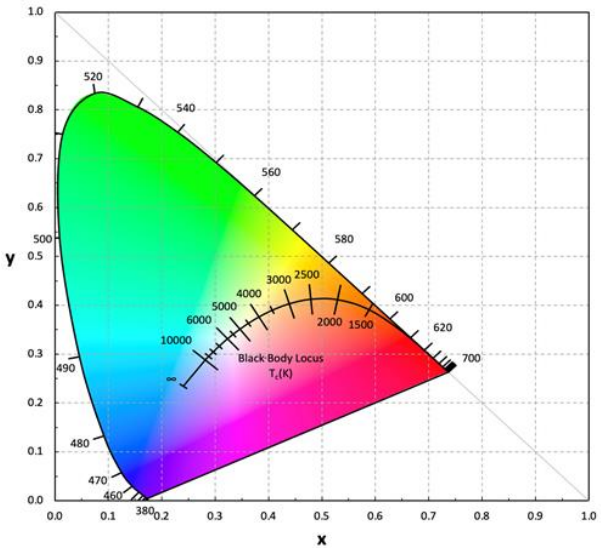

Fig 2.6: Planckian locus in CIE Chromaticity Diagram (CIE 1931)

However, recording a full spectrum for every sky condition can be costly. A simplified evaluation method known as correlated color temperature (CCT) was created by Max Planck in 1974 to describe the color appearance of light sources, measured in Kelvin(K). It provides an understanding of how “cool” (bluish) and “warm” (yellowish) the light appears to the human eye. CCT is determined by comparing the light emitted by a source to that of an ideal blackbody radiator. The temperature at which the blackbody radiator’s light matches the color of the light

source is considered its color temperature. Measured on Kelvin (K) scale, CCT values indicate different hues of light as shown in Fig.2.5. For example, 2700K, corresponds to warm light with a yellowish or reddish tint, similar to incandescent lighting and the natural light at sunrise or sunset. 6500K, corresponds to cooler, bluish light, akin to daylight or light from an overcast sky. The xy chromaticity space provides a way to graphically represent all human color vision, and the CCT gives us a numerical measure of the color appearance of a light source, relating it to the color of a blackbody radiator, which can be plotted on xy chromaticity space, representing the full range of colors visible to the human eye. The curve formed by the points is called the Plackian locus as shown in Fig 2.6. According to Hernandez-Andreas's (2001) evaluation and data collected by Inanici (2023), the CCTs of the sky range from 2500K to over 25,000K (Fig 2.7), and also fluctuate dramatically depending on the weather conditions (Fig 2.1.4) the time of day (Fig 2.8).

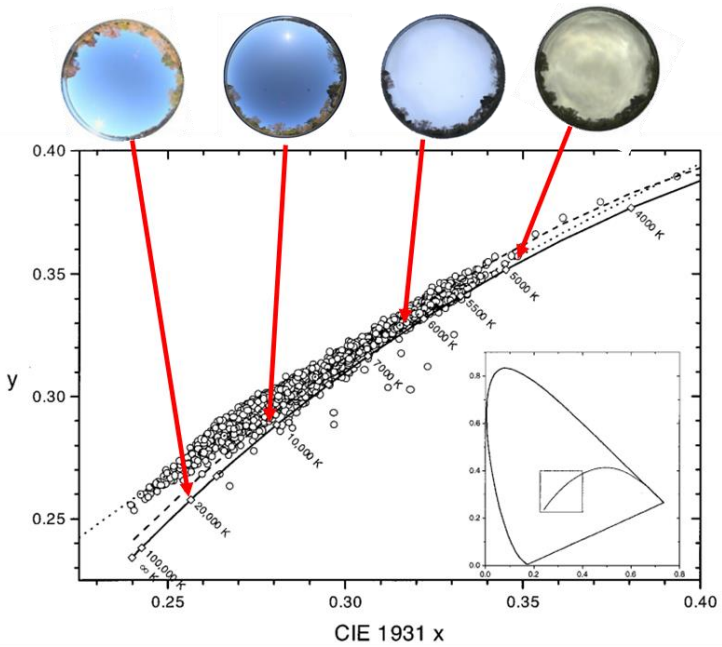

Fig 2.7: CCT of Granada, Spain (Hernandez-Andreas, et al 2001) and HDR skydome image in Seattle overlay (Inanici et al., 2023)

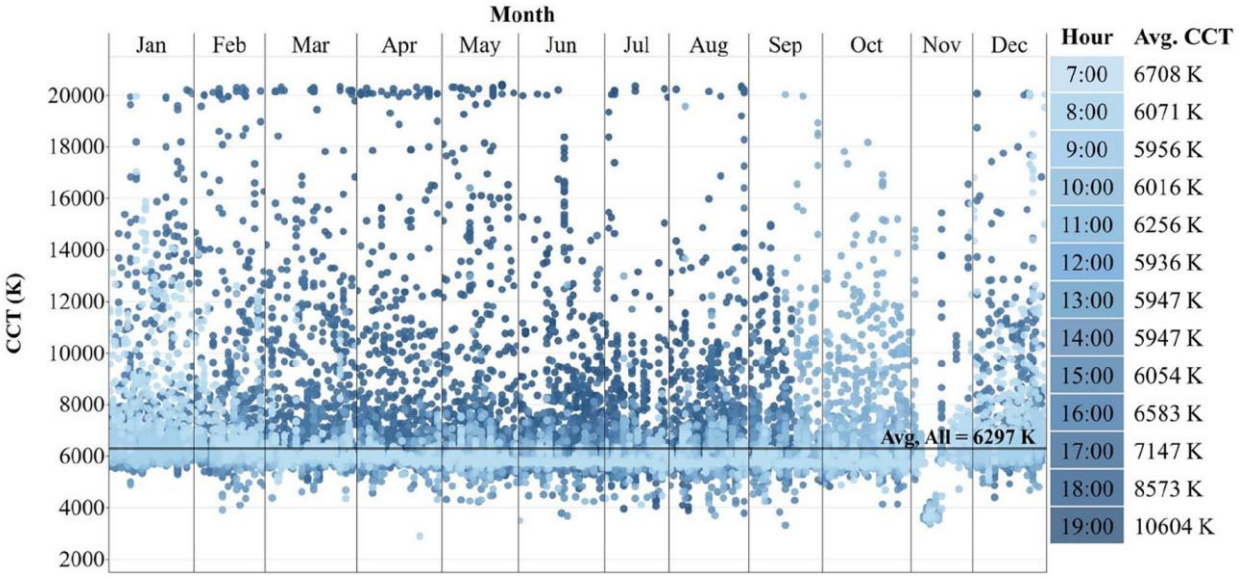

Fig 2.8: Annual CCT values for Golden, Colorado, USA (Inanici, et al. 2023)

2.1.2 — Electric Lighting

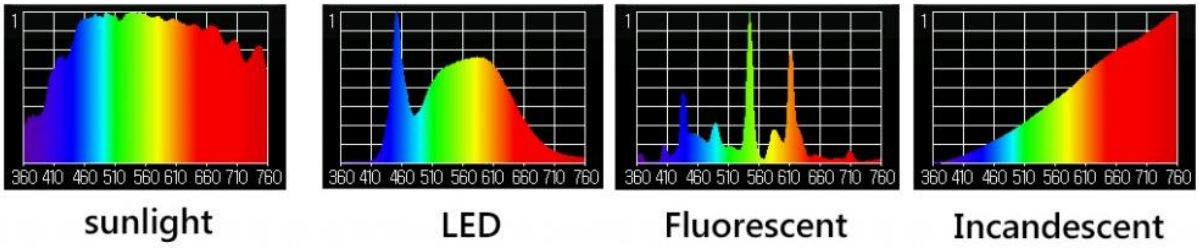

Fig 2.9: SPD comparison between sunlight and electric lights. (Sunlight Inside)

Electric light is a form of artificial light produced by the conversion of electrical energy into visible light. It is typically generated through the passage of electricity through a filament or other material that causes it to heat up and emit light. There are three common types of electric lighting, incandescent light, fluorescent, and Light-emitting diode (LED). Fig 2.9 shows the SPD of typical LED, fluorescent, and incandescent light. Incandescent lamps operate on the principle

of thermal radiation, with a tungsten filament heating up and emitting warm, yellowish light. Incandescent light is relatively inefficient and lacking in color accuracy. Fluorescent lamps utilize gas discharge, where mercury vapor excited by an electric current releases ultraviolet radiation (UV) that interacts with a phosphor coating to produce visible light that is commonly in white color (Boyce, 2022). It is more energy efficient than incandescent, but can prime to flickering and contain mercury which require careful disposal. LED, invented by Gary Pittman and James Biard in 1961, is a semiconductor device composed of two layers of doped semiconductor materials. When an electric current passes through the LED, electrons and holes (positively charged vacancies) recombine in the junction between these layers, releasing energy in the form of light. LEDs are the most common type of electric light because they are the most efficient and versatile lighting technology available today, offering a long lifespan, high color rendering, and controllability of color temperature and spectral output (Guo et al., 2015). They have drastically reduced energy consumption and contributed to sustainable building practices (IEA, 2021). Due to the increasing awareness of circadian health with lighting, many manufactures have launched many LEDs products that can mimic the spectra of natural daylight to regulate our circadian rhythms during the daytime. However, electric light is still considerably inferior to natural daylight in providing both enough illumination and circadian stimulus due to different SPD, thereby imposing significant energy usage when using LEDs to artificially mimic the same characteristics of daylight (Knoop et al. 2020).

Compared to electric lighting, which often exhibits unevenly concentrated spikes at specific wavelengths as shown in Fig 2.7, natural light generally has a high intensity of light across the entire visible spectrum. This broader spectral distribution is more beneficial for entrainment of the human circadian rhythm (Blume et al., 2019, Boyce et al., 2006, 2022).

2.1.3 — Shade Fabric (SF)

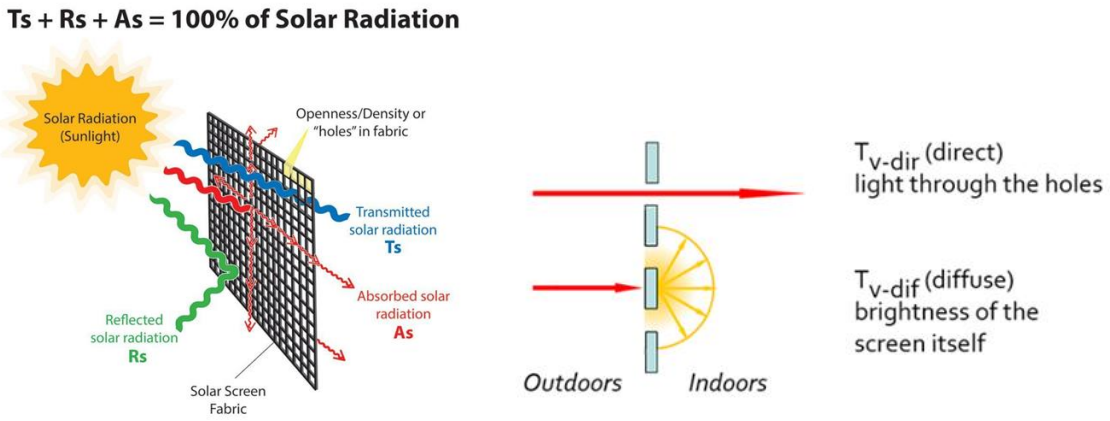

Fig.2.10: Shade Fabrics (SF) and lighting interactions (EN 14501 Standard)

Shade Fabrics (SF) are specially designed materials used to control the amount of natural light entering a space, thereby enhancing visual comfort and reducing glare. These fabrics are used in various applications, including window treatments like blinds, shades, and curtains, as well as in architectural elements like canopies and pergolas. Shade fabrics work based on their ability to alter the transmission (Ts), reflection (Rs), and absorption (As) of solar radiation as shown in Fig.2.10. According to the European standard EN 14501 (Blinds and Shutters, Thermal and Visual Comfort, Performance Characteristics and Classification), visual comfort and glare control are dictated by the specular transmission (Tv-dir) and diffuse transmission (Tv-dif) of SF. Tv-dir refers to the light directly passing through SF, controlled by the holes or open spaces in the SF known as openness factor (OF). The common OF are 1%, 3%, 5%, and 10% as shown in Fig 2.11. The greater the OF, more light will come through the shade which increases the visibility but also the heat gain and potential glare. Tv-dif, on the other hand, refers to the light scattered after passing through SF, controlled by the color of SF. Lighter color SF reflects energy with less glare control and lower heat gain, whereas darker SF absorbs energy with more glare

control (Fig.2.12) and higher heat gain. The commercial typical products take different levels of gray as the happy medium, or use light-exterior-dark-interior twill weave to provide both energy and glare benefits.

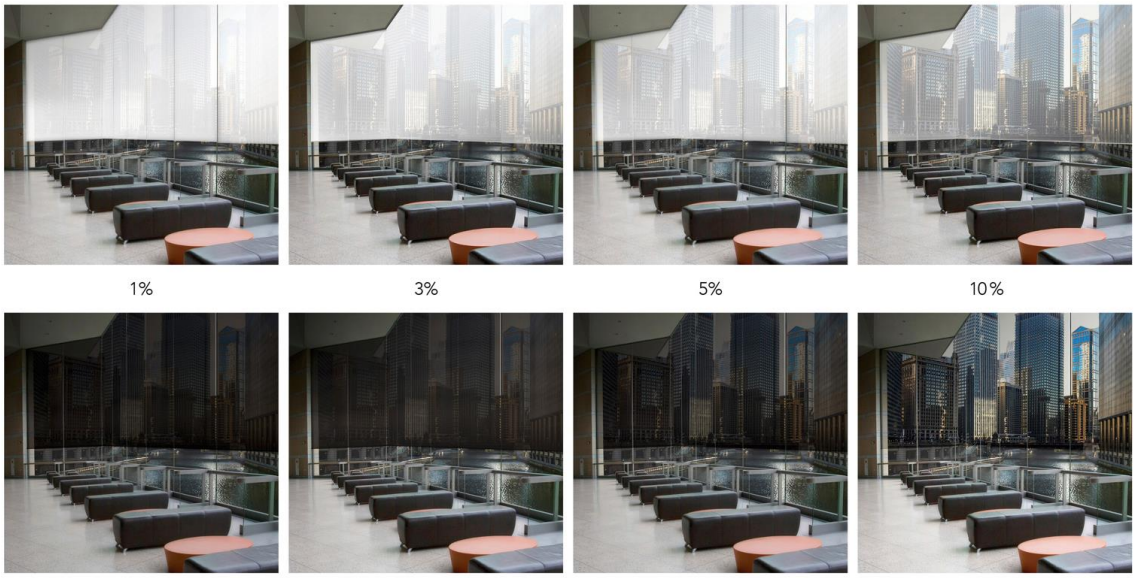

Fig.2.11: SF with different OF: 1%, 3%, 5%, 10% (Image: Mermet USA)

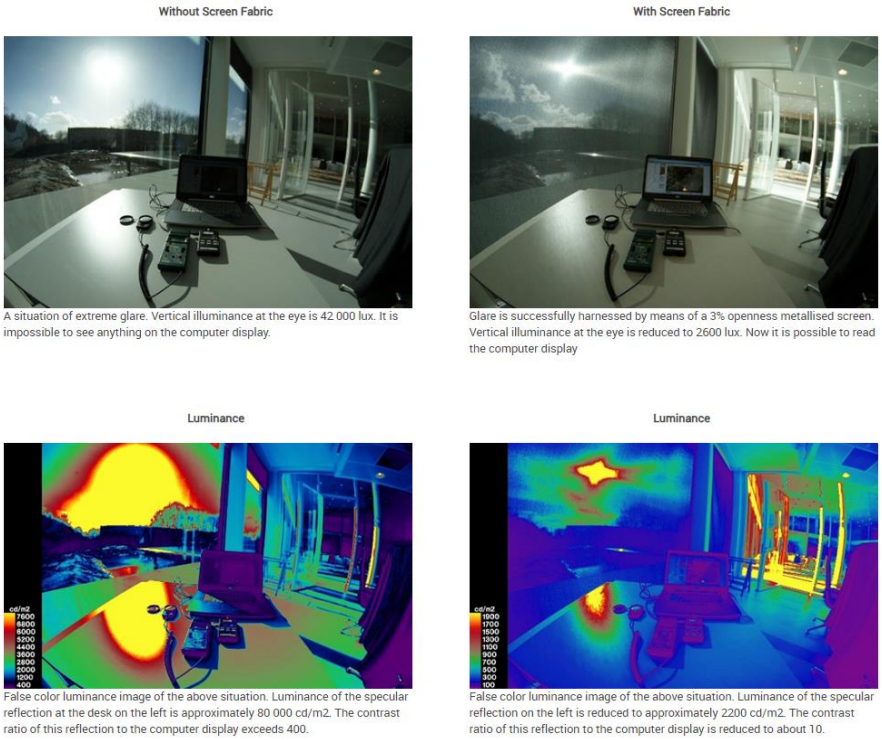

Fig.2.12: Luminance analysis with 3% OF (HunterDouglas)

FENESTRATION	FABRIC PROPERTIES								SHGC/G VALUE g-tot (glass & blind)			
	SOLAR OPTICAL								SINGLE		INSULATING	
	Ts (%)		Rs (%)		As(%)		Tv (%)		1/4 CL		1 HA	
COLOR	1%	3%	1%	3%	1%	3%	1%	3%	1%	3%	1%	3%
Brite White	15	18	72	70	13	12	14	17	0.26	0.28	0.20	0.21
Oyster	15	17	68	64	17	19	13	12	0.26	0.30	0.21	0.22
Oyster/Beige	10	11	60	55	30	34	9	8	0.31	0.32	0.23	0.23
Oyster/Pearl Gray	7	9	50	44	43	47	6	7	0.35	0.38	0.25	0.26
Beige	7	10	50	48	43	42	6	7	0.36	0.37	0.25	0.26
Beige/Pearl Gray	5	7	42	39	53	54	5	5	0.39	0.42	0.27	0.28
Pearl Gray	3	6	32	31	65	63	3	5	0.44	0.44	0.30	0.30
Charcoal	1	3	4	3	95	94	1	3	0.59	0.60	0.37	0.37
Charcoal/Gray	2	3	8	9	90	88	3	3	0.57	0.57	0.36	0.36
Charcoal/Chestnut	1	3	6	6	93	91	1	3	0.59	0.58	0.37	0.37
Charcoal/Alpaca	1	4	16	20	83	76	2	5	0.53	0.51	0.34	0.33
COLOR	5%	10%	5%	10%	5%	10%	5%	10%	5%	10%	5%	10%
Brite White	22	27	67	62	11	11	20	25	0.30	0.33	0.22	0.24
Oyster	21	27	61	57	18	16	14	21	0.30	0.35	0.23	0.24
Oyster/Beige	17	24	54	51	29	25	12	19	0.35	0.37	0.24	0.26
Oyster/Pearl Gray	14	20	45	45	41	35	10	16	0.39	0.41	0.27	0.27
Beige	14	19	47	44	39	37	10	16	0.40	0.43	0.27	0.28
Beige/Pearl Gray	11	17	38	39	51	44	9	15	0.43	0.44	0.29	0.30
Pearl Gray	10	16	31	30	59	54	9	14	0.47	0.49	0.30	0.31
Charcoal	4	10	4	4	92	86	5	11	0.60	0.62	0.37	0.37
Charcoal/Gray	5	12	9	8	86	80	6	14	0.57	0.60	0.36	0.37
Charcoal/Chestnut	6	11	6	5	88	84	6	12	0.59	0.61	0.37	0.37
Charcoal/Alpaca	7	12	18	15	75	73	9	16	0.53	0.57	0.34	0.35

Fig. 2.13: SF sample (Image: HunterDouglas SheerWeave®)

Currently, as commercial typical products primarily focus on using different levels of gray to resolve the duality of glare and visibility (Fig.2.13), they have yet to include the SPD analysis, thereby imposing a challenge to understand their circadian impacts. Also, there is a knowledge gap regarding different colors of SF and their impacts to both visual comfort and circadian stimulation.

2.1.4 — Venetian Blind (VB)

Fig.2.14: Perforated VB products and material samples (Images: TLC Flooring)

Other than SFs, Venetian blind (VB) is also a widely used solution for controlling natural light and mitigating glare in indoor environments. Unlike shade fabrics, which primarily filter light, Venetian blinds consist of horizontal slats that can be adjusted to control the amount and direction of incoming light. This adjustability allows users to fine-tune light levels to reduce glare without significantly compromising daylight availability. By tilting the slats, occupants can redirect sunlight to prevent direct glare while still allowing diffused light to enter, thus maintaining visual comfort and enhancing the overall lighting quality in the space. Moreover, the horizontal slats of VBs come in various materials such as aluminum, wood, or plastic, each offering different levels of light reflectance and absorption. Advanced materials may include perforated patterns, harnessing the diffuse quality of light, to maintain adequate light level indoor while providing privacy.

2.2 — Human Response to Light

This chapter will divide the human response to light into two major categories, the visual impact of light and the non-visual impact of light (Fig 2.14).

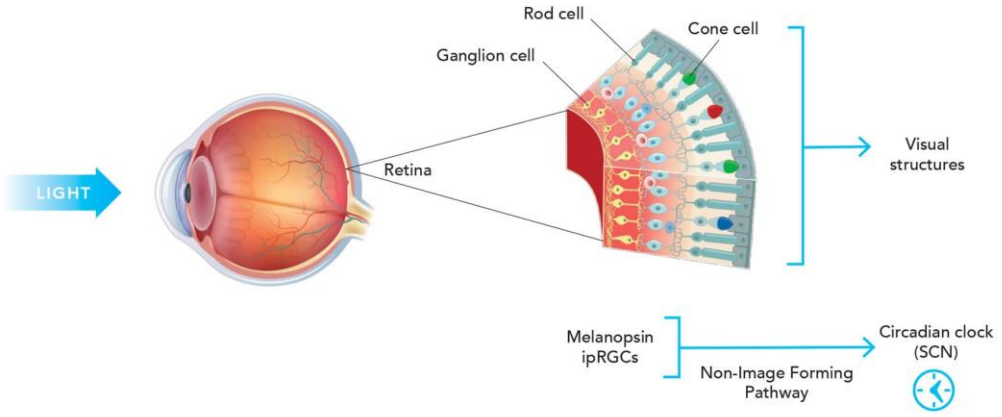

Fig 2.14: Light entering both visual and non-visual pathways (Jackson and Bollinger, 2022)

2.2.1 — Visual Impact of Light

The first function in the human ocular system is called the image forming (IF) pathway. The IF pathway is initiated when light enters the eyes through cornea, a transparent, dome-shaped structure that refracts light rays (Duke-Elder and Wybar, 1972). The size of the pupil, controlled by the iris, regulates the amount of light entering the eye. The lens, located behind the iris, further the incoming light rays onto the retina, a light-sensitive layer at the back of the eye (Fig 2.14). This process, called accommodation, allows for clear vision at different distances (Helmholtz, 1867). The retina contains two major types of photoreceptor cells (rods and cones) that have different light sensitivities (Brown and Wald, 1964). When light strikes these photoreceptor cells, it triggers a series of chemical reactions that convert light energy into electrical signals. This process, called phototransduction, is initiated by the absorption of light by photopigments within the photoreceptors (Boyce, 2014). The electrical signals generated by the photoreceptors travel through a network of neurons, starting with bipolar cells and horizontal cells within the retina. These signals are then linked to ganglion cells, whose axons form the optic nerve. The optic nerve transmits the visual information to the brian, specifically the visual cortex located in the occipital lobe (Kandel et al. 2000). The visual cortex interprets the electrical signals received from the retina, constructing the image we perceive. This complex involves the integration of information from both eyes and the activation of various brain areas represented for different aspects of vision, such as color, shape, and motion (Hubel and Wiesel, 1962).

2.2.1.1 — Rods and Cones

Rods are highly sensitive to light and are responsible for vision in dim environments. They do not contribute to color vision and have the spectral sensitivity peaks at around 505 nm, which is the blueish-green part of the spectrum, known as scotopic vision (Fig 2.15).

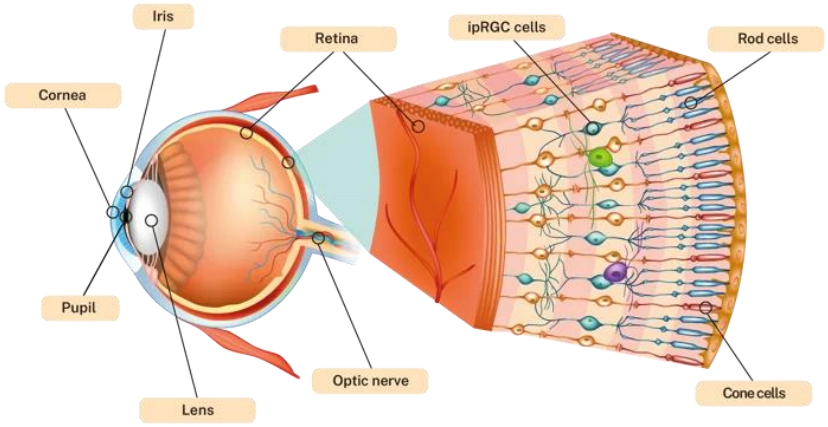

Fig 2.15: The anatomy of the human eye and retina (Image: Chromaviso)

Color is a visible electromagnetic spectrum in a certain range of wavelengths that a human eye can perceive through three types of cone photoreceptors sensitive to Short (S), Medium (M), and Long (L) wavelengths of light. According to CIE's standard spectral luminous efficiency function (Fig 2.16), the overall photopic vision contributes by cones peaks at around 555 nm. S,M,L cones are sensitive to different wavelengths, peaking at 420-440 nm (blue), 530-540 nm (green), and 560-580 nm (red) respectively.

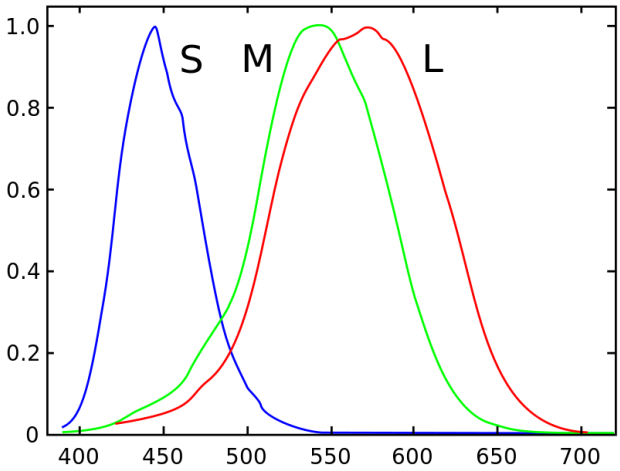

Fig 2.16: S,M,L Cones Sensitivity Curves (Stockman et al., 2000)

In 1924, the International Commission on Illumination (CIE) published a standardized photopic spectral sensitivity function based on the average human eye, called the CIE 1924 Luminosity Function, V(**λ**) (Wyszecki and Stiles 1982). These two major classes of photoreceptors, cones (OPN-1) and rods (OPN-2), peak at 498 nm wavelength, and 555 nm wavelength respectively (Fig 2.17).

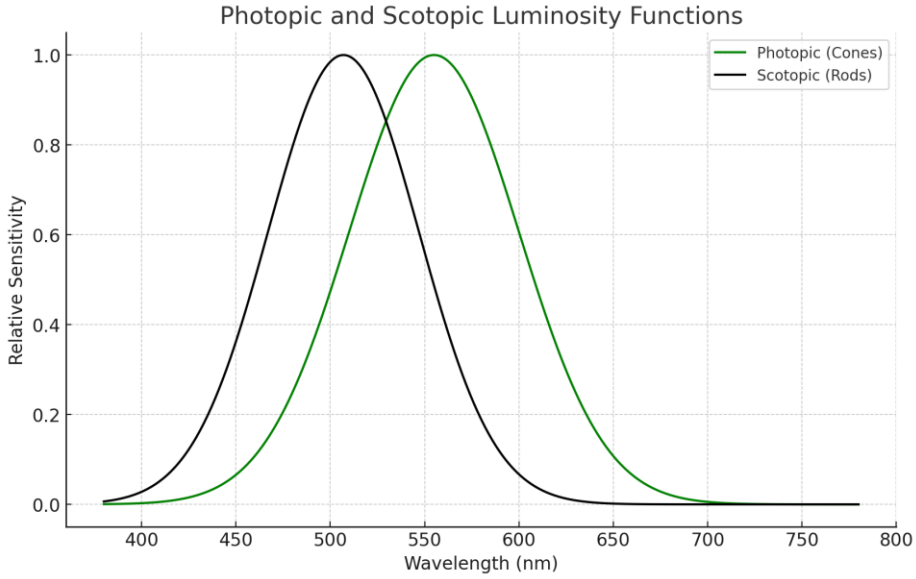

Fig 2.17: Simplified spectral sensitivity curves of rods and cones (CIE, 2004)

2.2.1.2 — Adequate light levels

Adequate light levels for the human visual system to the amount of illumination necessary for humans to see, perform tasks, and navigate their environment effectively and comfortably. The concept of "adequate" lighting is subjective and can vary depending on several factors such as the specific task being performed, the individual's age and visual acuity, and the context of the environment. Using a typical classroom as an example, Illuminating Engineering Society (IES) recommends a range of 30-50 foot-candles (323-538 lux) for classrooms. While CIE does not set specific levels, it suggests 50-100 foot-candles (538-1076 lux) for tasks requiring high visual acuity. The WELL v2 Standard by IWBI is more prescriptive for classrooms, advising 300-500 lux to balance both visual needs and circadian health. These guidelines are not fixed rules but serve as a foundation, acknowledging the need to adjust various activities, space configurations, individual preferences, and the impact of light's spectral qualities on both comfort and circadian rhythms.

2.2.1.3 — Glare

Fig 2.18: Disability glare caused by headlight (Image: EHS Works) and discomfort glare caused by poor lighting (Image: KULeuven)

According to IES, “glare” refers to “the sensation produced by luminances within the visual field that are sufficiently greater than the luminance to which the eyes are adapted to cause annoyance, discomfort, or loss in visual performance or visibility” (IES). It is a multifaceted problem contributed by a variety of factors, such as the luminance, size, quantity, location, and direction of the glare source, as well as the background luminance and the differences between an individual's visual perception. Generally speaking, there are two types of glare: disability glare and discomfort glare. Disability glare directly reduces visual performance by scattering light within the eye, making it difficult to see clearly (Boyce, 1981). This is often associated with high-luminance sources such as headlights or bright sunlight. Discomfort glare, on the other hand, does not necessarily impair visual acuity but can cause annoyance, eye strain, and fatigue (Rea, 2000). It is often associated with poorly designed lighting systems or reflective surfaces that create unwanted reflections (Fig 2.18). Figure 2.19. shows the useful region of the human eye in terms of adaptation level, if the object luminance is too high or low compared to the adaptation luminance, the visual performance would be impaired. However, adaptation takes time, and once the eye is adapted, the range would drop from spanning about 14 decades to 4-5 orders of magnitude. (CLEAR 2013)

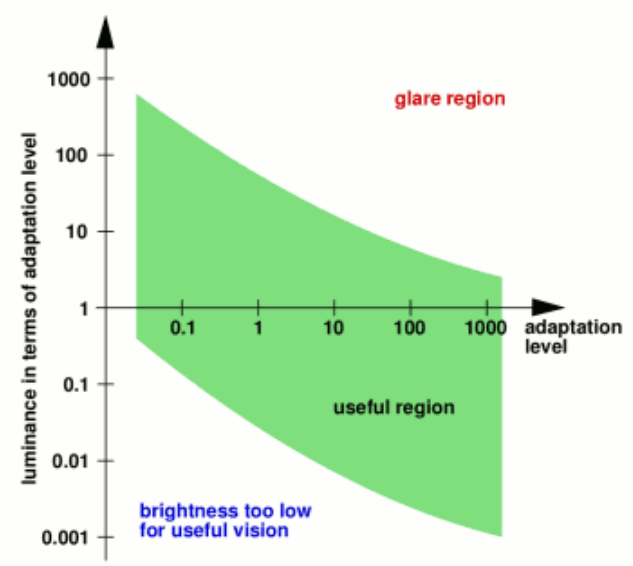

Fig 2.19: Adaptation level graph (CLEAR 2013)

There are many glare metrics to evaluate the visual discomfort caused by excessive brightness or contrast in a person's field of vision. These metrics are important in various fields, including lighting design, architecture, and vision science. Important glare metrics that align closely with the objective of this study would include Unified Glare Rating (UGR), and Daylight Glare Probability (DGP).

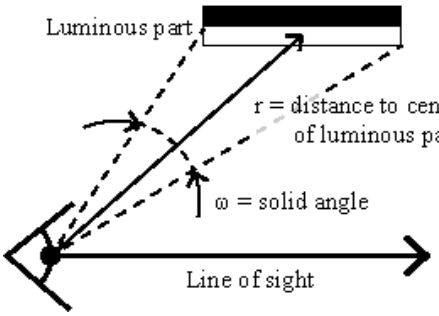

$$\mathrm{UGR} = 8 \log \left[\frac{0.25}{L_b} \sum \frac{L_s^2 \omega}{p^2} \right]$$

UGR	
13 – 16	Just Perceptible
16 – 19	Perceptible
19 – 22	Just Acceptable
22 – 25	Unacceptable
25 – 28	Just Uncomfortable
> 28	Uncomfortable

Fig 2.20: UGR Formula and Scale (CIE 1995)

UGR, established by “CIE 117:1995 Discomfort Glare in Interior Lighting”, assesses the likelihood of discomfort glare, defined as “glare that causes discomfort without necessarily impairing the vision of objects.” Glare impairs the vision of objects is defined as “Disability Glare” and is excluded from this metric. Fig 2.20 shows the formula and the scale of UGR, where L_b (in cd/m²) is the background luminance “represented by the illuminance at the eye excluding the direct light from the glare sources”; the summation contains factors for each light source within the field of view of the observer that includes: L_s (in cd/m²) as the average luminance of light source in the direction of the observer; ω (in sr) as the solid angle of the light source at the eye of the observer; and p as the Guth position index, a factor that accounts for the position of the luminaire in the observer's field of view (NEMA LS 20001-2021).

The UGR scale typically ranges from 10 to 30, where lower values indicate less glare. UGR < 19 is considered acceptable for most indoor environments; UGR > 28 is seen as uncomfortable for most people. The UGR formula takes into account the brightness of multiple light sources, their positions relative to the viewer, and the contrast with the background. This makes it a comprehensive tool for assessing the visual comfort in spaces with artificial lighting. Despite being widely used in lighting design, UGR has various limitations as documented by CIE 117, for example, UGR is for indoor lighting only and for uniform background luminance, not for small (subtending < 0.00003 sr) and large (subtending > 0.1) light sources, as well as indirect lighting. Additionally, p only defines the upper visual field hence the UGR formula cannot be used to evaluate discomfort glare from lights located below the line of sight (Kent et al., 2016). These limitations make UGR not a feasible metric for this study in simulation regarding glare from natural daylight.

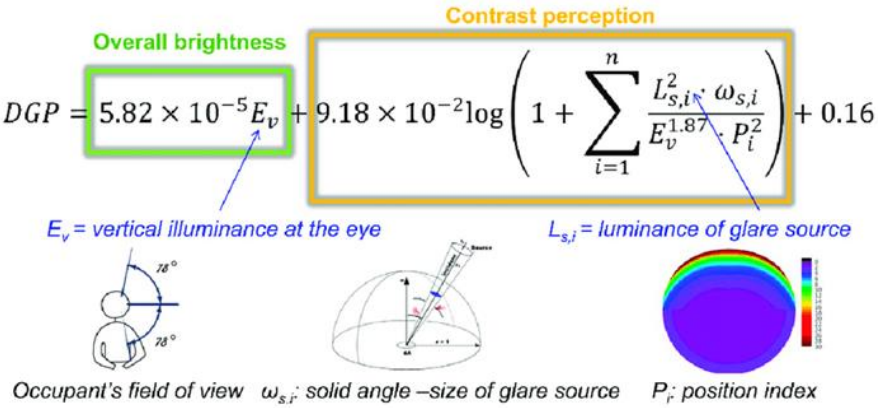

$$DGPs = \underbrace{6.22 \cdot 10^{-5} \cdot E_v}_{\text{illuminance term}} + \underbrace{0.184}_{\text{constant term}}$$

DGP	
< 0.34	Imperceptible
0.34 – 0.38	Perceptible
0.38 – 0.45	Disturbing
> 0.45	Intolerable

Fig 2.21: DGP formula, Simplified DGPs formula , and DGP Scale

(Wienold and Christoffersen, 2006)

DGP, on the other hand, developed by Wienold and Christoffersen (2006), is the most updated metric used to quantify the likelihood of discomfort glare in indoor spaces due to daylight. Fig.2.21 shows the formulas and the DGP Scale. It is formed by 2 major components: overall brightness, contrast perception. Overall brightness represents the overall brightness perceived by the occupants where E_v is the vertical illuminance at the eye. Contrast perception quantifies how much brighter glare sources are compared to the surrounding light, affecting discomfort levels where: $L_{s,i}$ as the luminance of glare source *i* (in cd/m^2); ω (in sr) as the solid angle ; and *Pi* as the Guth position index (Wienold and Christoffersen, 2006). DGP can help evaluate the effectiveness of the design in controlling glare from natural light sources while allowing for circadian benefits of daylight.

This study utilizes simplified DGP (DGPs) to facilitate a feasible workflow to test different alternatives. DGPs are entirely based on the linear function of vertical Eye illuminance (Ev) which is arguably more useful for the initial evaluation. The DGP value ranges from 0 to 1: DGP < 0.34 means the glare is not perceptible; DGP (0.34-0.38) is perceptible; DGP (0.38-0.45) is disturbing, and DGP > 0.45 is intolerable (Fig 2.18). After using 0.34 as the DGP value, the DGP formula concludes 2657 lx as threshold for the E_v where the human eye perceives perceptible glare.

2.2.2 — Non-visual Impact of Light

Chronobiology is the scientific study of biological rhythms and cyclic phenomena in living organisms. It explores the timing of biological events, the internal and external factors that regulate these events, and the mechanisms underlying their control. One of the central focuses of chronobiology is the circadian rhythm, which is the approx. 24-hour cycle in the physiological processes of living beings including humans, plants, animals, and even microbes.

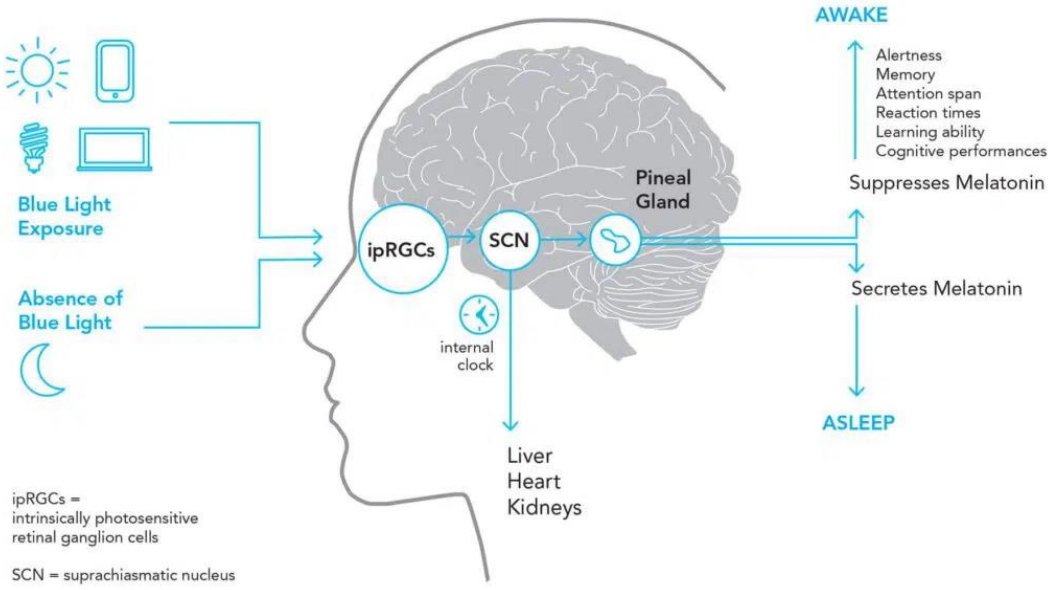

Fig 2.22: The interactional relationship between blue light and melatonin regulation

Alongside the well-known image-forming pathway, there is a non-visual function within the human visual system called non-image-forming (NIF) pathway (Fig 2.22). It plays a crucial role in regulating our internal clock known as circadian rhythm. It is activated by the 5th type of photosensitive cells known as intrinsically photosensitive retinal ganglion cells (ipRGCs) that express a unique photopigment called melanopsin, sensitive to blue light (Hattar et al., 2002). When blue light strikes ipRGCs, it triggers a cascade of biochemical reactions, converting light signals into electrical signals that initiates the non-visual response. ipRGCs extend projections to various brain areas, bypassing the visual cortex. These include the suprachiasmatic nucleus (SCN), the brain's master clock controlling circadian rhythms, and olivary pretectal nucleus (OPN), responsible for the pupillary light reflex, and hypothalamus (Lucas et al., 2001).

SCN is the brain's master clock that receives information from ipRGCs about the day-night cycle, adjusting our internal clock accordingly. Light exposure in the morning suppresses melatonin production, promoting alertness and wakefulness. Conversely, darkness leads to melatonin release, promoting sleepiness and preparing the body for rest, controlling circadian rhythms (Gooley et al., 2001; Blume et al., 2019). However, circadian rhythm is not exactly 24 hours but ranges between 23.7 and 25.1 hours (Lockley 2009). This endogenous rhythm is generated by a series of biochemical feedback loops within the cells of the SCN. Pupillary light reflex is a mechanism that protects the retina from excessive light and improves visual acuity (Lucas et al., 2001).

Other than the endogenous rhythm that may cause the circadian rhythm to naturally fall out of synchronization, there are other common reasons causing circadian rhythm disorder such

as shift work, jet lag, advanced and delayed sleep phase syndromes, and unusual environmental photoperiod. These disruptions can adversely affect health, leading to sleep disorders, obesity, These disruptions can adversely affect health, leading to sleep disorders, obesity, depression, bipolar disorder, and seasonal affective disorder (Lockley 2009). To maintain synchronization with environmental time, the circadian pacemaker requires a daily phase shift to counteract the natural drift in phase determined by its endogenous period (Lockley 2009). Resetting circadian rhythms involves the timing, intensity, duration, and pattern of light exposure, along with wavelength and photic history.

2.2.2.1 — ipRGCs (Melaposin, Neuropsin)

Intrinsically Photosensitive Retinal Ganglion Cells (ipRGCs), are discovered in mice byBrainard et al. and Thapan et al. in 2001. are a small population (1-5%) of specialized retinal ganglion cells that are directly sensitive to light, independent of the IF pathways (Fig.2.15). In addition, ipRGCs are sensitive from 380 to 580 nm and peaks at around 480-500 nm (Enezi et al, 2011). ipRGCs contain three special photopigments called encephalopsin (OPN-3), melanopsin (OPN-4) and neuropsin (OPN-5) (Tarttelin 2003; Sung, 2004; Panda, 2002) as shown in Fig 2.23. The response curve for OPN-3 is not known. OPN-4 is a photopigment primarily sensitive to blue light (480-500 nm range). It plays a crucial role in regulating circadian rhythms, pupillary light reflex, mood and alertness, and seasonal adaptations. OPN-5 is another photopigment present in a subset of RGCs, mainly sensitive to ultraviolet (UV) light. Its exact functions are still under investigation but recent studies have highlighted the role of OPN-5 to be responsible for metabolism (Zhang et al., 2020; Yoon et al., 2023). In addition, Zhu et al. (2018) has investigated the effects of UV light exposure on spatial learning and memory in mice, and found that moderate UV light exposure improved learning and memory performance in mice,

suggesting it may enhance cognitive function, but more research is need to addressed the specific role of OPN-5. Since UV light exposure is classified as Group 1 carcinogen, the sensitivity peak of OPN-5 would be adjusted to the shortest wavelength (380 nm) of the visible light (CDC 2023).

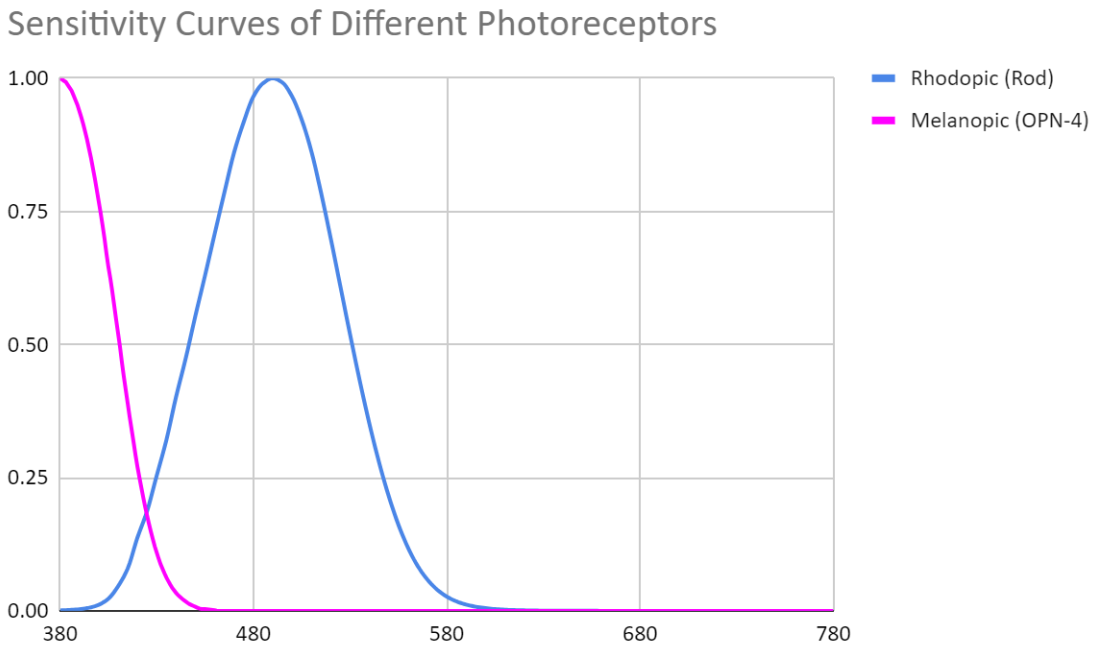

Fig 2.23: Sensitivity curves of Rod, OPN-4, and OPN-5 (CIE)

2.2.2.2 — EML and other metrics

Equivalent Melanopic Lux (EML) is a specialized unit, proposed by Lucas et al. (2014), measures the biological impact of light on the human circadian system(CIE, 2013). Unlike traditional light measurements like lux, which focus on overall brightness perceived by our eyes, EML is a measure that represents the effectiveness of a light source in stimulating the melanopsin-containing ipRGCs (OPN-4) in the human eye. It translates the melanopic impact of any given light source into an equivalent photopic lux value. By incorporating a melanopic

weighting function that assigns greater value to blue wavelengths, EML provides a more accurate picture of light's potential to regulate our internal clock. This allows for the design of lighting environments that promote optimal health and well-being, from stimulating alertness during the day to facilitating restful sleep at night. EML plays a vital role in research on circadian rhythm disorders and the development of new lighting technologies that optimize human health. In the WELL standard, in order to measure the biological effects of light on humans. To optimize circadian health in an indoor environment, the WELL v2 Q4 2022 standard prescribes an ideal daily EML exposure threshold to be met in chapter L03. (Fig 2.24) It suggests a minimum amount of 275 EML for 4 hours per day before noon. However, this study argues that higher EML in exchange of shorter exposure time is more feasible given the effect of 275 EML for 4 hours and 1100 EML for 1 hour can both fulfill the required circadian entrainment.

For workstations used during the daytime, electric lighting is used to achieve the following thresholds:

a. The following light levels are achieved for at least four hours (beginning by noon at the latest) at a height of 18 in above the work-plane for all workstations in regularly occupied spaces:

Tier	Threshold		Threshold for Projects with Enhanced Daylight	Points
1	At least 150 EML [136 M-EDI(D65)]	OR	The project achieves at least 120 EML [109 M-EDI(D65)] and either L05 Part 1 or L06 Part 1	1
2	At least 275 EML [250 lux M-EDI(D65)][11]	OR	The project achieves at least 180 EML [163 M-EDI(D65)] and either L05 Part 1 or L06 Part 1	3

b. The light levels are achieved on the vertical plane at eye level to simulate the light entering the eye of the occupant.

Fig 2.24: WELL v2 L03 Circadian Lighting Threshold (IWBI 2020)

Defined by the CIE S 026/E:2018 documentation, melanopic equivalent daylight illuminance (m-EDI) is also a metric used to quantify the melanopic stimulus provided by a light source as if it were daylight. Unlike EML, m-EDI does not directly measure the sensitivity of melanopsin, but instead expresses the effect of a given light spectrum in terms of an equivalent illuminance of standard daylight (D65). It is calculated using the melanopic sensitivity curve normalized to the CIE D65 daylight spectrum. The calculation involves applying a weighting

function to the SPD of the light source and comparing it to the response under standard daylight conditions. In the context of this study, where multiple sky settings other than CIE D65 are stimulated, EML is a more useful metric for glare-circadian balance assessment as it offers a more direct assessment of circadian impact of lighting.

M/P Ratio could be another useful metric as it helps in understanding the effectiveness of light in stimulating the circadian impact relative to its visual brightness. It is particularly relevant when considering the balance between visual comfort (reducing glare) and maintaining a healthy circadian stimulus through appropriate light exposure. The general equation for M/P ratio is the melanopic luminous flux divided by the photopic luminous flux (IES). Higher M/P ratio signifies a light source with a greater influence on the circadian system relative to its visual impact. Lower M/P ratio suggests a light source that is more focused on visual comfort than circadian stimulation. However, the primary limitation of using the M/P ratio as a metric for evaluating the glare-circadian balance is the lack of a standardized calculation method (Miller and Irvin 2019). Currently, there are four different methods to determine the M/P ratio, each yielding significantly different results due to variations in how the melanopic and photopic response functions are weighted and normalized. This inconsistency can lead to confusion and misinterpretation of a light source's effectiveness in supporting both visual and non-visual (circadian) functions. Without a unified approach, it is challenging to make reliable comparisons or decisions based on M/P ratios. This inconsistency underscores the need for the lighting and health community to agree on a single, standardized calculation method to ensure clarity and reliability in the application of M/P ratios.

2.3 Balancing — Glare and Circadian Stimulus

Balancing the opposing forces - maximizing the positive effects of daylight while minimizing glare - is a crucial and rewarding challenge in building design. Jalali and colleagues propose a comprehensive framework for integrating circadian lighting design into architectural practice, introducing VITALS criteria (Vertical light, Intensity, Timing, Appearance, Location, Spectrum) as guidelines for human-centric lighting design. They also include dynamic lighting techniques and tools for analysis such as Solemma ALFA and LARK Spectral Light, and reference standards such as LEED and WELL Building Standard for ensuring adequate lighting conditions (Jalai et al,. 2024). Building on their work, this study aims to further explore the practical implementation of these principles by investigating the optimal threshold of 2657 lx and 275 EML that supports circadian health without causing discomfort from glare. By leveraging simulation tools like LARK 3.0, this study will focus on the comparative analysis of shade fabrics and their properties, aiming to find solutions that harmonize the need for visual comfort with the circadian requirements of building occupants.

2.4 — Simulation of Visual and Non-visual Lighting

2.4.1 — Radiance and The .RAD file format

Radiance, developed by the Lawrence Berkeley National Laboratory (LBNL), is a leading tool in architectural lighting analysis (Ward and Shakespeare, 1998). Known for its accuracy and flexibility, Radiance uses advanced ray-tracing and radiosity algorithms to simulate light interactions with high precision (Mardaljevic, 2000). This makes it capable of accurately modeling complex phenomena such as interreflections and diffusion, essential for realistic lighting simulations. Radiance is particularly proficient in daylighting simulation, allowing

comprehensive analysis of how natural light infiltrates interior spaces throughout the day and year (Reinhart, 2001). This capability is invaluable for designing spaces that optimize natural light while mitigating issues like glare and overheating (Nabil and Mardaljevic, 2005). A key strength of Radiance is its ability to model a wide range of material properties and light sources, enabling highly accurate simulations that closely mimic real-world conditions. This is crucial for architects and lighting designers in predicting light interactions with various surfaces and materials. Radiance consists of over 150 command-line tools, each performing specific functions. The typical workflow involves importing the CAD model, compiling it with luminaires, placing them, rendering an HDR image, converting it to a false-color image, and displaying the result. This modular approach offers great versatility and customization for diverse project requirements (LBNL, 2023).

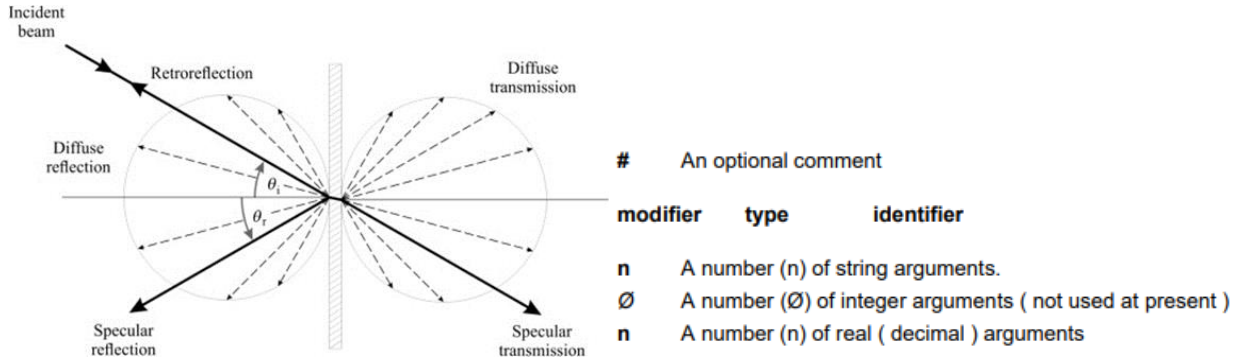

Fig.2.25: Light-material interactions in radiance and .rad file format structure (LBNL)

According to the Radiance Users Manual (1992), the .rad file format in Radiance is used to define the physical properties of materials and objects within a scene. The structure of these files includes definitions for various primitive types such as polygons, spheres, cylinders, and more, each of which can be assigned specific material properties. As shown in Fig.2.25 , radiance calculates specular and diffuse part of light reflections and transmission. A typical structure of a .rad file include: Optional comments (lines begins with "#") for file descriptions; "Modifiers" that must be either the word "void" or a name of a previously defined primitive; "Types" as the second field specifies the type of primitive (e.g., "metal", "trans", "BRDTfunc"); identifier as the unique name with which to label the primitive; and "Arguments" as the specific parameters for the material such as the transmittance and reflectance values.

2.4.1.1. — Trans Material

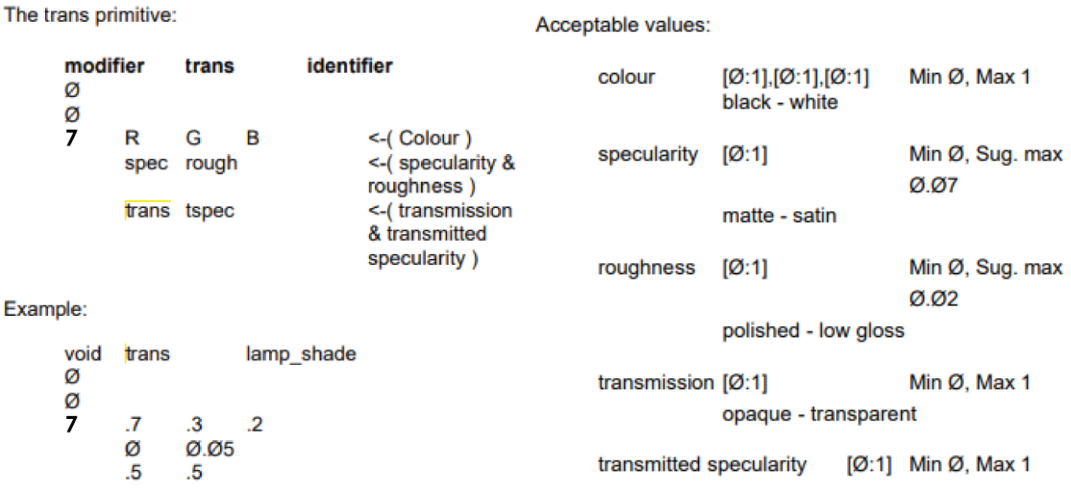

Fig.2.26: Material parameter of Trans .rad file and example (LBNL)

The “Trans” material in Radiance is designed to model infinitely thin translucent surfaces. This material type allows users to specify the transmission, reflection, and scattering properties of surfaces, thereby influencing how light is diffused and transmitted through the material. As shown in Fig.2.26, there are 7 arguments describing: “R, G, B” as the color reflectances; “spec” as the specular reflection; “rough” as the roughness of the material; “trans” as transmission; and “tspec” as the transmitted specularity. The transmissivity is the fraction of penetrating light that passes through the material. The transmitted specular component is the fraction of transmitted light that is not diffusely scattered. Transmitted and diffuse light is modified by the material color. In the context of this study, materials for SF require more flexibility than Trans material format for a more accurate simulation.

2.4.1.2. — BRTDfunc Material

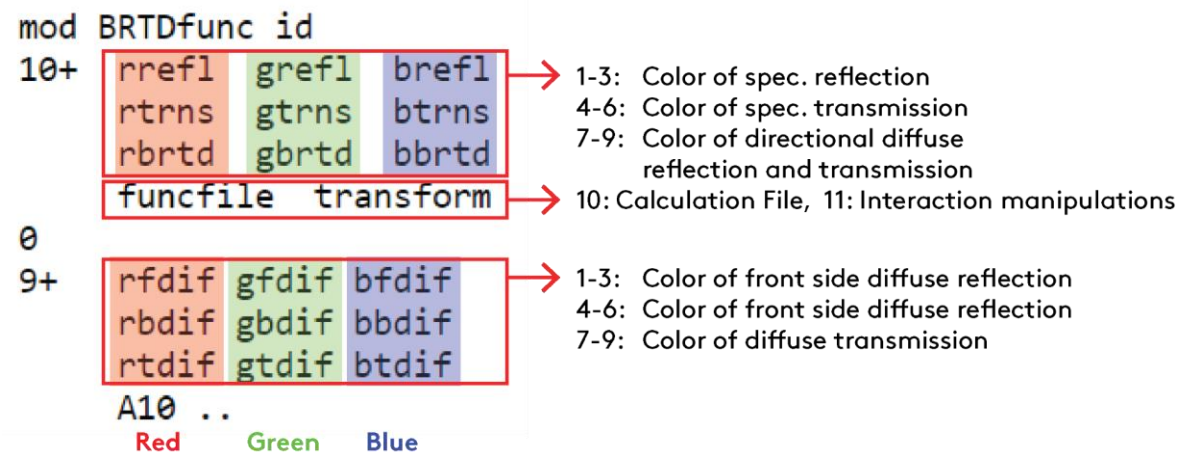

Fig.2.27: BRTDfunc file structure

Bidirectional Reflectance Transmittance Distribution function (BRTDfunc), provides extensive flexibility for simulating surface reflectance and transmittance, offering functions for spectrally-dependent specular rays and reflectance/transmittance distribution functions. This material is particularly useful for accurately modeling complex light interactions with surfaces, including specular and diffuse components of both reflection and transmission. As shown in Fig.2.27, BRTDfunc file contains: “rrefl, grefl, brefl” as the colors of specular reflection; “rtrns, gtrns, btrns” as the colors of specular transmission; “rbrtd, gbrtd, bbrtd” as colors the directional diffuse reflection and transmission based on the direction of the incident light and its solid angle; “funcfile” as the mathematical functions that define customized light interactions; “transform” as the transformation parameters applied to the surface; “rfdif, gfdif, bfdif” as the colors of diffuse reflection for the front side of the surface; “rbdif, gbdif, bbdif” as the colors of diffuse reflection for the back side of the surface; and “rtdif, gtdif, btdif” as the colors of diffuse transmission of the material. Additionally, the sum of reflected diffuse, transmitted diffuse, reflected specular,

transmitted specular and the integrated directional diffuse component should never be greater than one due to optical physics. After a quick HDR rendering test as comparison as shown in 2.28, this study concludes BRDTfunc is a better file format to depict how light interacts with shade fabrics of different colors and OF.

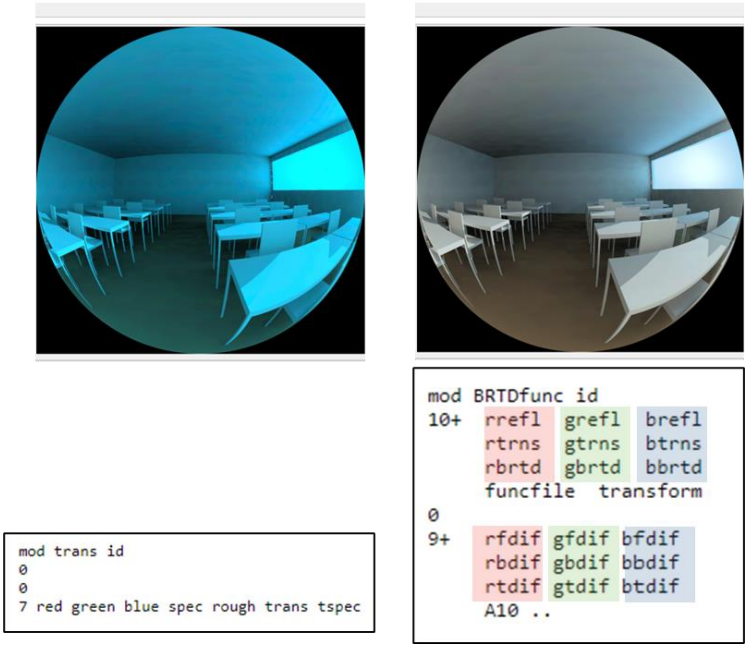

Fig.2.28: HDR rendering comparison between Trans and BRTDfunc material (LBNL)

2.4.2 — ALFA, LARK, CircaLight

There are three available simulation platforms that can perform circadian light assessment: ALFA, LARK, and CircaLight.

ALFA – ALFA () is a direct plugin to Rhino3D. It uses precomputed spectral sun and sky data from the libRadtran radiative transfer library. It allows users to choose between

different sky conditions and ground spectra. One of the limitations, as with other simulation tools, is the challenge in accurately modeling complex dynamic sky conditions, such as varying cloud cover. (Balakrishnan et al., 2023; Ibrahim & Elghali, 2023)

LARK – Lark was originally developed by University of Washington and ZGF Architects LLP as a collaboration. (Inanici et al, 2015) It is provided as an open source and freely available plugin for Rhino Grasshopper that helps architects, lighting designers and researchers investigate circadian light metrics within a daylighting workflow. It allows users to define the color of skies, glazing and building materials based on spectral data. The latest version, Lark 3.0 is a continuous development of multispectral lighting simulation tool that can be used to compute both photopic and melanotic lighting values, as well as neuropic lighting values. It also utilizes multi-channel simulation and allows users to divide the spectra in any number of channels for understanding circadian responses. It can be tailored to specific contexts, such as healthcare environments like Neonatal Intensive Care Units. (Jung, Cheng, Brennan, Inanici 2023)

CircaLight – CircaLight is a new open-source tool designed as a plug-in for Grasshopper in the Rhino3D environment. (Aguilar-Carrasco et al., 2023) It facilitates the computation of various metrics that measure the influence of both natural and artificial light on circadian rhythms, taking into account the spectral reflectance of interior surfaces. The tool can be incorporated with other Grasshopper plugins like Solemma or Ladybug, offering data on the Circadian Stimulus, Equivalent Melanopic Lux, and the Melanopic Photopic ratio—current metrics associated with circadian rhythms. The study assesses CircaLight's reliability by comparing its results with other validated software. The findings demonstrate that CircaLight is a precise parametric tool, with an error margin of less than ±10%, even in challenging scenarios.

Comparison – Balakrishnan and Jakubiec introduces a unique framework to compare spectral daylight platforms concerning their visual, spectral, and colorimetric accuracy in complex daylight scenes in their paper investigated and compared LARK and ALFA as the spectral daylight simulation platform. They concluded that LARK and ALFA are the foremost accessible and user-friendly interfaces for the daylight community to conduct spectral daylight simulations. Both platforms were designed to compute circadian lighting. Both LARK and ALFA can produce spectral renders that offer richer color information compared to non-spectral standard RGB daylight simulations. These renders represent physically accurate color perceptions. The Root Mean Square Error (RMSE) between Lark and ALFA differs mainly in how they represent the sun and sky. LARK tends to have a lower RMSE than ALFA in conditions where the sun's effect is minimal, such as during overcast, evening, and morning skies. In these conditions, the measured spectral irradiance accurately represents the entire sky, making LARK's generated sky closely match the real sky's colorimetric properties. However, when the sun is present and the sky's color varies, the measured irradiance is just an average representation. As a result, LARK's input averages out the distinct color contrasts seen in different parts of the sky. In clear sky conditions, ALFA performs better with lower RMSEs than LARK. Currently, neither platform can simulate clouds, leading to significant errors when the sun is partly obscured. However, an update to LARK (v3.0) has weighed the CCT of the sun and sky based on direct and diffuse global horizontal irradiance.

CircaLight is developed after the validation established by Balakrishnan and Jakubiec. Its paper did not provide a base-line model for validation but instead comparing it result with the simulation of ALFA, which imposes a validity issue as ALFA’s simulation accuracy deviates from the actual measurement of the site under different materials, timing, and weather conditions

as shown below (Balakrishnan, Jakubiec, 2019). Therefore, it becomes difficult to validate the accuracy of CircaLight by only looking at its relative performance to ALFA's simulation result.

Chapter 3 — Methodology

First, this study performs lighting simulations for a standard classroom without any shading devices as a baseline model, to have a basic understanding of the lighting condition of the standard classroom on summer and winter solstices. Then, this study performs additional simulations for commercial typical SF of different OFs, to find out the ideal product for further investigations, and to understand the photopic and melanopic lighting impact of conventional shade fabrics. After selecting the ideal openness factor, this paper will implement a color adjustment in the Radiance material file and create a theoretical shade fabric based on related opsin sensitivity of human eyes to maximize the melanopic stimulation while preserving the same photopic light level. Then, this study will simulate different color variations of SF to demonstrate the potential alternatives for different photopic and melanopic lighting requirements. Apart from exploring color variations, this research also investigates other fenestration systems such as venetian blinds that allow more controls to manipulate indoor lighting behavior.

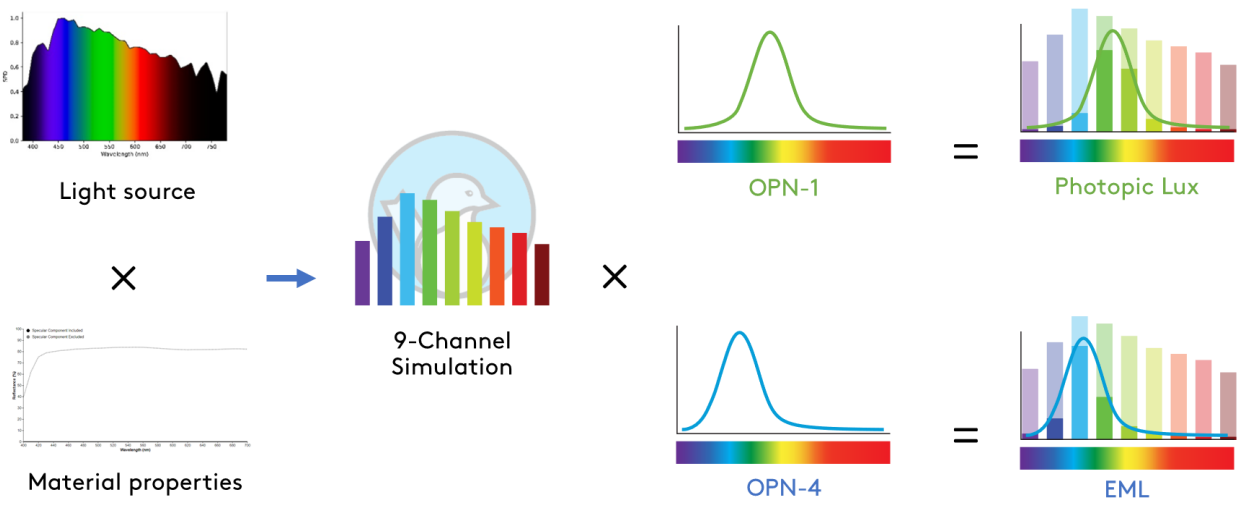

Fig.3.1: Simulation process

The research utilizes LARK Spectral Lighting 3.0 (9-Channel) within Rhino3D to perform all simulations. The SPD of light sources and material properties are converted into 9 spectral channels with the following spectral intervals: B1(380-420 nm); B2(420-460 nm); B3(460-500 nm); G1(500-530 nm); G2(530-559 nm); G3(559-588 nm); R1(588-609 nm); R2(609-631 nm); and R3(631-780 nm). The resulting data is weighted with the photopic (OPN-1) and melanopic (OPN-4) sensitivity coefficients to compute the glare (in lx) and circadian lighting (in EML) conditions.

For result analysis, this study creates grid based simulations for light distribution condition analysis, sectional graphs for light penetration analysis, and HDR renders with false color mapping to understand the human visual and non-visual responses.

3.1. — Simulation Setting

According to the National Center for Education Statistics (Fig.3.2), the typical class size in US public schools is 15-23 students. The most frequently observed class size in US public schools in 2020 to 2021 was 19 students. Therefore, a standard classroom for 20 to 25 students, 30 ft wide by 30 ft deep with a 9 ft ceiling height, is modeled (Fig.3.3). This classroom is set to be located in Seattle, WA and has a south facing window of 27 ft wide by 4 ft high, making up 40% window to wall ratio (WWR%). The south facing window is sitting 3 ft from ground with a head height of 7 ft. The simulation time includes the summer solstice (12:00 pm on June 21st) and winter solstice (12:00 pm on December 21st). The weather is set to clear sky to study the glare-circadian condition of the classroom under the maximum direct daylight. As recorded in Inanici's work, the CCT (Fig 2.8) is never static but highly dynamic throughout the day. Therefore, four different correlated color temperatures (5500K, 6500K, 13000K, 25000K) are

included in the simulations to depict a comprehensive analysis to understand how shade fabric affects the lighting condition under different times of the day.

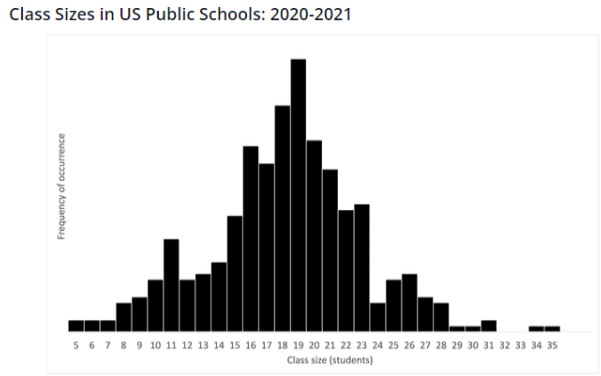

Estimated Classroom Sizes for Different Class Sizes

Class size (students)	Classroom size (roomy, 45 sq ft/student)	Classroom size (compact, 35 sq ft/student)
15	675 sq ft (26 by 26 ft)	525 sq ft (23 by 23 ft)
18	810 sq ft (28 by 29 ft)	630 sq ft (25 by 25 ft)
20	900 sq ft (30 by 30 ft)	700 sq ft (26 by 27 ft)
22	990 sq ft (31 by 32 ft)	770 sq ft (28 by 28 ft)
25	1125 sq ft (34 by 33 ft)	875 sq ft (30 by 29 ft)
30	1350 sq ft (37 by 37 ft)	1050 sq ft (32 by 33 ft)
40	1800 sq ft (42 by 43 ft)	1400 sq ft (37 by 38 ft)
50	2250 sq ft (47 by 48 ft)	1750 sq ft (42 by 42 ft)

Fig 3.2:. Class size distribution 2020-2021 (NCES)

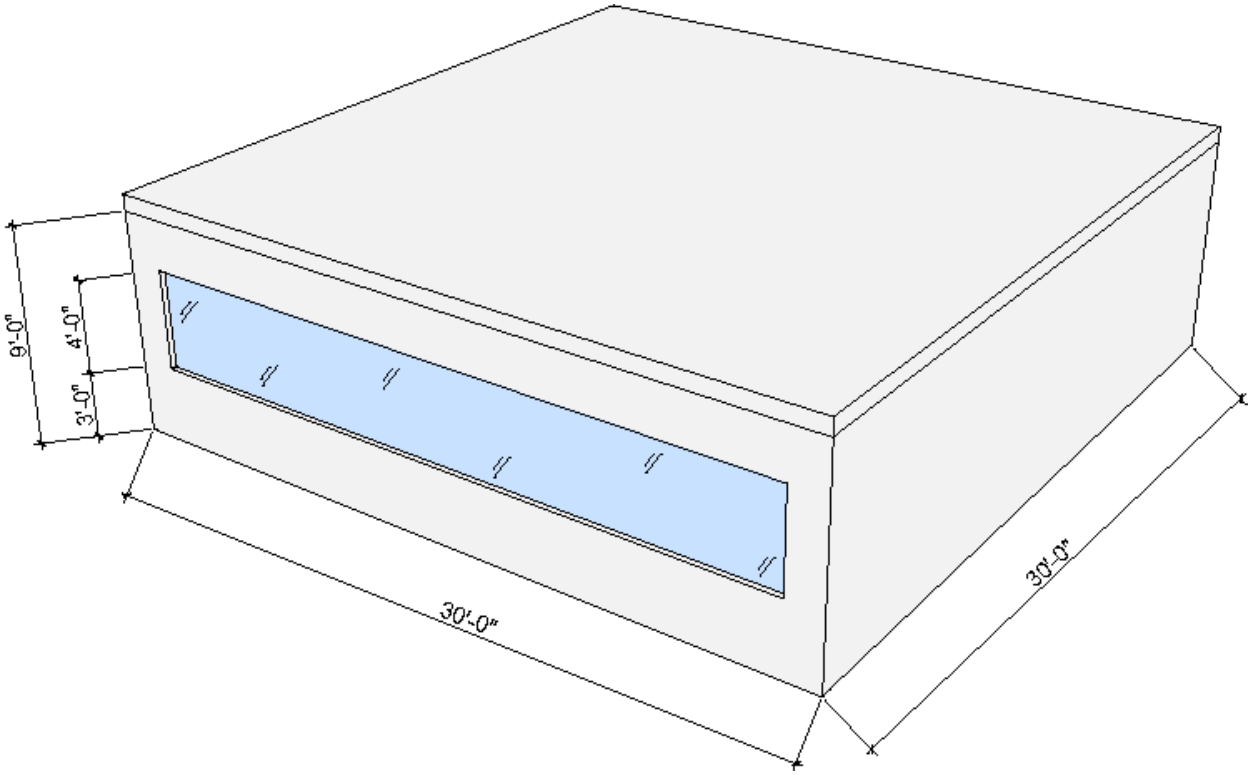

Fig 3.3: Standard classroom model in Rhino 3D

3.1.1 — Simulating Typical Shade Fabrics (Typ.SF)

For simulating commercial typical SF (Typ.SF), this paper investigates the commercial typical product as shown in Fig.3.3. This fabric is called SheerWeave® manufactured by Hunter Douglas Architectural. There are 4 different openness factors, 1%, 3%, 5%, and 10%. Each openness factor comes with different Solar Transmittance (Ts), Solar Reflectance (Rs), Solar Absorptance (As), and Visual Transmittance (Tv). Since lighting simulation only focuses on visual impacts, this paper has translated Ts, Rs, As into visual properties proportionally based on the ratio between Ts and Tv, before computing their material in BRTDfunc format (Fig.3.4).

SheerWeave® 2500 1%, 2410 3%, 2390 5%, 2360 10%

FENESTRATION	FABRIC PROPERTIES								SHGC/G VALUE g-tot (glass & blind)			
	SOLAR OPTICAL								SINGLE		INSULATING	
	Ts (%)		Rs (%)		As(%)		Tv (%)		1/4 CL		1 HA	
COLOR	1%	3%	1%	3%	1%	3%	1%	3%	1%	3%	1%	3%
Pearl Gray	10	16	31	30	59	54	9	14	0.47	0.49	0.30	0.31
COLOR	5%	10%	5%	10%	5%	10%	5%	10%	5%	10%	5%	10%
Pearl Gray	10	16	31	30	59	54	9	14	0.47	0.49	0.30	0.31

Fig.3.3: Typ.SF sample (SheerWeave® 2360) (image: Hunter Douglas Architectural)

#V20 Pearl Gray 1% OF

```
#V20 Pearl Gray 1% OF
void BRTDfunc final_gy1
10
    0.125 0.125 0.125
    0.01 0.01 0.01
    0 0 0
    C:\lark\temp\shade_cal_folder\shade_kchiu.cal
0
9
    0.263 0.263 0.263
    0.263 0.263 0.263
    0.04 0.04 0.04
```

#V20 Pearl Gray 3% OF

```
#V20 Pearl Gray 3% OF
void BRTDfunc final_gy3
10
    0.125 0.125 0.125
    0.03 0.03 0.03
    0 0 0
    C:\lark\temp\shade_cal_folder\shade_kchiu.cal
0
9
    0.263 0.263 0.263
    0.263 0.263 0.263
    0.04 0.04 0.04
```

#V20 Pearl Gray 5% OF

```
#V20 Pearl Gray 5% OF
void BRTDfunc final_gy5
10
    0.125 0.125 0.125
    0.05 0.05 0.05
    0 0 0
    C:\lark\temp\shade_cal_folder\shade_kchiu.cal
0
9
    0.263 0.263 0.263
    0.263 0.263 0.263
    0.04 0.04 0.04
```

#V20 Pearl Gray 10% OF

```
#V20 Pearl Gray 10% OF
void BRTDfunc final_gy10
10
    0.125 0.125 0.125
    0.1 0.1 0.1
    0 0 0
    C:\lark\temp\shade_cal_folder\shade_kchiu.cal
0
9
    0.263 0.263 0.263
    0.263 0.263 0.263
    0.04 0.04 0.04
```

Fig.3.4: BRTDfunc material description for V20 Pearl Gray with 1%, 3%, 5%, 10% OF

3.1.2 — Simulating Spectrally-Selective SF (SSF)

To investigate how SFs can be manipulated to improve the glare-circadian balance, this study has created an Excel-based calculator. This calculator takes in considerations of human photopic and melanopic sensitivity coefficients to reconfigure the BRTDfunc material properties, so that the new type of SF, named Spectrally-Selective Shade Fabrics (SSF), can retain the same photopic impact while adjusting melanopic impact of shading after applying the color adjustments. Fig. 3.5 shows this process for theV20 Pearl Gray 10% OF. For example, the color of light transmission of Typ.SF is 0.1 throughout the B1 to R3, hence both photopic and melanopic impacts should expect 0.1. After adjusting the color ratio as shown in "Adjust Ratio" for blue (B1-B3 as 1.0), green (G1-G3 as 0.55), and red (R1-R3 as 0.1) spectra, the calculated colors of transmissions for SSF become 0.217 as blue; 0.119 as green; and 0.022 as red. In this case, the total photopic impact remains 0.1 as the Typ.SF but the melanopic impact is 0.178 that is theoretically 7.8% more effective in maintaining the melanopic stimulus.

Spectrum	Channels-Trans	Gray-P	Gray-M	Channels-Colored	Pho	Mel	Channels-color2	Color-P	Color-M
B1	**0.1**	0.00002760813738	0.00119	1	0.000276081373	0.0119	0.2165206164	0.00005977730923	0.002576595335
B2	**0.1**	0.0009098397499	0.01784	1	0.009098397499	0.1784	0.2165206164	0.001969990635	0.03862727797
B3	**0.1**	0.00555902089	0.04165	1	0.0555902089	0.4165	0.2165206164	0.0120364263	0.09018083673
G1	**0.1**	0.01640711022	0.0268842588	0.55	0.09023910619	0.1478634234	0.119086339	0.01953862689	0.03201547958
G2	**0.1**	0.02503559048	0.01033	0.55	0.1376957476	0.056815	0.119086339	0.02981396816	0.01230161882
G3	**0.1**	0.02597542495	0.0019	0.55	0.1428648372	0.01045	0.119086339	0.03093318262	0.002262640441
R1	**0.1**	0.01301770719	0.00017	0.1	0.01301770719	0.00017	0.02165206164	0.002818601985	0.000036808504
R2	**0.1**	0.008108571837	0.00002963	0.1	0.008108571837	0.00002963	0.02165206164	0.001755672972	0.000006415505
R3	**0.1**	0.004959126549	0.0000061112	0.1	0.004959126549	0.0000061112	0.02165206164	0.001073753137	0.000001323200
	Total	0.1	0.1		0.4618497844	0.8221341646		0.1	0.1780089961
		Photopic T	Melanopic T						
	T coef	**0.138**			4.618497844			**0.138**	
	Total T	0.0138	0.0138					0.0138	0.02456524146

Fig 3.5: Recomputing the R,G,B diffuse transmittance for maximizing melanopic responses

This study explores SSF with 10%OF under blue, purple, and orange color based on their opsin(OPN) sensitivities features as shown in Fig.3.6. Their BRTDfunc material properties are recorded as shown in Fig.3.6. Given a similar photopic light impacts (integral area of dashed

lines) between SFs, the melanopic light impacts (integral area of blue and purple solid lines) of SSF(Blue) and SSF(Purple) are significantly higher than Typ.SF; whereas the melanopic light impact (integral area of orange solid lines) of SSF(Orange) diminished. The purpose of this study is to investigate how these changes of sensitivity affect the glare-circadian balance of the classroom lighting.

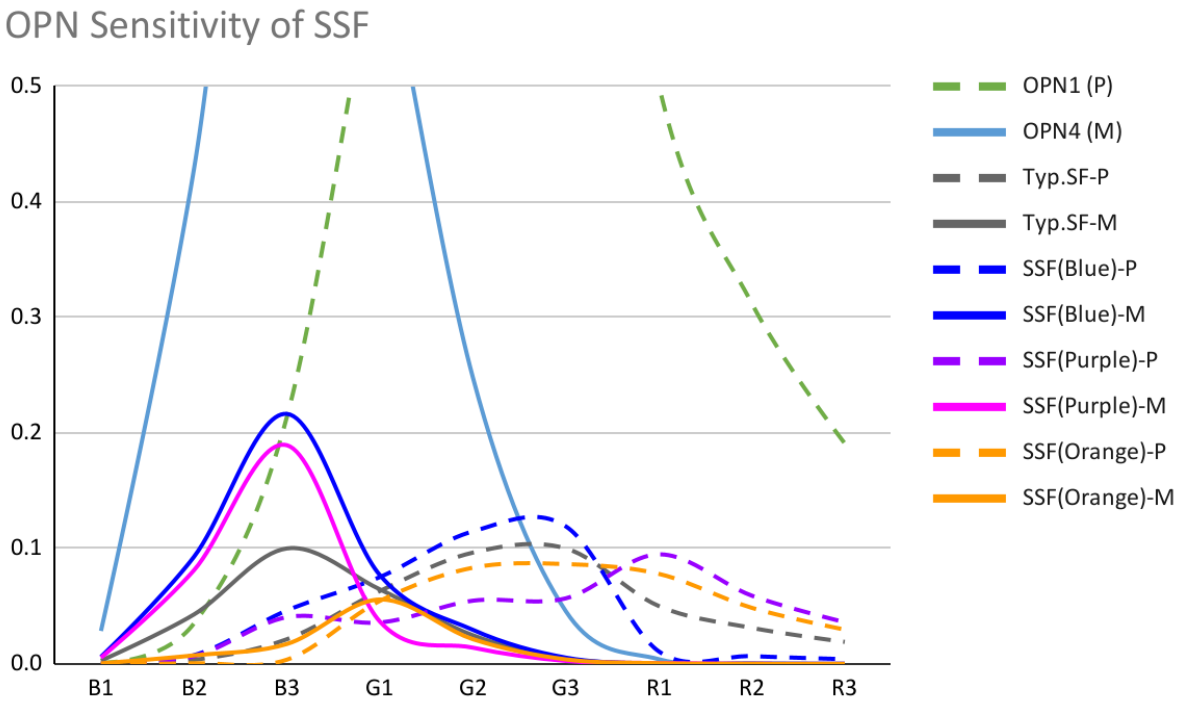

Fig 3.6: Normalized photopic and melanopic responsive curves in 9-channels representation

One thing worths notice is that, unlike simulating Typ.SFs in 9-channels simulation, SSFs in 9-channel simulation requires additional BRTDfunc files for blue (B1-B3), green (G1-G3), and red (R1-R3) spectra, as one BRTDfunc file is only design to take 3 channels for light tracing calculation. Therefore, one SSF with 9-channels simulation would require 3 BRTDfunc files in total as shown in Fig.3.7.

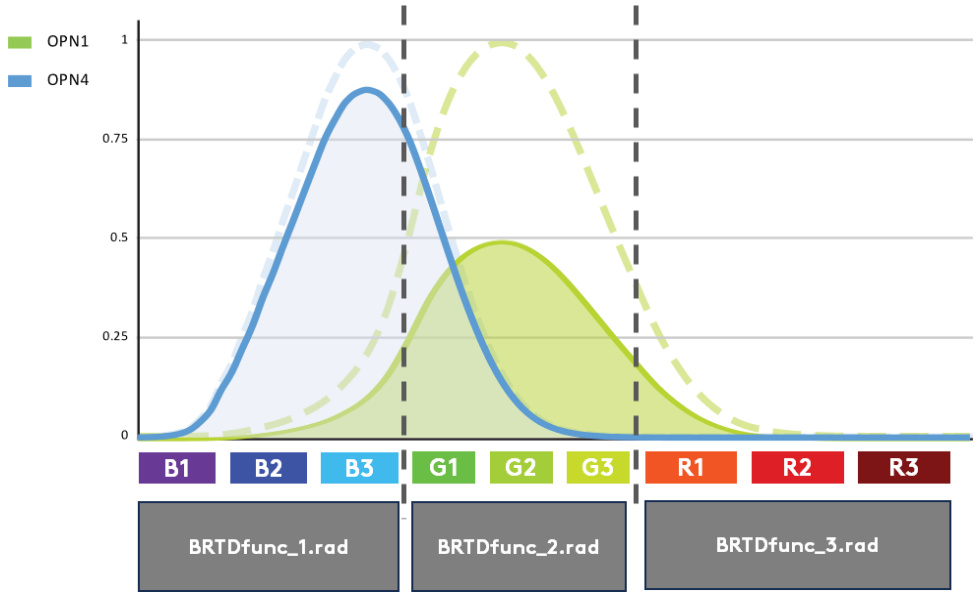

Fig 3.7: Additional BRTDfunc files for 9-channel simulation

3.1.3 — Simulating Venetian Blind (VB)

Apart from investigating how SSF impacts the glare-circadian balance, this study also makes a simulation to compare how SFs and VBs affect the lighting conditions. Similar to simulating SFs, this study first models a commercial typical product shown in Fig.3.8 with standard 5 cm slat width, followed by color adjustments to see how changing colors for VBs would impact the lighting condition.

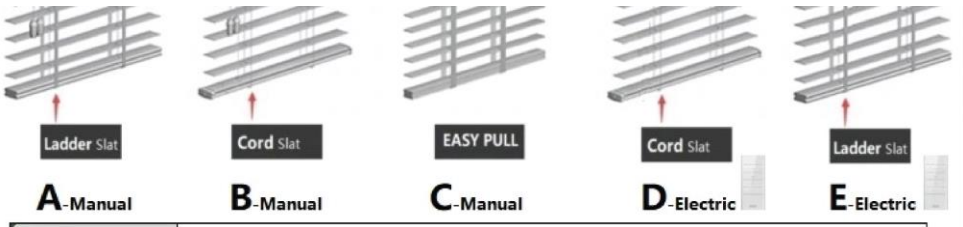

Name	Venetian Horizontal Blinds
Slat	5cm (standard)or 3.5cm (Contact us)
System	Manual Cord.Ladder.EasyPull | Electric
Customize	Wide (30-250)cm | (12"-118")inch.High (30-350)cm | (12"- 138")inch

Fig.3.8: VBs standard product specification. (Image: Karlleo)

3.2. — Data Visualization

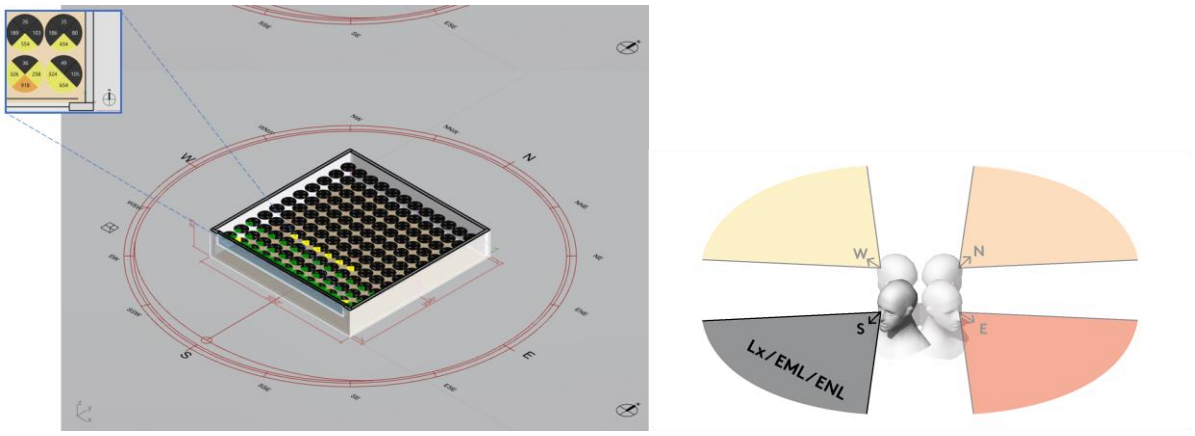

Fig 3.9 Illustration of cone shape data visualization for photopic lux

In the classroom, a grid simulation is performed at 44 inches from ground to mimic how occupants perceive light at sitting eye level, as shown in Fig 3.9 above. Each grid point is a disc shape splitted into 4 cones as the occupants' visual perceptions facing toward north, east, south, and west directions. Each cone displays a value that indicates the incoming light intensity either in photopic lux or EML from their facing directions.

The color of the cones indicates the glare and circadian light situation. As shown in Fig 3.10, there are 3 different legends for photopic lighting, melanopic lighting, and neuropic lighting simulations. When the photopic lux is less than 300 lux, cones will become gray to indicate insufficient light; when it is higher than 2657 lux, cones will become red to indicate a glare issue. When the melanopic lux is lower than 275 EML, cones will become gray to indicate insufficient circadian light stimulation. Unlike glare caused by photopic light, there is no upper limit to melanopic light. Since the WELL building standard is suggesting 275 EML ast the minimum melanopic light for at least 4 hours, this paper is setting the theoretic upper threshold 4 times higher than 275 EML, suggesting 1100 EML can shorten the time needed for circadian entrainment from 4 hours to 1 hour. Since more research is needed to establish the requirement for neuropic entertainment, this paper holds the same calibration for neuropic lighting conditions.

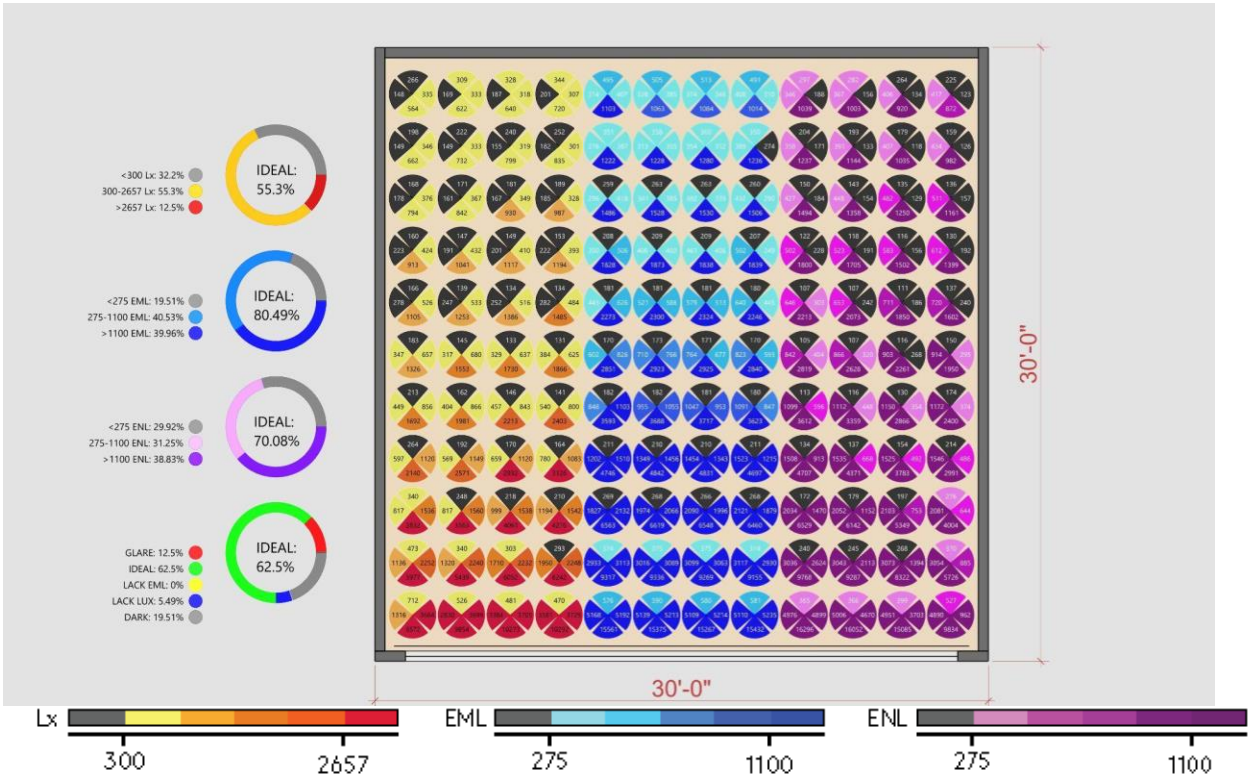

Fig 3.10: Example of photopic, melanopic, and neuropic simulations of the standard classroom

To have a direct understanding of glare-circadian balance conditions, this paper creates a balance comparison between photopic and melanopic light stimulation as shown in Fig 3.11 below. According to the legend, there are in total 5 situations: “Glare” in red label as photopic lux over 2657 lx; “Ideal” in green label as photopic lux between 300 lx and 2657 lx and EML over 275; “Fair” in yellow label as photopic lux between 300 lx and 2657 lx but EML below 275; “DIM” as photopic below 300 lx and EML over 275; and “Underlit” as both photopic lux and EML are below the threshold. On the other hand, the pie charts next to grid simulation present the percentage of ideal lighting conditions in the classroom. Using Fig 3.12 as an example, 62.5% of all simulated locations in the classroom have an ideal glare-circadian light balance; 12.5% of the locations have a glare issue; 5.49% of the locations have enough melanopic light but lacking photopic light; and 19.51% of the locations do not have enough both the photopic and melanopic light.

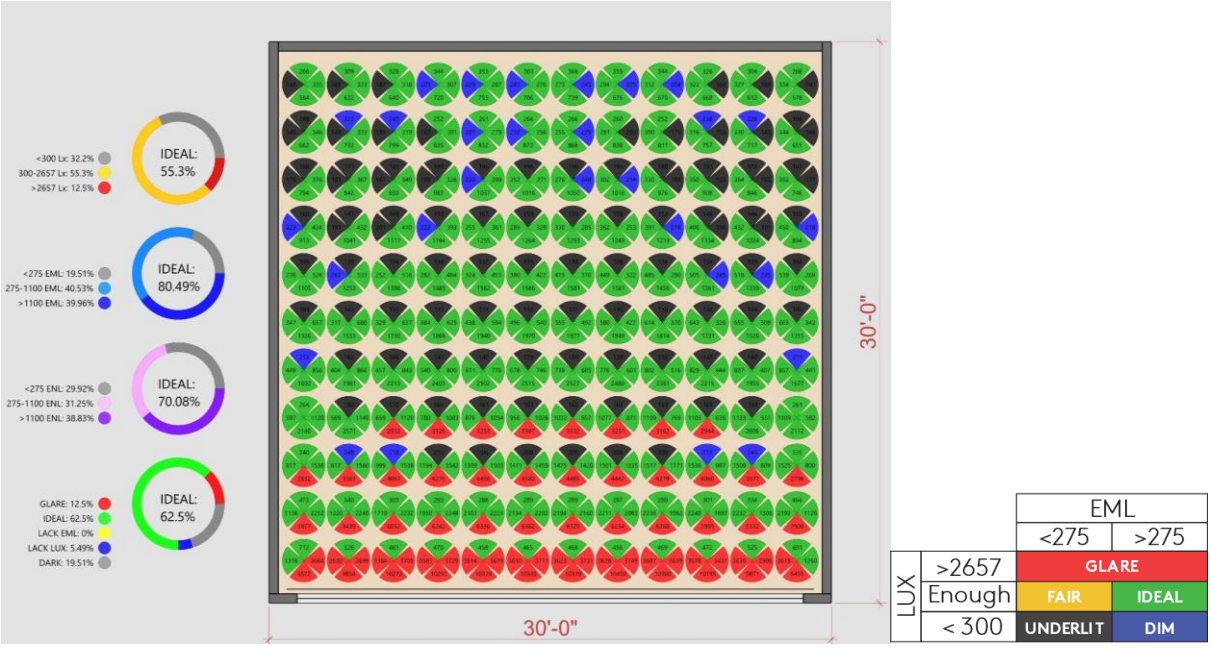

Fig 3.11: Example of Glare-Circadian Balance simulation of the standard classroom

Moreover, this paper analyzes light penetrations to understand how each shade device impacts the photopic and melanopic illuminance per depth, under 4 view orientations on summer and winter solstices as shown in Fig.3.12 below. There are two types of graphs: photopic light penetration (in red) with a corresponding legend OPN1(lx) of threshold 300 - 2657 lx ; and melanopic light penetration (in blue) with legend OPN4(EML) of threshold 275 - 1100 EML. Photopic graph beyonds the 2657 lx threshold predicts a glare issue at the belonging depth of the classroom. Any graph below their lower threshold (300 lx or 275 EML) predicts an underlit problem. As various CCTs of sky are included in simulation, the melanopic light penetration graph will include a poché area to indicate the melanopic stimulus from 5500 K to 25000 K. Four view orientations include: “S” as south where occupants gaze toward the window; “E/W” as east and west where occupants gaze parallel to the window; and “N” where occupants gaze toward the rear wall.

Finally, this study includes simulated HDR images to demonstrate human visual sensation of the classroom as shown in Fig. 3.13. The camera is set at the center of the west wall, gazing toward the east, parallel to the window as shown in Fig.3.14, at the sitting eye level under 5500K and 25000K sky CCT. The time is set at 9:00am to mimic the visual sensation to the human eye in the morning. Additionally, false color mappings are included to analyze the change of photopic luminance (in cd/m^2) and melanopic luminance (in $EMcd/m^2$) to the human eye.

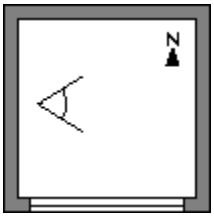

Fig.3.14: HDR camera position

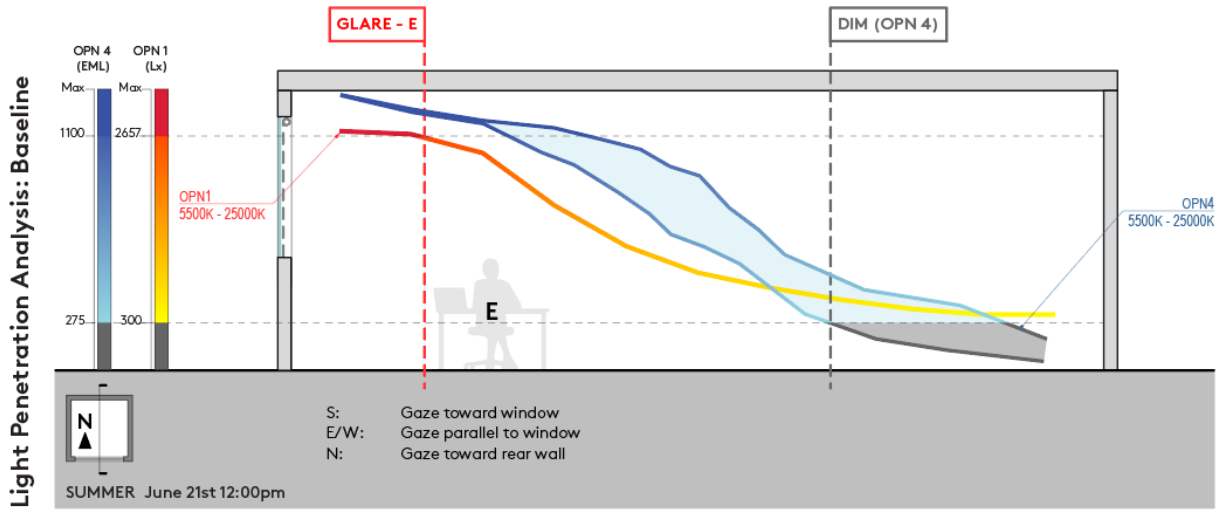

Fig 3.12: Light penetration of baseline model on summer solstice

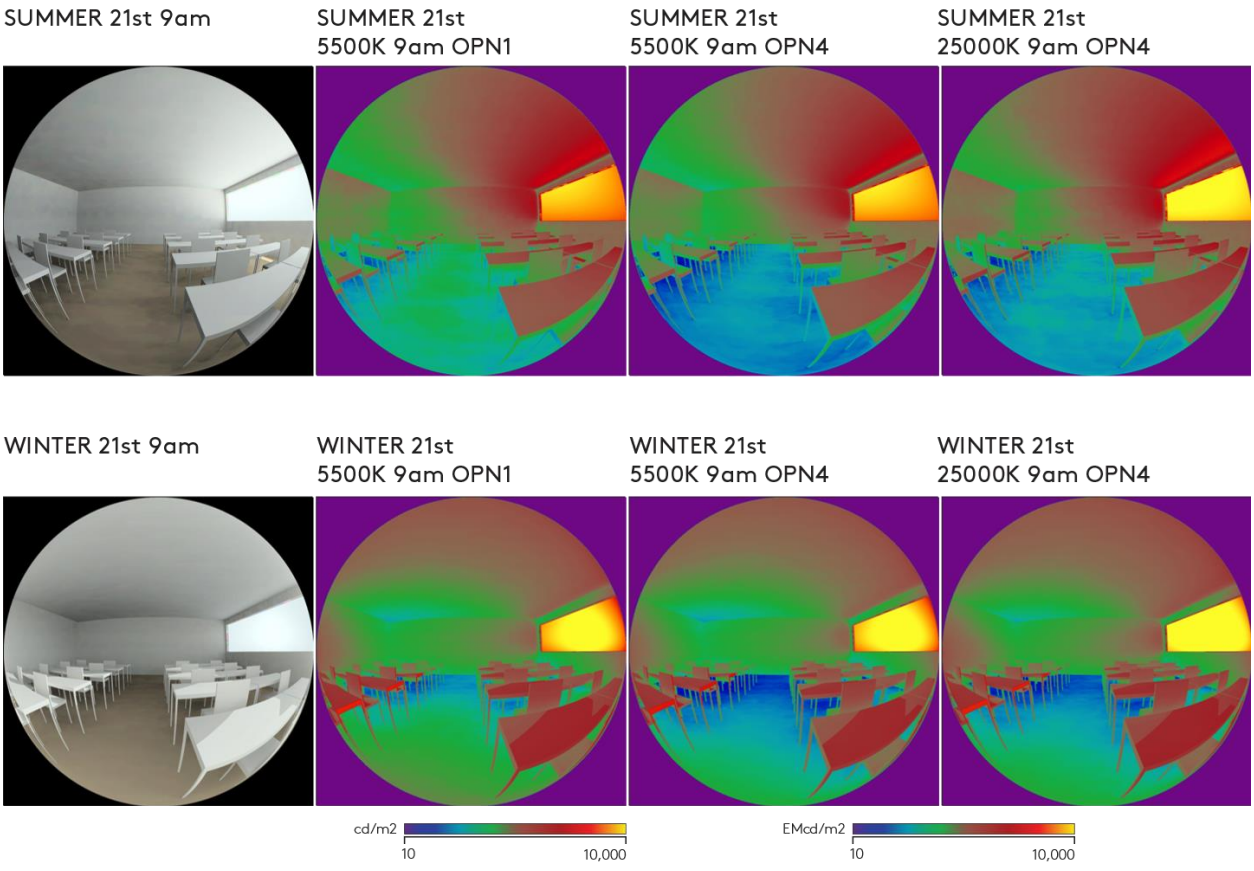

Fig.3.13: Simulated HDR images

Chapter 4 — Result and Discussion:

4.1. — Baseline

Before further discussion about the effect of shade fabrics, a series of light simulations has been performed for a fundamental understanding as a baseline model shown below.

Fig.4.1 and Fig.4.2 display the photopic light distributions of the classroom under CCT 6500K on summer solstice and winter solstice. In summer, 64.02% of the classroom area has an ideal photopic light level between 300 lx and 2657 lx; 20.27% of the area has glare issues with photopic light over 2657 lx; and 15.72% of the area has underlit problem with photopic light below 300 lx. In terms of light distribution, most of the glare issues concentrate on the view gazing toward the window and area close to the window. This implies a need for shading to achieve visual comfort. On the other hand, the central area gazing toward the rear wall and the back corners of the classroom shows underlit problems and implies a need for light compensation from electric light. In winter, 70.83% of the classroom area has an ideal photopic light; 29.17% of the area has glare issues; and 0% of the area has underlit problems. In terms of light distribution, most of the glare issues heavily concentrated on the view gazing toward the window and the area nearby the window. Although the ideal area has increased, there is a more serious glare issue in the class during winter, which implies a need for shading to achieve visual comfort.

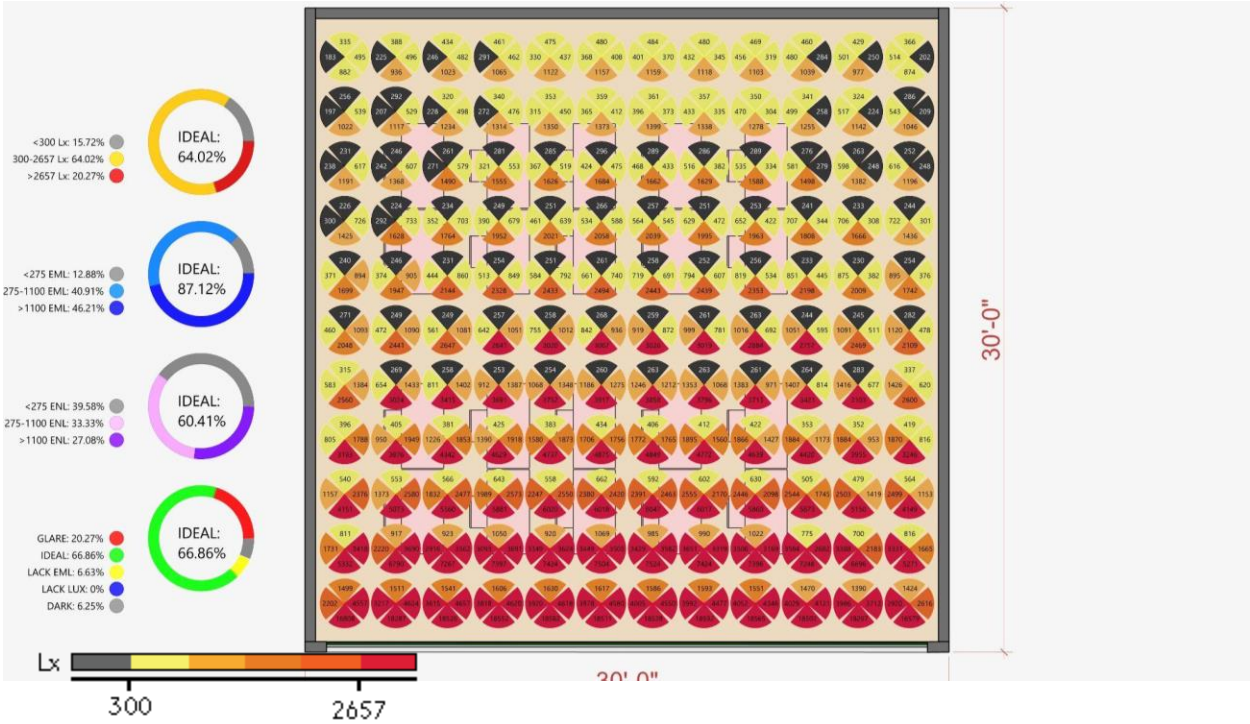

Fig.4.1: Daylight distribution under CCT 6500K on summer solstice

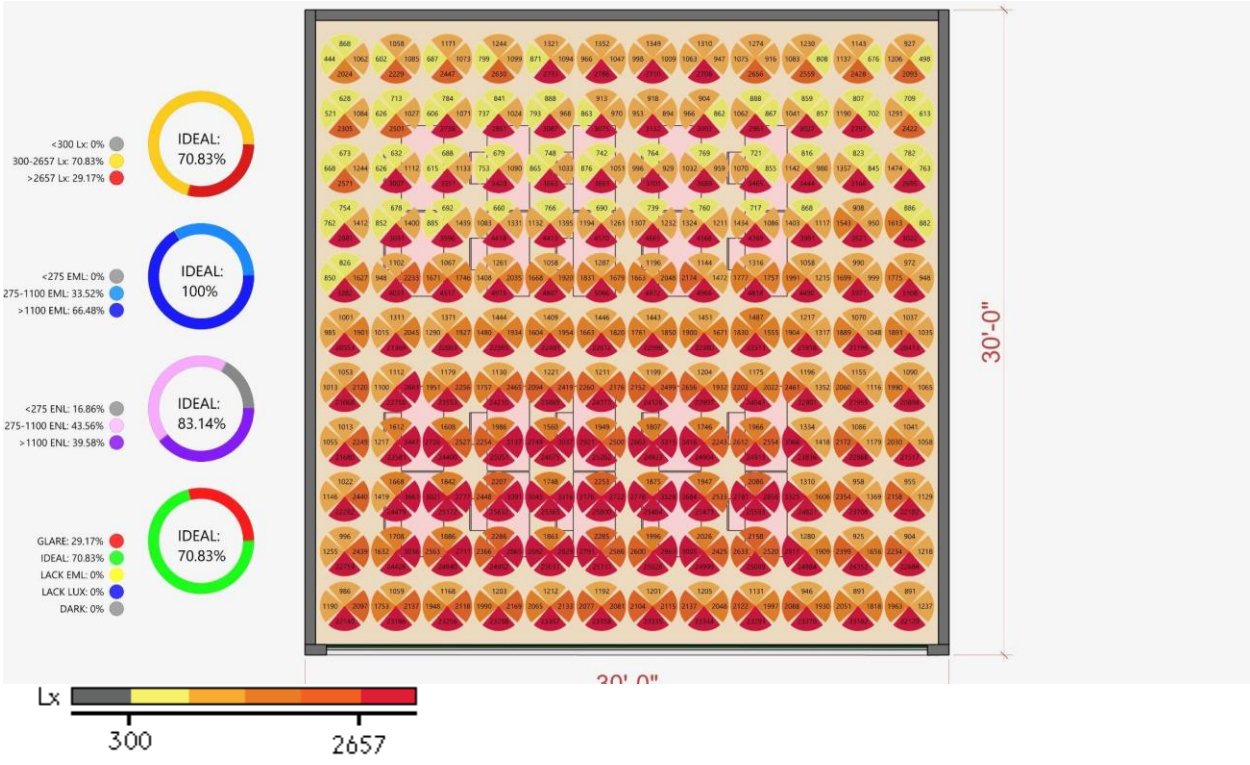

Fig.4.2: Daylight distribution under CCT 6500K on winter solstice

Fig.4.3 and Fig.4.4 display the melanopic light distributions of the classroom under CCT 6500K on summer solstice and winter solstice. In summer, every location in the classroom has enough melanopic stimulation from the south direction. 87.12% of the area has an ideal melanopic lighting over 275 EML; 46.21% of the area has high melanopic lighting over 1100 EML; 12.88% of the area has an underlit problem with melanopic illuminance below 275 EML. In terms of the light distribution, circadian entrainment is mostly satisfied by the area near the window from all view orientations, and nearly half of the area can fully entrain circadian health within 1 hour. The central area gazing toward the rear wall and the deeper corners of the classroom presents underlit problems and implies a need for circadian light compensation. In winter, 100% of the area has melanopic lighting over 275 EML; and 66.48% of the area has high melanopic lighting over 1100 EML, which implies about ⅓ of the area can fully entrain occupants' circadian health within 1 hour.

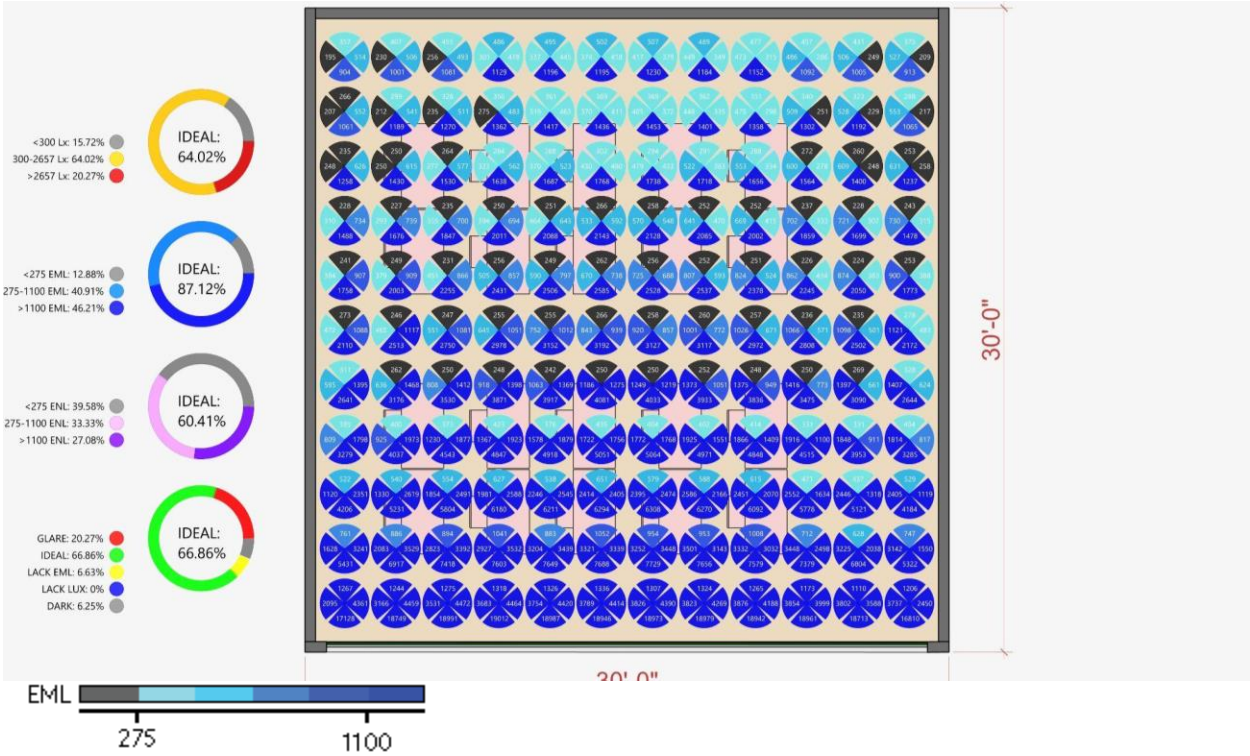

Fig.4.3: EML distribution under CCT 6500K on summer solstice

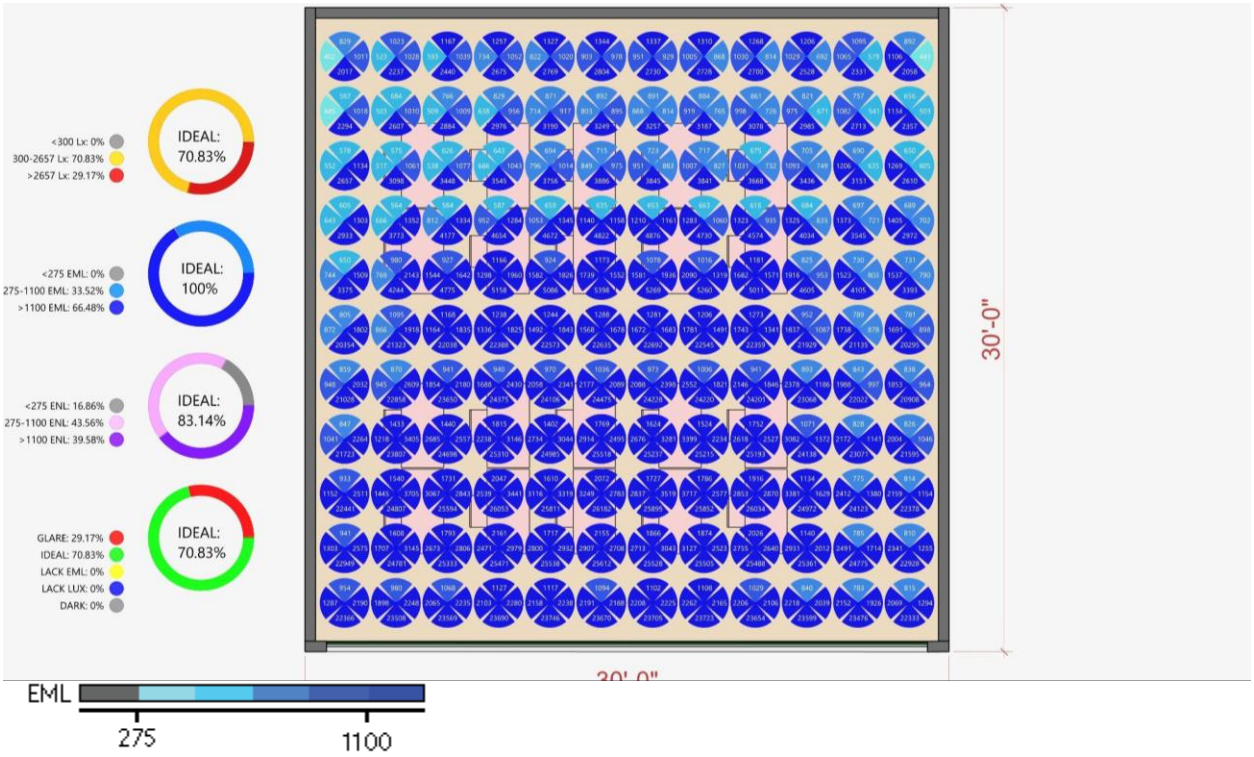

Fig.4.4: EML distribution under CCT 6500K on winter solstice

Fig.4.5 and Fig.4.6 display the glare-circadian balance condition of the classroom under CCT 6500K on summer solstice and winter solstice. In summer, 66.86% of the area present an ideal lighting balance with photopic light between 300 lx and 2657 lx while melanopic light over 275 EML ; 20.27% of the area presents glare problem; 6.63% of the area present an under-entrain condition with adequate photopic light but lacking melanopic light; 6.25% of the area present a totally-underlit problem where both photopic and melanopic light are missing. In terms of the balance distribution, glare issues only happen at the area close by the window, as well as view gazing toward the window near the central area. Most of the ideal balance concentrated at location near the rear wall of the classroom. Certain locations in the central area gazing toward the rear wall, and near the corners at the end may experience either under-entrain or underlit problems. It implies occupants' circadian rhythm may not be fully entrained and require additional circadian stimulus and photopic light from electric light to achieve circadian entrainment with visual comfort. In winter, 70.83% of the area presents an ideal light balance; 29.17% of the area presents an glare issue; 0% of the area presents any underlit problem. The balance distribution shows there are significant glare issues from the south direction across most locations, and the area near the window gazing parallel to the window. This implies a need of shading to avoid discomfort glare.

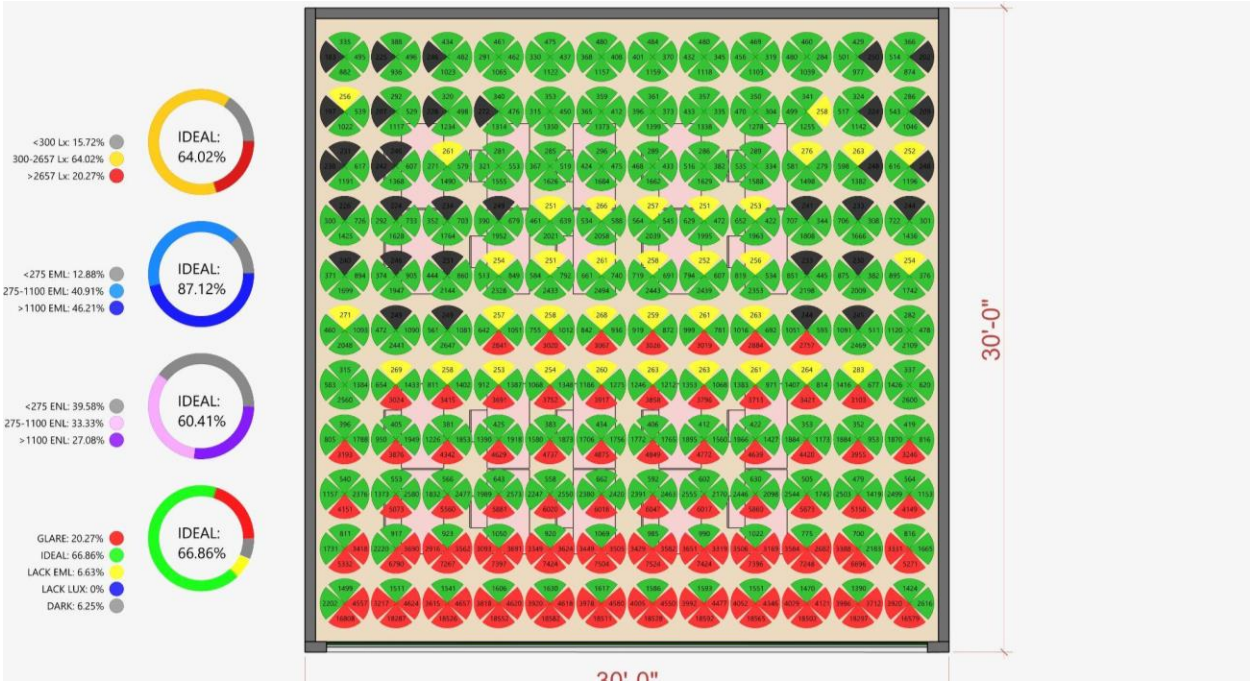

		EML	
		<275	>275
LUX	>2657	GLARE	
	Enough	FAIR	IDEAL
	< 300	UNDERLIT	DIM

Fig 4.5: Glare-circadian comparison under CCT 6500K on summer solstice

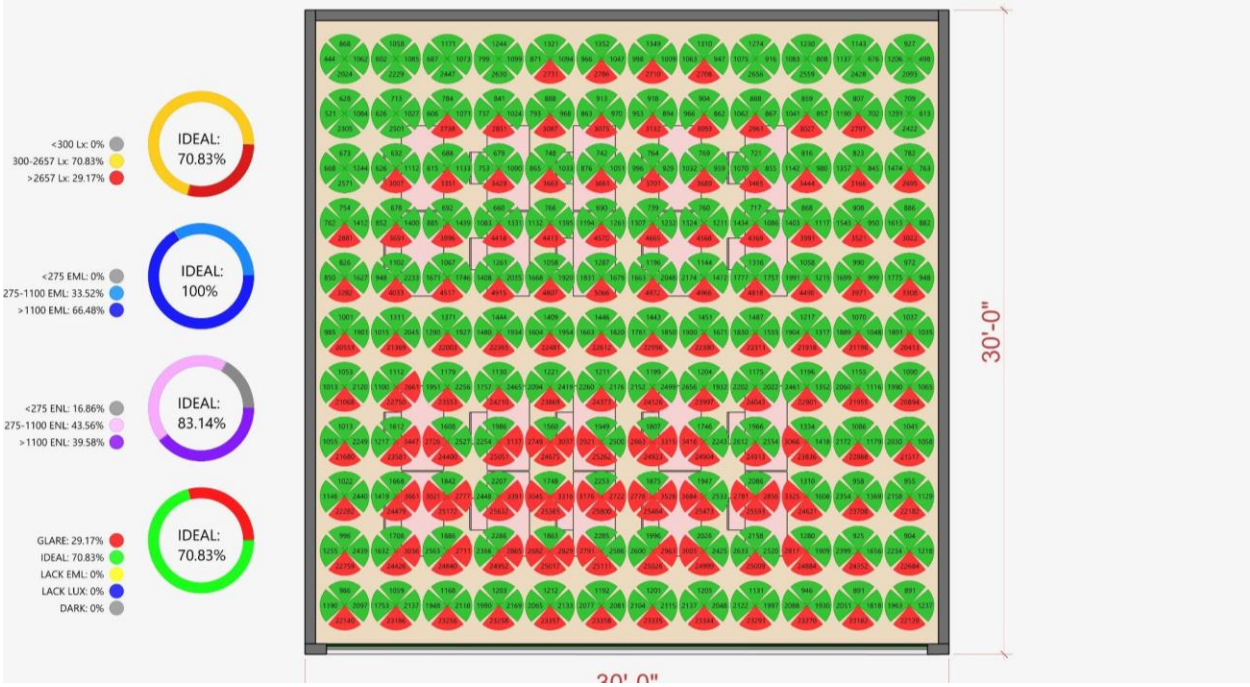

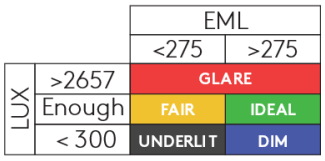

Fig 4.6: Glare-circadian comparison under CCT 6500K on winter solstice

Fig.4.7 and Fig.4.8 display the photopic and melanopic light penetration of 4 view orientations under CCT sky conditions from 5500 K to 25000 K. While the photopic illuminance remains very similar, the melanopic illuminance per depth varies drastically based on view orientations and sky CCT. Melanopic light penetration is positively related to sky CCT, meaning higher CCT increases melanopic light penetration under the same photopic illuminance. In summer, gazing toward the window within 15 ft would experience glare issue; gazing parallel to the window within 5 ft would experience glare issue; and gazing toward the rear wall between 10 to 20 ft would experience under-entrain problem when the sky CCT is low. In winter, gazing toward the window at any depth would experience glare issues; gazing parallel to the window between 5 to 10 ft would experience glare issues.

As simulations take place at 12:00pm, the sun position is orthogonal to the south, hence the simulation of view orientations toward east and west are close to identical. This result is expected to differ more drastically in the morning and evening time. Overall, both photopic and melanopic light levels diminish proportionally per depth, until approximately 5 to 10 ft from the rear wall where the light levels increase due to the rear wall reflectance. The general photopic and melanopic light levels in winter are higher than summer, and the diminishing rate is more gentle, indicating a more even light distribution throughout the classroom. During winter, this compensation of light from reflectance is more significant in which both photopic and melanopic light levels of gazing toward the rear wall exceed the light levels of gazing parallel to the window.

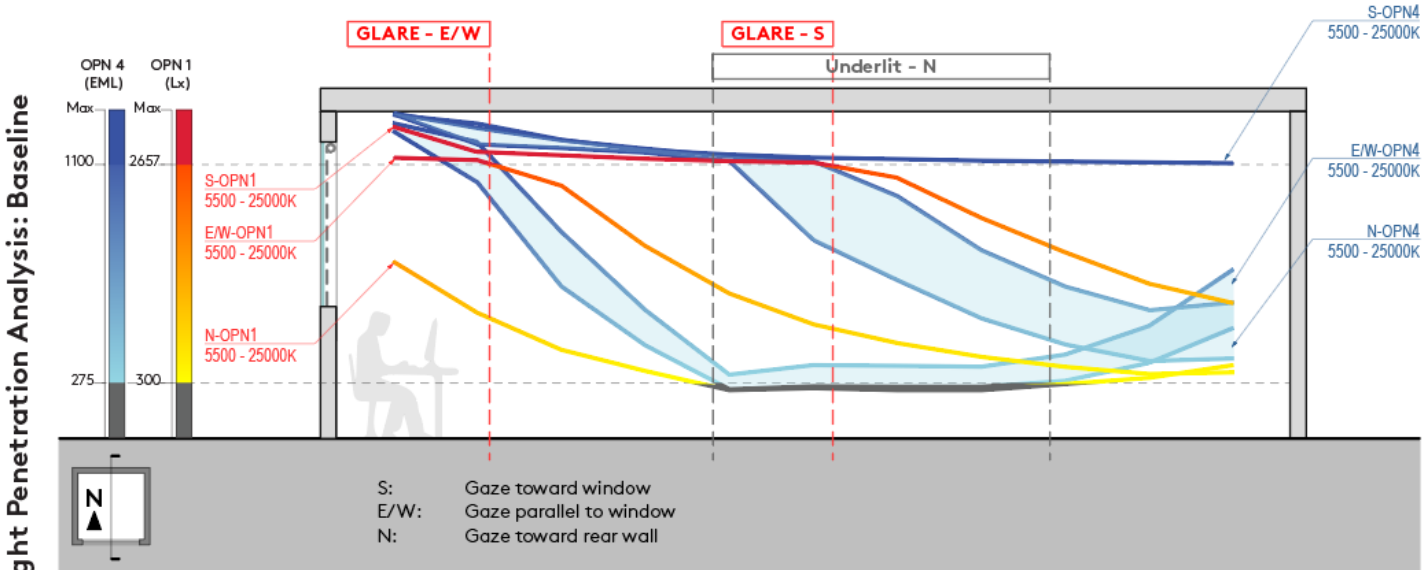

Fig 4.7: Photopic and melanopic light penetration on 4 view orientations on summer solstice

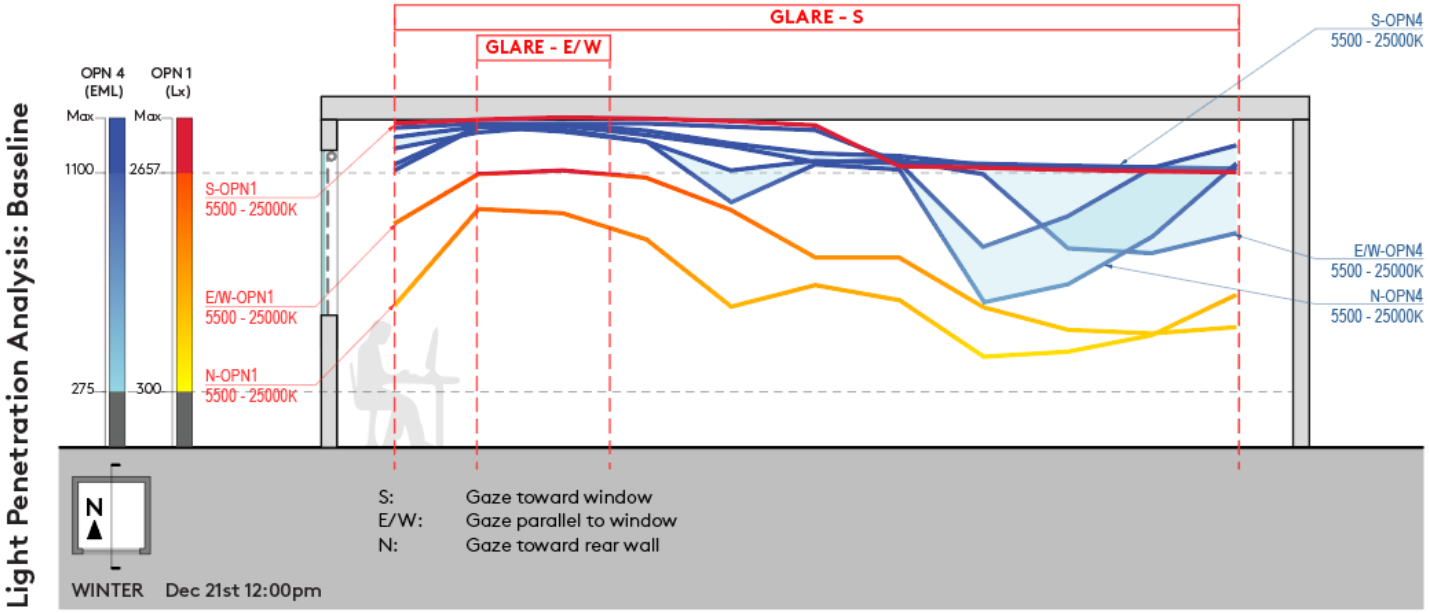

Fig 4.8: Photopic and melanopic light penetration on 4 view orientations on winter solstice

For HDR image simulations, after performing false color mapping on both photopic and melanopic luminance, the classroom appears to be evenly lit but with potential glare from the window, and the light pattern for both photopic and melanopic lighting conditions align with the light penetration study. In summer, the sun angle is higher, hence the light level close to the window is high and has a significant drop when passing through the central area of the classroom. The table surfaces close to the window appear to be reflecting substantial amounts of light and potentially cause discomfort glare. Melanopic light levels under 5500K and 25000K CCT have very similar distribution, but the window and the floor, under 25000 CCT, emit and reflect slightly more melanopic light to the human eye. In winter, the sun angle is lower, hence more photopic light concentrates on the window. All table surfaces have higher luminance reading, implying a more serious glare potential. When compared to summer, the false color mapping on the ceiling area suggests a more even and slightly less intensive lit environment. The melanopic stimulus reflected by the floor behaves reciprocal to the summer situation, with a significant drop when approaching the east wall due to the sun angle in the winter morning.

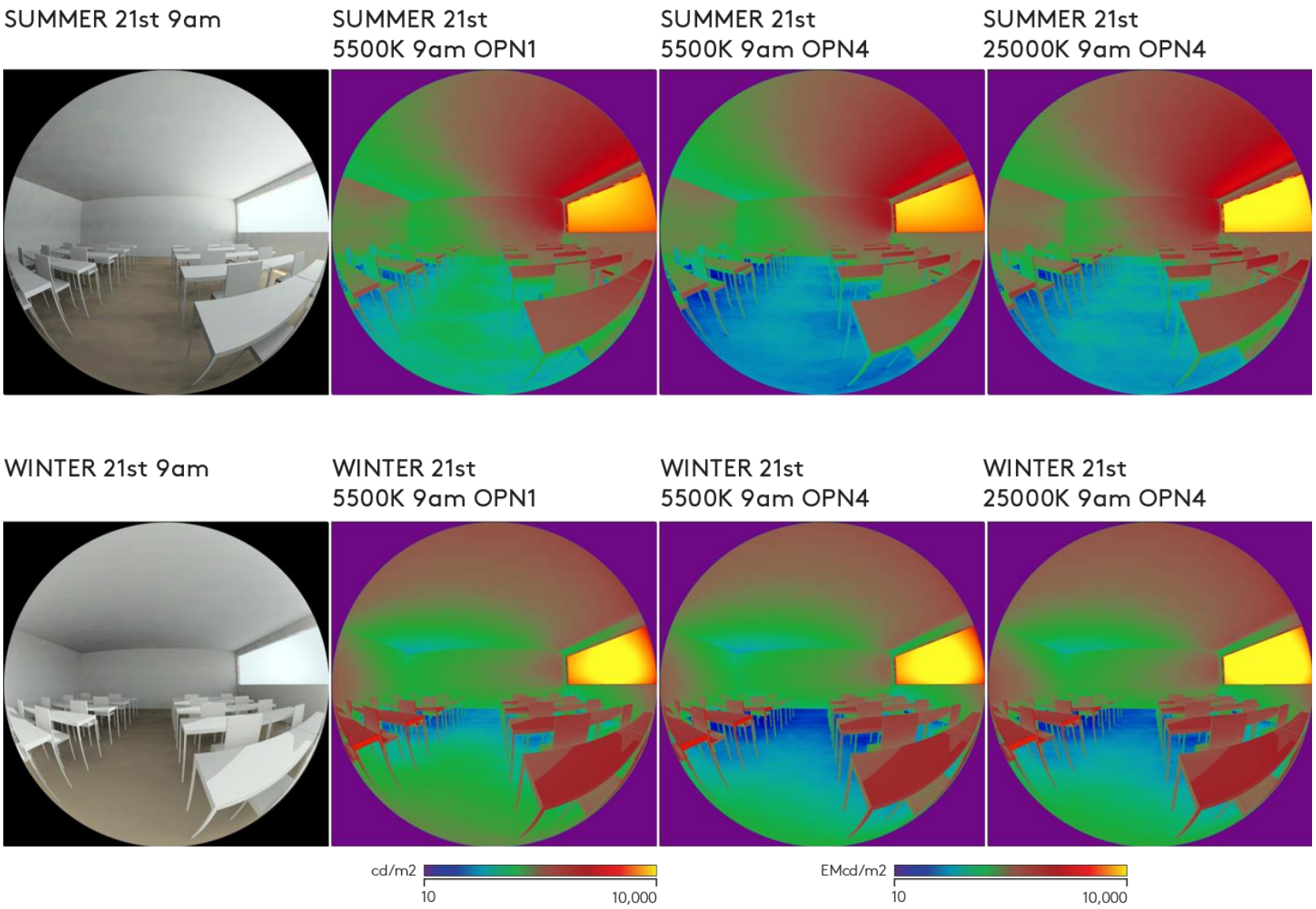

Fig.4.9: HDR image simulations on summer and winter solstice

4.2. — Typical Shade Fabric (Typ.SF) with 1%, 3%, 5%, 10% OF

According to the industry typical shade product, there are 4 common levels of openness factors: 1%, 3%, 5%, and 10%. Using SheerWeave® 2360 (Fig.3.3) as an example, a light simulation is performed to find out the ideal openness factor (OF) for further investigation. Fig.4.10 to Fig.4.13 display the glare-circadian balance condition of the classroom under CCT 6500K on summer solstice and winter solstice, with Typ.SFs OF of 1%, 3%, 5%, and 10% deployed, respectively.

After deploying Typ.SF 1% OF in summer, 6.82% of the classroom area has ideal photopic illuminance; 0% of the area has glare issue; 93.18% of the area has underlit problems with photopic illuminance under 300 lx; 7.58% of the area has enough melanopic illuminance and none of those area have melanopic light higher 1100 EML; 92.42% of the area has under-entrainment problem. Overall, 6.82% of the area presents an ideal lighting balance; 0.76% of the area is dim; and 92.42% of the area is underlit. In winter, 13.64% of the classroom area has both ideal photopic and melanopic stimulus; 0% of the area has glare issues; and 86.36% of the area has underlit problems based on both ideal photopic and melanopic illuminance. Overall, only the location near the window with view orientation gazing toward the window appears to have ideal visual comfort and circadian entertainment. It shows Typ.SF with 1% OF can effectively filter most photopic illuminance but would require a substantial amount of lighting compensation from electric light for lack of photopic illuminance and melanopic stimulus.

After deploying Typ.SF 3% OF in summer, 13.26% of the classroom area has ideal photopic illuminance; 0% of the area has glare issues; and 86.74% of the area has underlit problems with photopic illuminance under 300 lx; 14.02% of the area has enough melanopic illuminance and none of those area have melanopic light higher 1100 EML; 85.98% of the area

has under-entrainment problem. Overall, 13.26% of the area presents an ideal lighting balance; 0.57% of the area is dim; and 86.17% is underlit. In winter, 13.64% of the classroom area has ideal photopic illuminance; 0% of the area has glare issues; and 86.36% of the area has underlit problems with photopic illuminance under 300 lx; 18.37% of the area has ideal melanopic illuminance; 4.92% of it has melanopic light higher 1100 EML; 81.63% of the area has under-entrainment problem. Overall, 13.64% of the area presents an ideal lighting balance; 4.73% of the area is dim; and 81.63% is underlit. It shows that using Typ.SF with 3% OF performs slightly better than 1% OF but would also require a substantial amount of lighting compensation from electric light for lack of photopic illuminance and melanopic stimulus.

After deploying Typ.SF 5% OF in summer, 18.94% of the classroom area has ideal photopic illuminance; 0% of the area has glare issues; and 81.06% of the area has underlit problems with photopic illuminance under 300 lx; 19.88% of the area has enough melanopic illuminance; 2.27% of it has melanopic light higher than 1100 EML; 80.11% of the area has under-entrainment problem. Overall, 18.94 of the area presents an ideal lighting balance; 0.95% of the area is dim; and 80.11% is underlit. In winter, 23.86% of the classroom area has ideal photopic illuminance; 0% of the area has glare issues; and 76.14% of the area has underlit problems with photopic illuminance under 300 lx; 27.09% of the area has ideal melanopic illuminance; 13.64% of it has melanopic light higher 1100 EML; 72.92% of the area has under-entrainment problem. Overall, 23.86% of the area presents an ideal lighting balance; 3.22% of the area is dim; and 72.92% is underlit. It shows that using Typ.SF with 5% OF performs better than 1% OF and 3% OF but would also require a substantial amount of lighting compensation 75+% to 80+% of the area.

After deploying Typ.SF 10% OF in summer, 27.46% of the classroom area has ideal photopic illuminance; 0% of the area has glare issues; and 72.56% of the area has underlit problems with photopic illuminance under 300 lx; 30.68% of the area has enough melanopic illuminance; 3.79% of it has melanopic light higher than 1100 EML; 69.32% of the area has under-entrainment problem. Overall, 27.46 of the area presents an ideal lighting balance; 3.22% of the area is dim; and 69.32% is underlit. In winter, 33.14% of the classroom area has ideal photopic illuminance; 7.2% of the area has glare issues; and 59.66% of the area has underlit problems with photopic illuminance under 300 lx; 42.24% of the area has ideal melanopic illuminance; 13.64% of it has melanopic light higher 1100 EML; 57.77% of the area has under-entrainment problem. Overall, 33.14% of the area presents an ideal lighting balance; 7.2% of the area has glare issues; 1.7% of the area is dim; and 57.95% is underlit. It shows that using Typ.SF with 10% OF performs the best among all OF. It is effective in preventing discomfort glare for at least half the year but it is also the only option that has remaining glare problems just slightly above 2657 lx for location near the window with view orientation gazing toward the window.

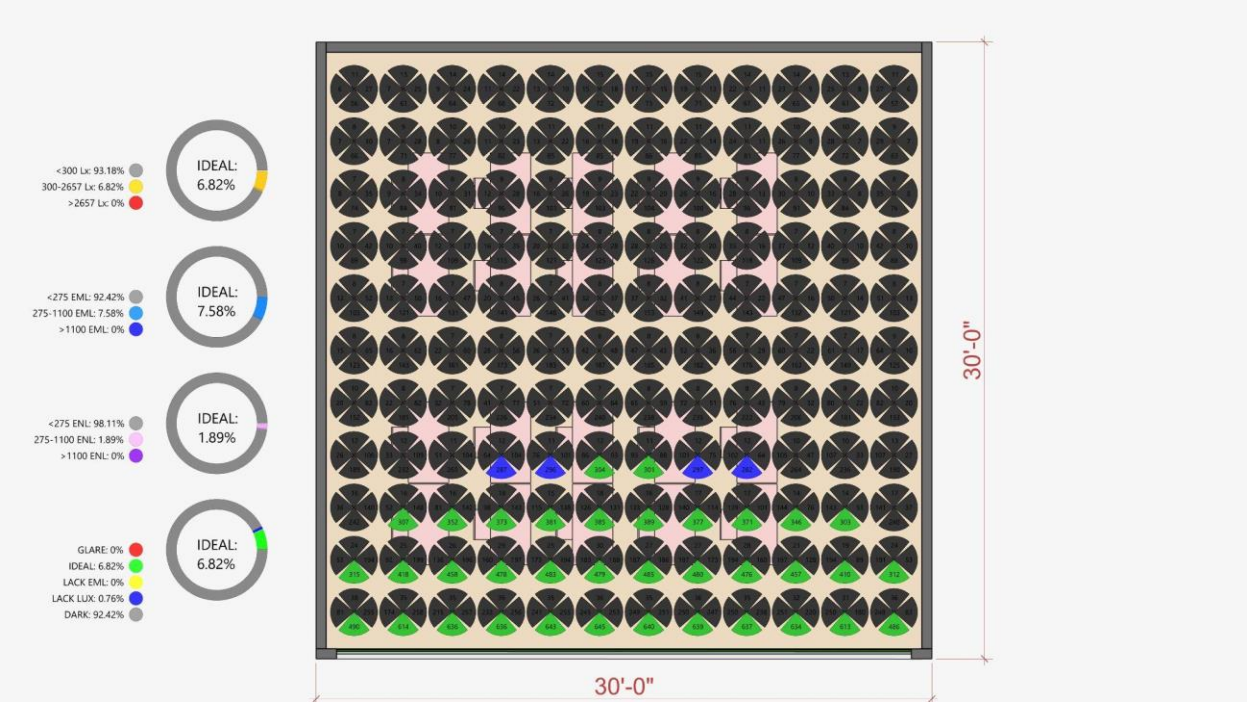

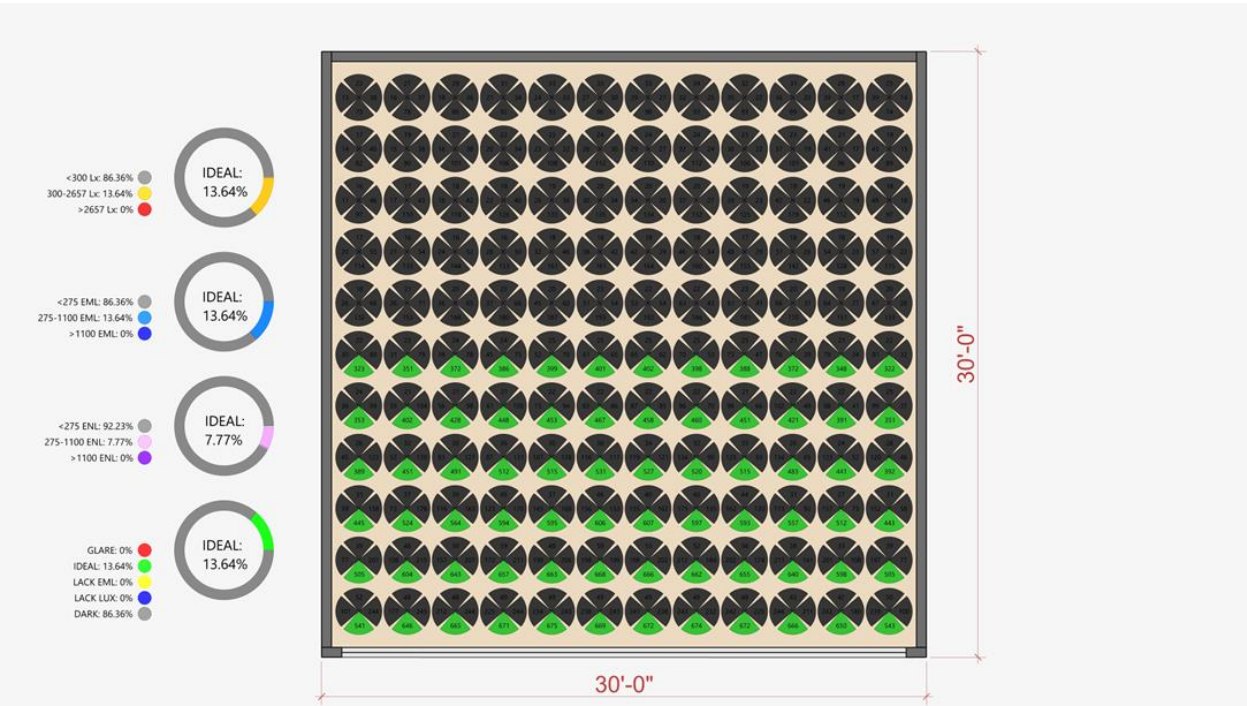

		EML	
		<275	>275
LUX	>2657	GLARE	
	Enough	FAIR	IDEAL
	< 300	UNDERLIT	DIM

Fig.4.10: Glare-Circadian Balance with Typ.SF 1% OF on summer solstice and winter solstice

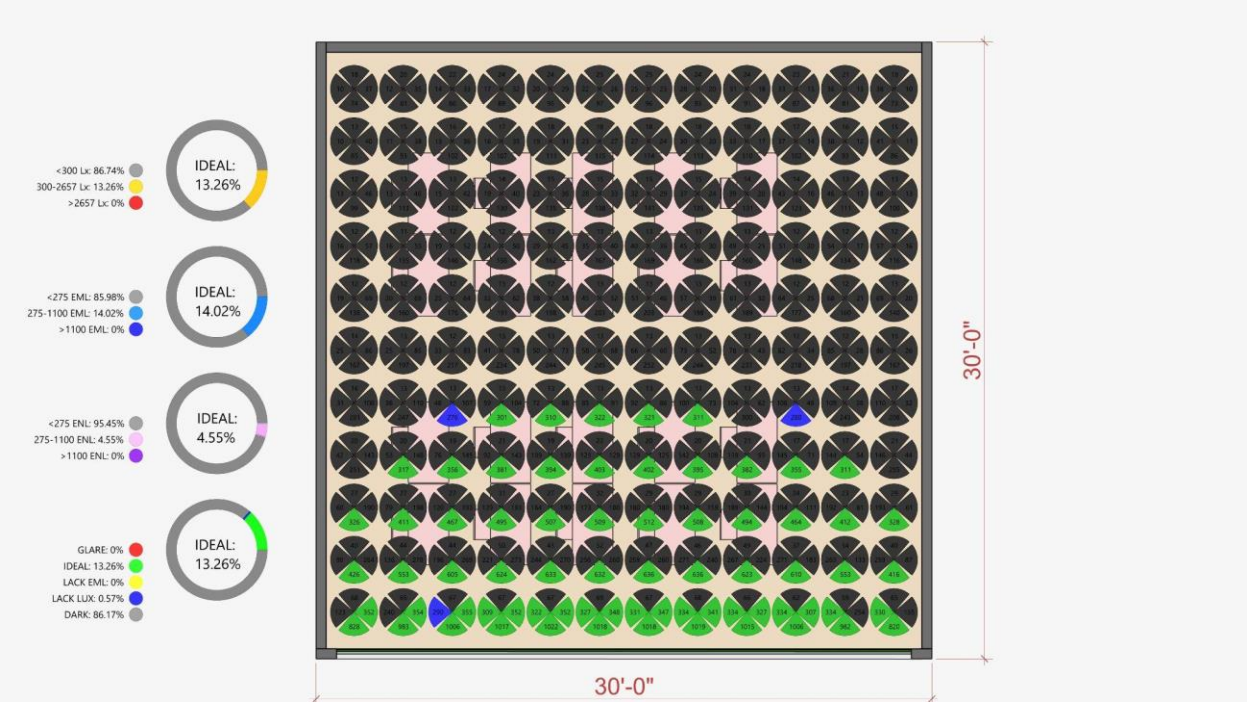

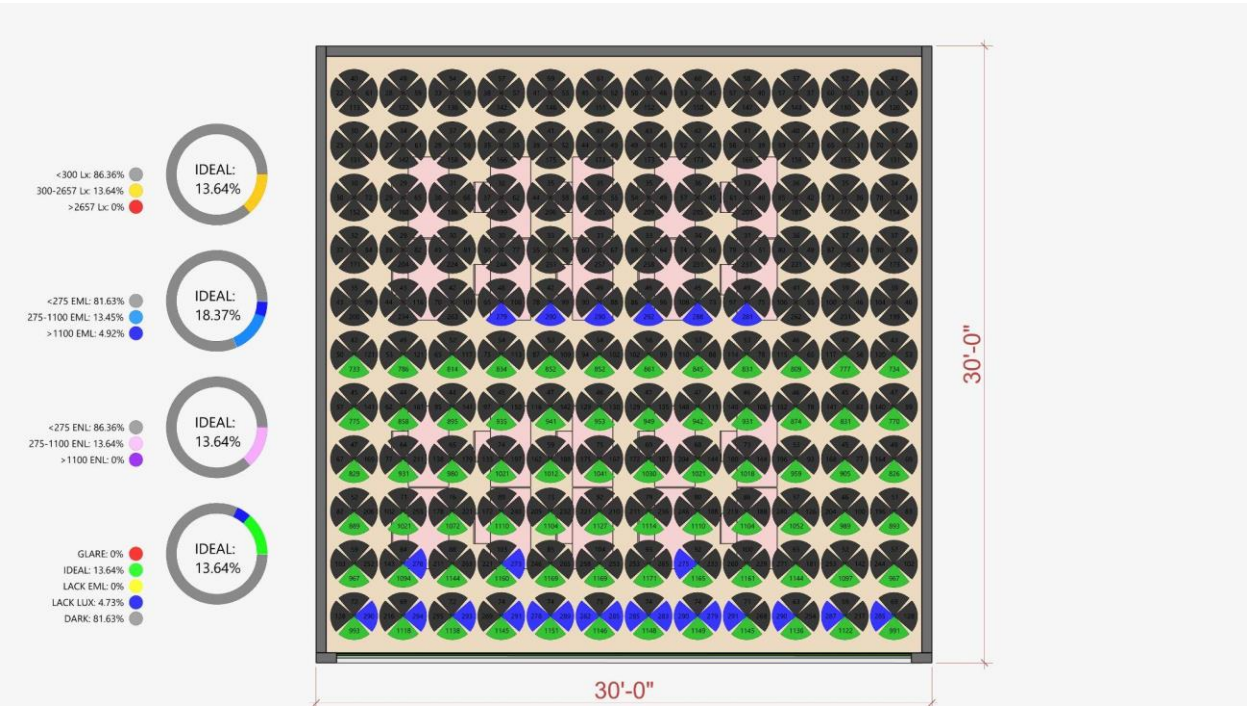

LUX	EML <275	EML >275
>2657	GLARE	
Enough	FAIR	IDEAL
< 300	UNDERLIT	DIM

Fig.4.11: Glare-Circadian Balance with Typ.SF 3% OF on Summer solstice and winter solstice

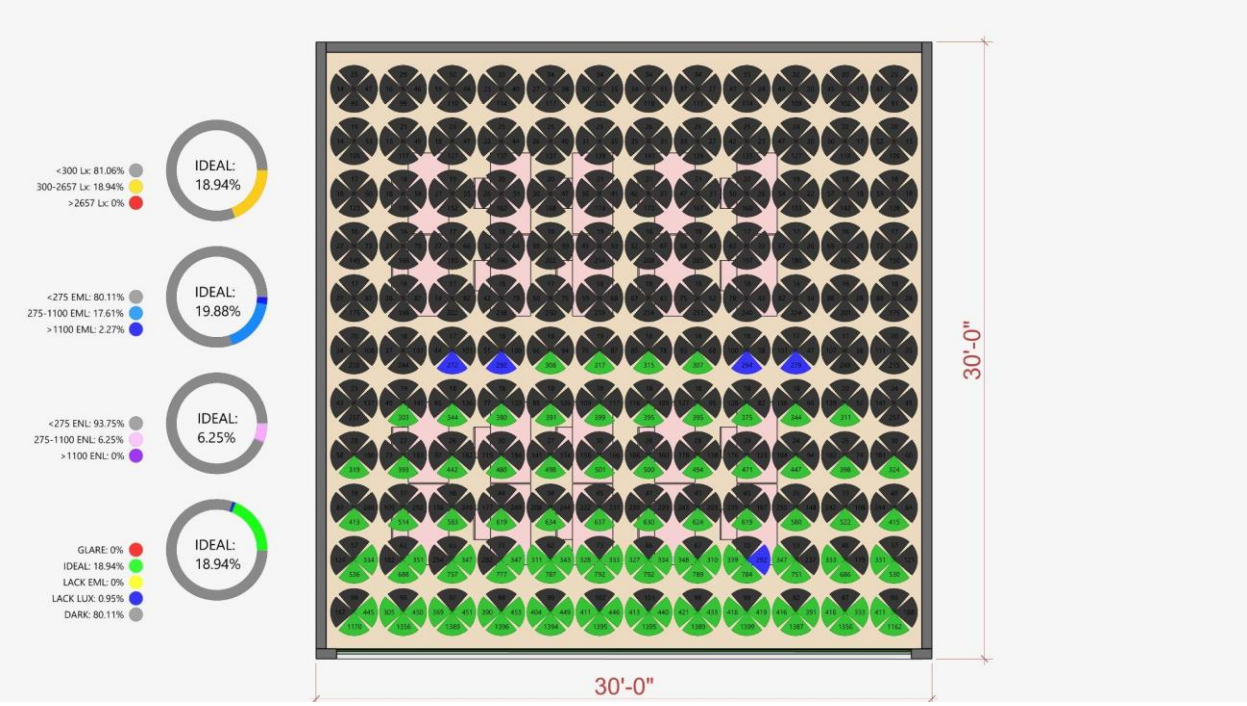

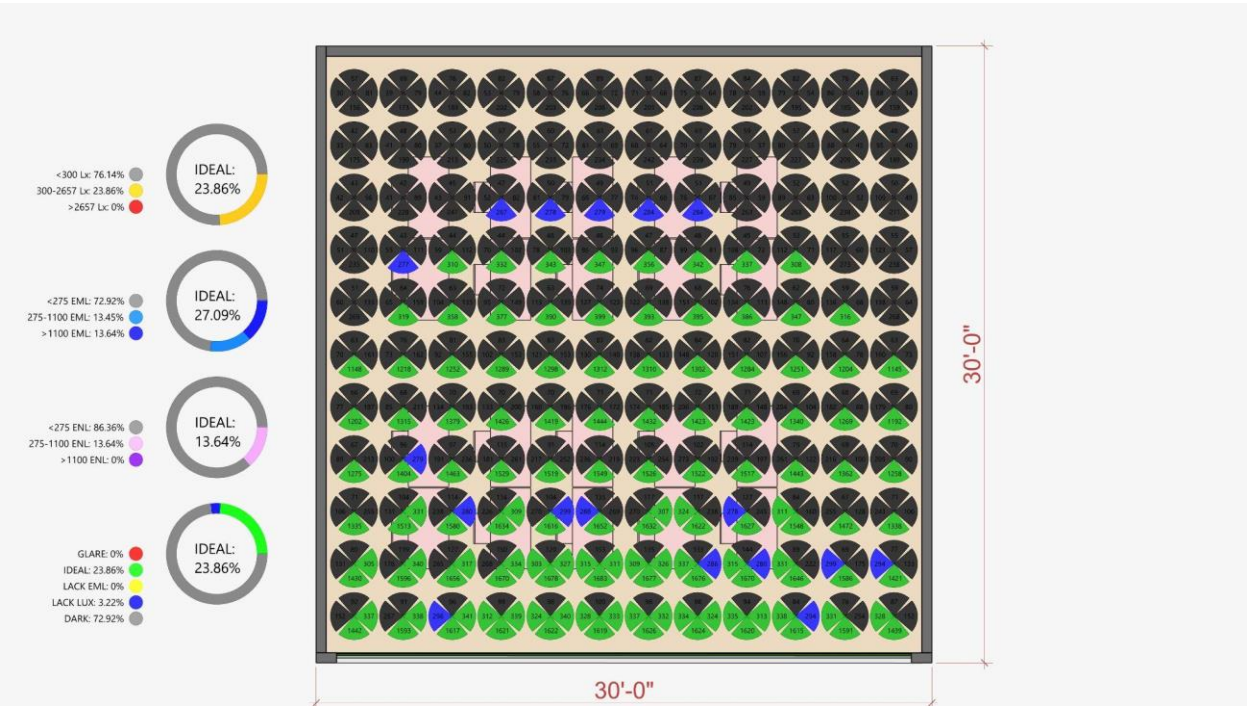

LUX	EML <275	EML >275
>2657	GLARE	
Enough	FAIR	IDEAL
< 300	UNDERLIT	DIM

Fig.4.12: Glare-Circadian Balance with Typ.SF 5% OF on Summer solstice and winter solstice

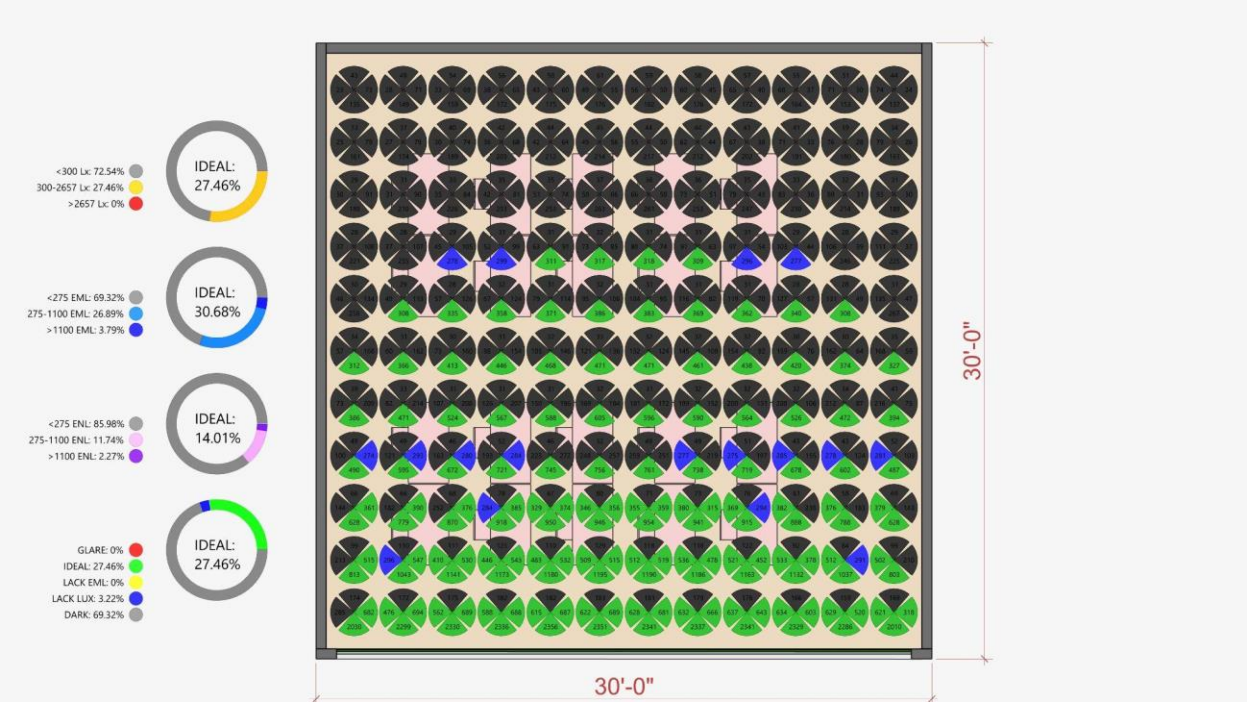

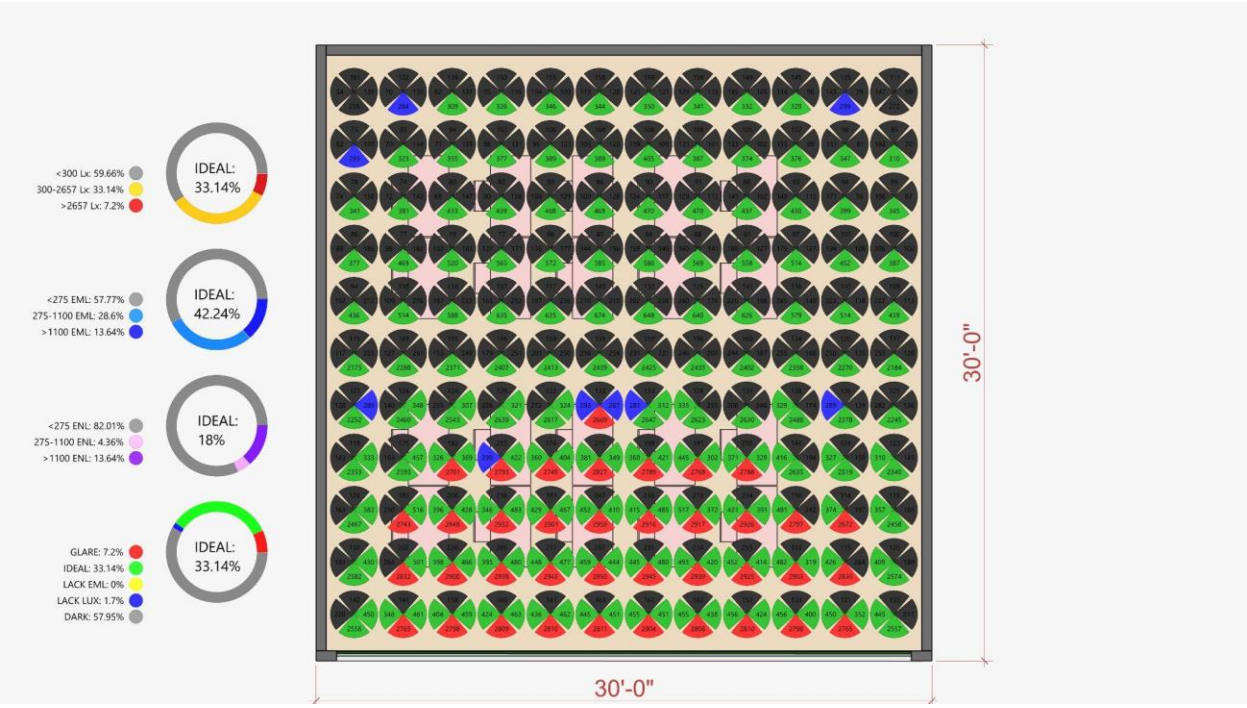

		EML	
		<275	>275
LUX	>2657	GLARE	
	Enough	FAIR	IDEAL
	< 300	UNDERLIT	DIM

Fig.4.13: Glare-Circadian Balance with Typ.SF 10% OF on Summer solstice and winter solstice

Figures 4.14 and 4.15 illustrate the photopic and melanopic light penetration for the view gazing toward the window under CCT sky conditions ranging from 5500 K to 25000 K. The OF value of SF is crucial in controlling light penetration. Lower OF values are highly effective but significantly reduce photopic illuminance, potentially causing underlit conditions approximately 10 feet away from the window. From the glare-circadian balance graphs, only south-oriented views show a tangible difference in results. Therefore, the light penetration graphs will focus on comparing how different OF values affect photopic illuminance at various depths for views gazing toward the window.

In summer, both photopic and melanopic illuminance diminish progressively with increasing depth from the window. The 10% openness factor (OF) provides the best visual comfort among the options, though it can still cause underlit conditions in deeper spaces. This OF maintains an ideal balance up to about 20 feet, where "dim" lighting conditions emerge. Between approximately 22 to 25 feet, melanopic illuminance falls below 275 EML, resulting in underlit conditions depending on the sky's CCT. The 1% OF performs the worst, maintaining an ideal balance only up to about 10 feet. In winter, all OF options exhibit a significant drop in daylight illuminance beyond 15 feet from the window. The 10% OF effectively suppresses photopic illumination but still has glare issues, with levels just above the threshold, ranging from 2669 lx to just under 3000 lx as shown in Figure 4.13. However, it is the only option that retains melanopic stimulus throughout the entire classroom, ensuring circadian entrainment. The second-best option, the 5% OF, fully mitigates glare and maintains good light penetration up to about 20 feet from the window, potentially providing melanopic stimulus to the entire classroom under high CCT.

Overall, photopic and melanopic illuminance are generally higher in winter under sunny conditions, with a more gradual decline until a sudden drop beyond 15 feet. After comparing all OF values, the typical shade fabric (Typ.SF) with a 10% OF appears to require the least supplemental lighting from electric sources. This option also offers promising opportunities for color explorations.

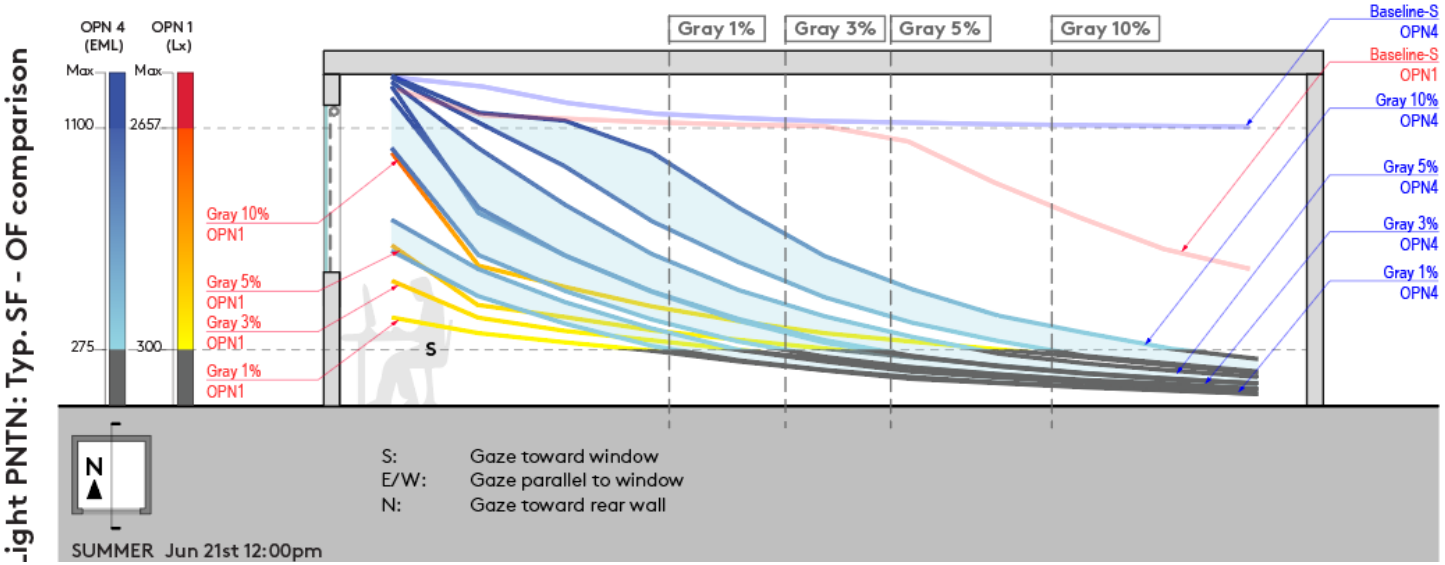

Fig 4.14: Photopic and melanopic light penetration with Typ.SF (1%, 3%, 5%, 10%) on summer solstice

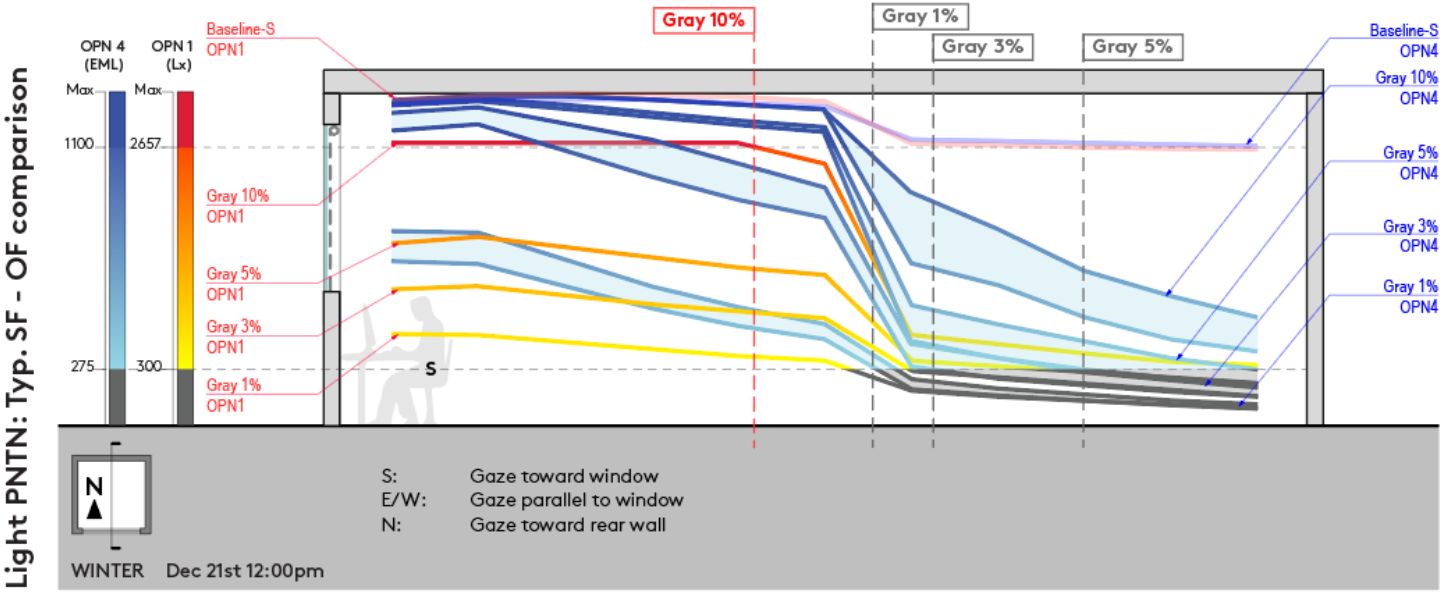

Fig 4.15: Photopic and melanopic light penetration with Typ.SF (1%, 3%, 5%, 10%) on winter solstice

Figures 4.17 and 4.18 display the HDR image simulations for different OF values on the summer solstice and winter solstice. They indicate that the baseline condition without shading results in very high photopic and melanopic luminance levels near the window. The false color mapping shows bright yellow and brown regions, indicating luminance levels up to 10,000 cd/m² and EMcd/m², respectively. This high intensity can cause significant glare and visual discomfort.

In summer, introducing the Typ.SF with a 10% OF reduces these luminance levels significantly. The reduction brings photopic luminance into a more manageable range, predominantly in blue and green shades as luminance well below the 10,000 cd/m². Similarly, melanopic luminance also sees a substantial decrease. However, this reduction does not eliminate all high-intensity spots, maintaining some bright areas near the window, which suggests a balance between reducing glare and retaining adequate light levels.

In winter, the baseline condition shows lower photopic and melanopic luminance levels compared to summer but still with a noticeable gradient (regions in yellow and red tones) from the window to the back of the room. With the 10% OF, the reduction in luminance levels is less pronounced than in summer. The photopic luminance is distributed more evenly, with cooler shades indicating lower but still adequate light levels. Melanopic luminance follows a similar trend, showing a reduction that avoids excessive intensity while maintaining enough light to support visual and circadian needs.

Overall, it is evident that the Typ. SF with 10% OF significantly reduces both photopic and melanopic luminance levels. This reduction is beneficial for minimizing glare and ensuring visual comfort, particularly near the window where the highest luminance levels occur. However, both summer and winter simulations show an increase in purple regions at the rear of the classroom, suggesting a potential risk of underlit conditions under lower sky CCT.

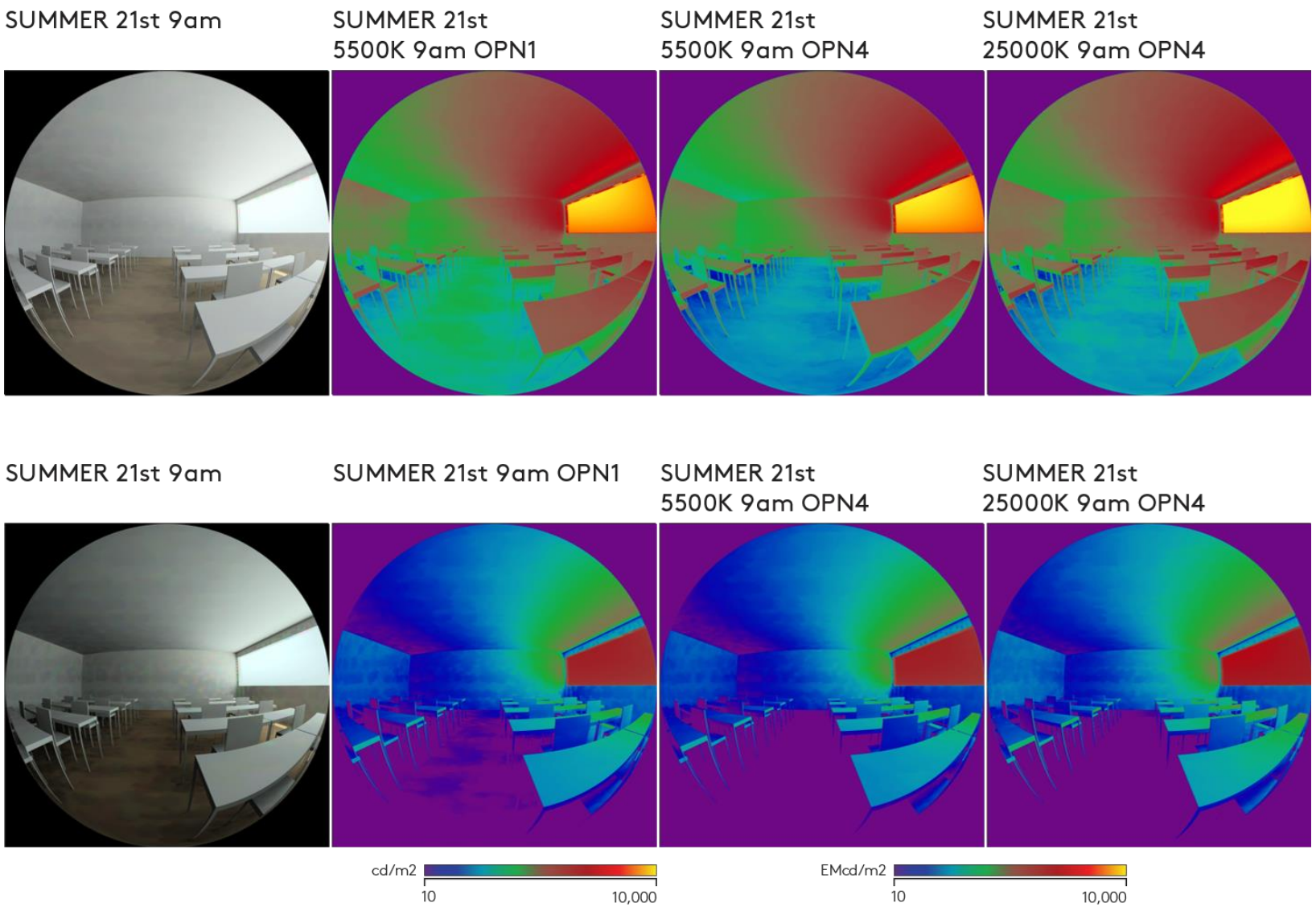

Fig.4.17: HDR image simulation comparing baseline (top row) and Typ.SF 10% OF (bottom row) on summer solstice

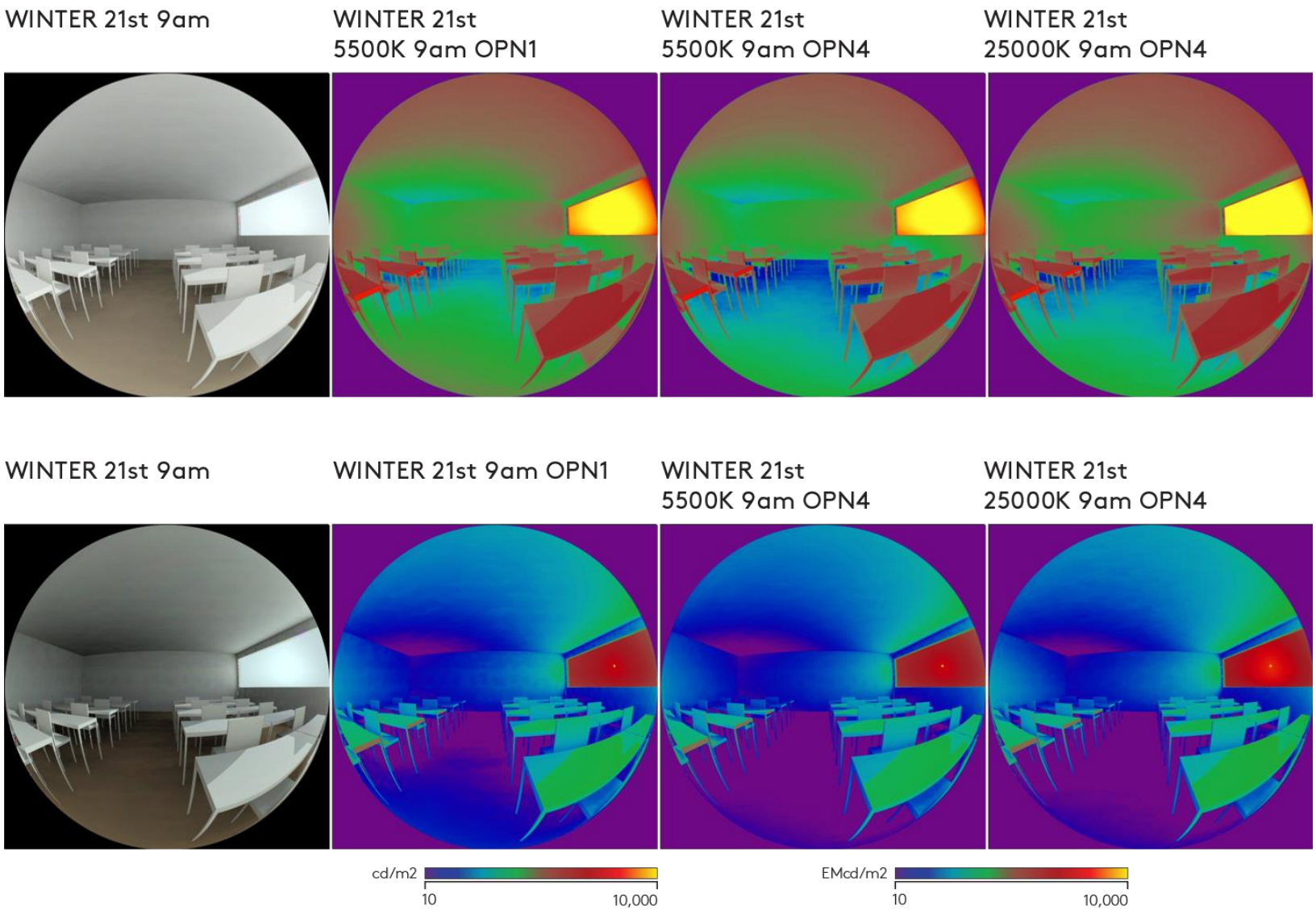

Fig.4.18: HDR image simulation comparing baseline (top row) and Typ.SF 10% OF (bottom row) on winter solstice

4.3. — Typ.SF and SSF

As Typ.SF 10% OF perform the best among all other OF options, this study has adjusted the color transmittances of the material, via BRTDfunc description, according to the photopic and melanopic sensitivities of the human eye. In short, three Spectrally-selective Shade Fabrics (SSFs) are created for three different colors: “SSF(Blue)” with reconfigured B-G-R ratio as “1:0.55:0.1”; “SSF(Purple)” with reconfigured B-G-R ratio as “1:0.3:1”; and “SSF(Orange)” with reconfigured B-G-R ratio as “0.1:0.5:0.9”.

After deploying SSF(Blue) in summer, 27.65% of the classroom area has ideal photopic illuminance; 0% of the area has glare issues; 72.35% of the area has underlit problems with photopic illuminance under 300 lx; 41.1% of the area has ideal melanopic illuminance; 7.58% of it has melanopic light higher 1100 EML; 69.32% of the area has under-entrainment problem. Overall, 27.46% of the area presents an ideal lighting balance; 3.22% of the area is dim; and 69.32% of the area is underlit. In winter, 32.77% of the classroom area has ideal photopic illuminance; 8.33% of the area has glare issues; and 58.9% of the area has underlit problems with photopic illuminance under 300 lx; 57.01% of the area has ideal melanopic illuminance; 14.02% of it has melanopic light higher 1100 EML; 42.99% of the area has under-entrainment problem. Overall, 33.14% of the area presents an ideal lighting balance; 8.33% of the area has glare issues; 15.91% of the area is dim; and 42.99% of the area is underlit (Fig.4.19).

After deploying SSF(Purple) in summer, 25.95% of the classroom area has ideal photopic illuminance; 0% of the area has glare issues; 74.05% of the area has underlit problems with photopic illuminance under 300 lx; 34.85% of the area has ideal melanopic illuminance; 5.3% of it has melanopic light higher 1100 EML; 65.15% of the area has under-entrainment problem. Overall, 25.95% of the area presents an ideal lighting balance; 8.71% of the area is dim; and

65.34% of the area is underlit. In winter, 36.36% of the classroom area has ideal photopic illuminance; 2.65% of the area has glare issues; and 60.99% of the area has underlit problems with photopic illuminance under 300 lx; 48.49% of the area has ideal melanopic illuminance; 13.64% of it has melanopic light higher 1100 EML; 51.51% of the area has under-entrainment problem. Overall, 36.36% of the area presents an ideal lighting balance; 8.33% of the area has glare issues; 2.65% of the area is dim; and 42.99% of the area is underlit (Fig.4.20).

After deploying SSF(Orange) in summer, 27.27% of the classroom area has ideal photopic illuminance; 0% of the area has glare issues; 72.73% of the area has underlit problems with photopic illuminance under 300 lx; 19.31% of the area has ideal melanopic illuminance; 1.89% of it has melanopic light higher 1100 EML; 80.69% of the area has under-entrainment problem. Overall, 19.32% of the area presents an ideal lighting balance; 7.95% of the area has enough photopic light but lacks melanopic illuminance; and 72.73% of the area is underlit. In winter, 33.71% of the classroom area has ideal photopic illuminance; 6.82% of the area has glare issues; and 59.47% of the area has underlit problems with photopic illuminance under 300 lx; 24.81% of the area has ideal melanopic illuminance; 12.5% of it has melanopic light higher 1100 EML; 75.19% of the area has under-entrainment problem. Overall, 17.99% of the area presents an ideal lighting balance; 6.82% of the area has glare issues; 15.72% of the area has enough photopic light but lacks melanopic illuminance; and 42.99% of the area is underlit(Fig.4.21).

After comparing the performance between Typ.SF 10% OF and SSFs, it shows that, under the same photopic illuminance, color adjustment based on photopic and melanopic sensitivities of the human eye can improve the overall lighting condition by enhancing melanopic illumination through the space. While SSF(Purple) appears to mitigate more glare and hence achieves a slighting better glare-circadian balance effect, SSF(Blue), particularly, can

improve the circadian lighting condition by about 10% in summer, and 15% in winter, showing the enhancement effect is more prominent in winter. SSF(Orange), on the other hand, has a similar shading effect compared to Typ.SF but suppresses more melanopic illuminance with about -11% in summer, and -17% in winter.

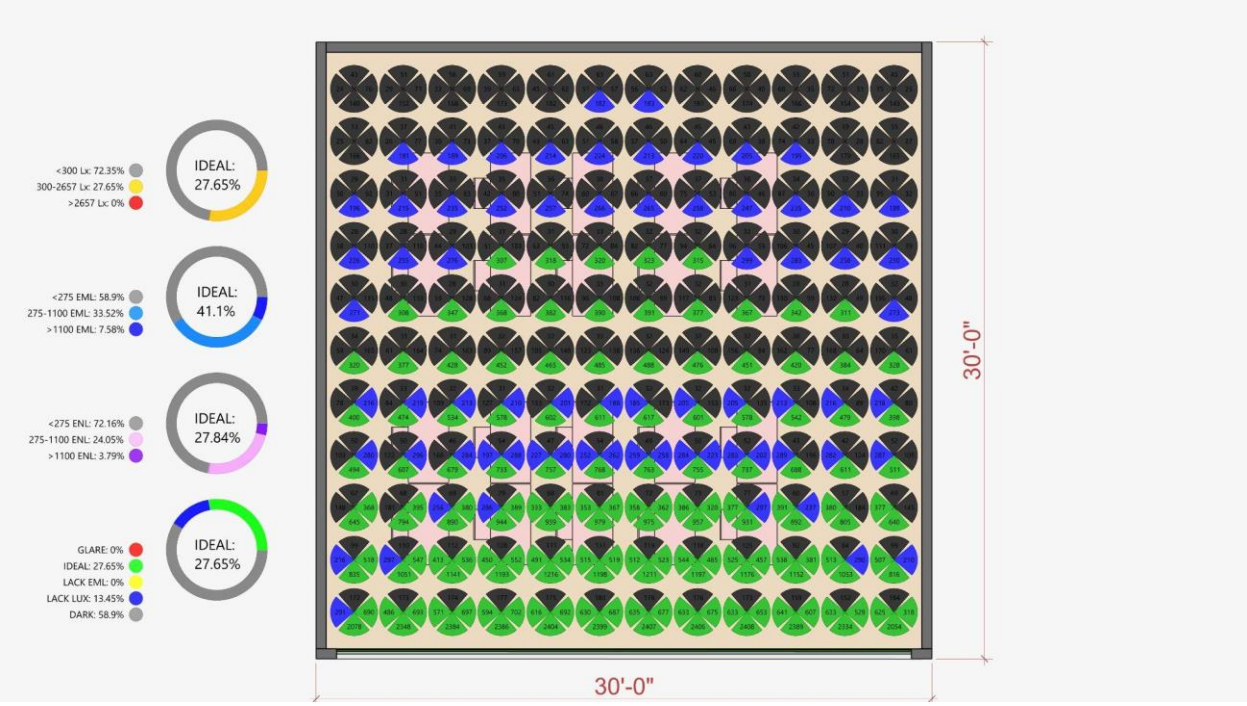

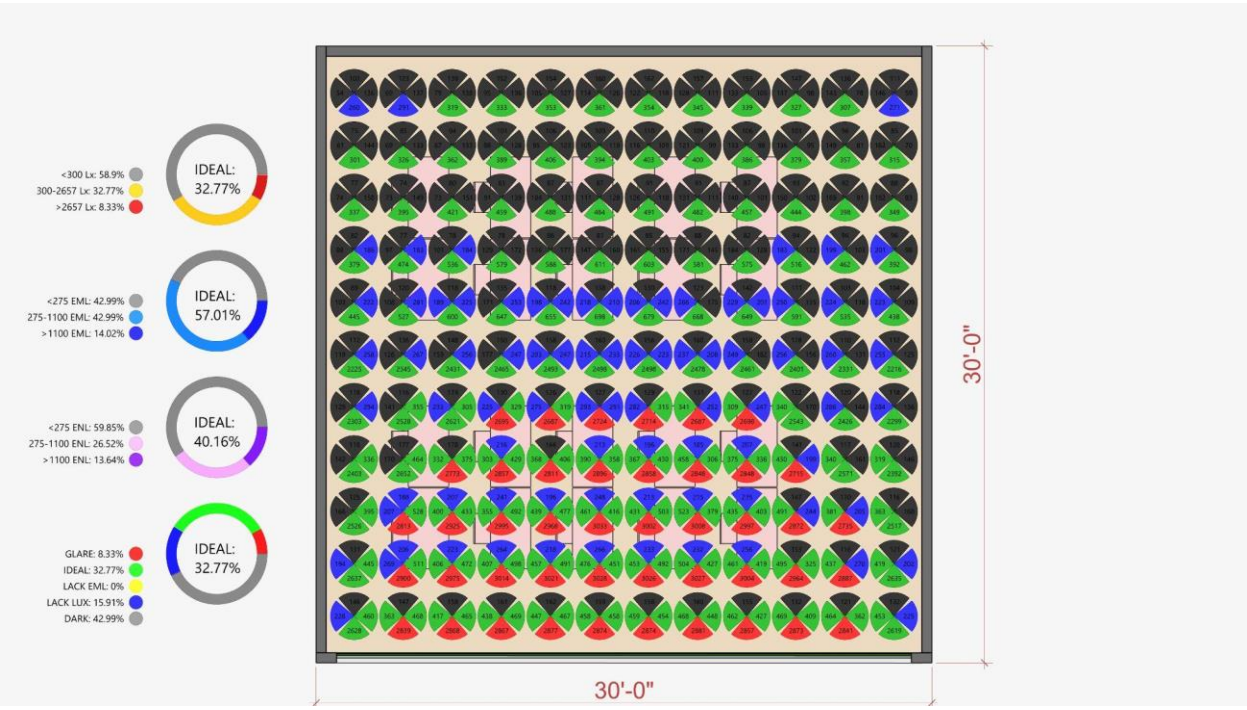

		EML	
		<275	>275
LUX	>2657	GLARE	
	Enough	FAIR	IDEAL
	< 300	UNDERLIT	DIM

Fig.4.19: Glare-Circadian Balance with SSF(Blue) on Summer solstice and winter solstice

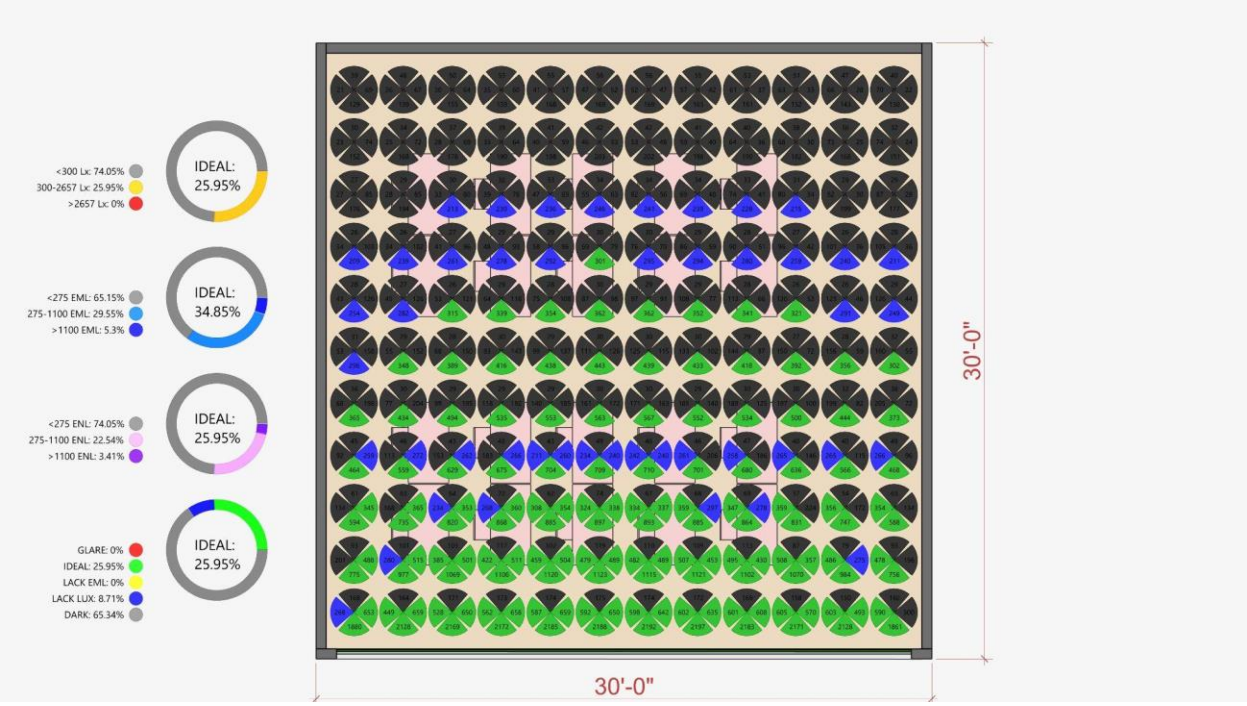

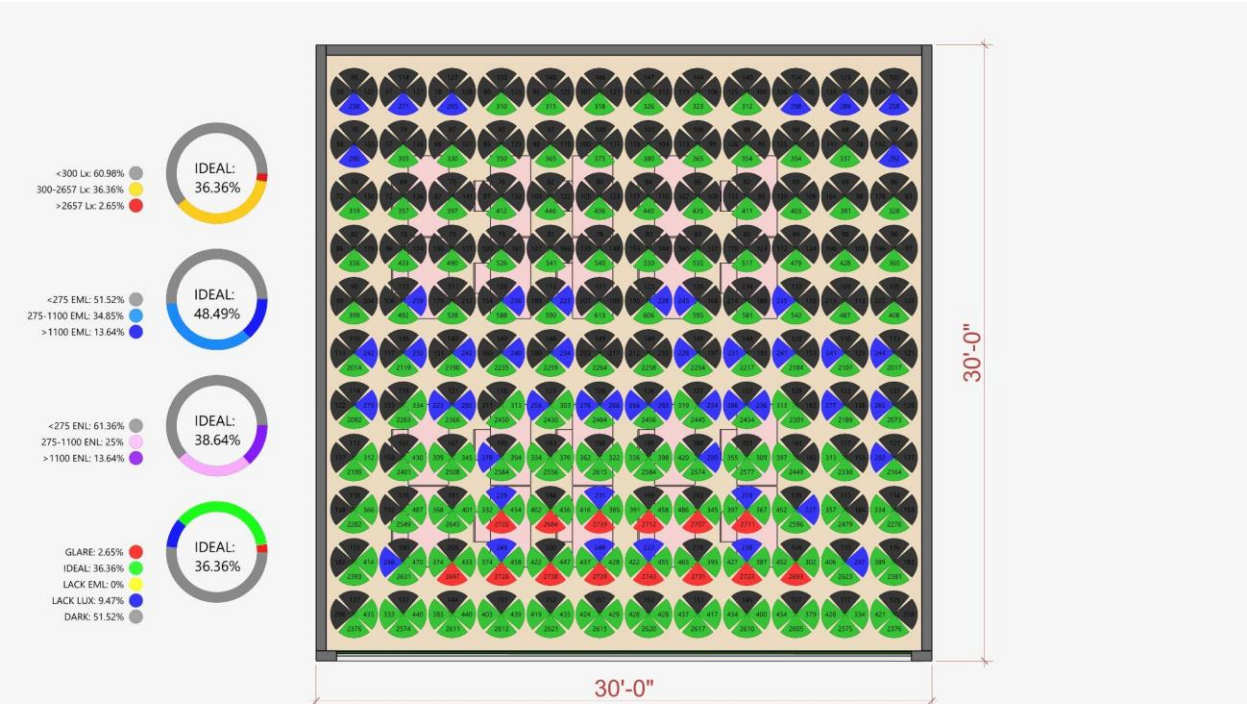

LUX	EML <275	EML >275
>2657	GLARE	
Enough	FAIR	IDEAL
< 300	UNDERLIT	DIM

Fig.4.20: Glare-Circadian Balance with SSF(Purple) on Summer solstice and winter solstice

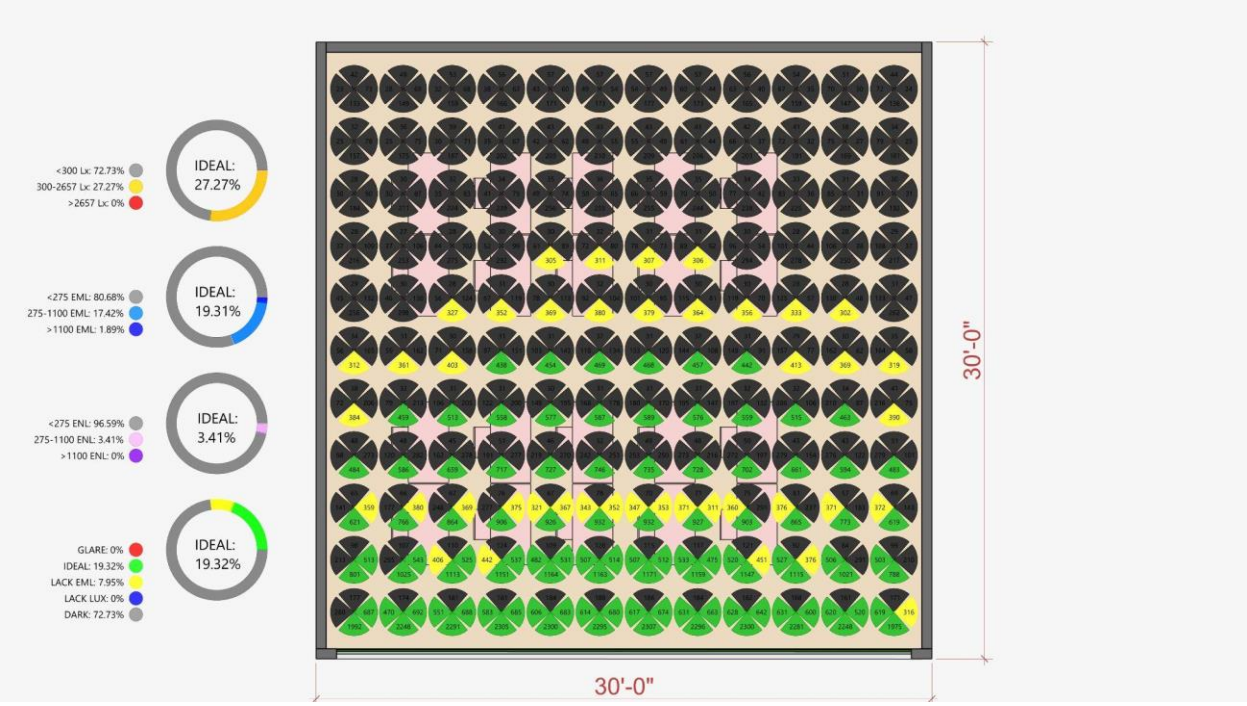

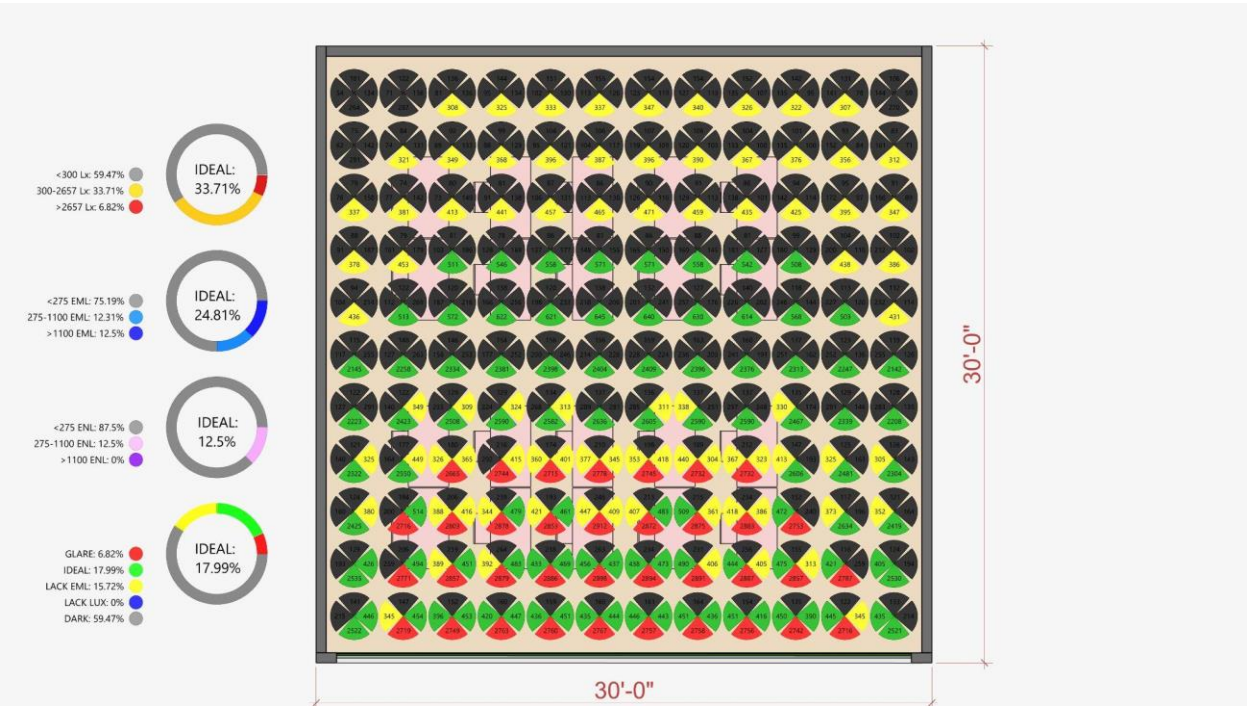

LUX	EML <275	EML >275
>2657	GLARE	
Enough	FAIR	IDEAL
< 300	UNDERLIT	DIM

Fig.4.21: Glare-Circadian Balance with SSF(Orange) on Summer solstice and winter solstice

Figures 4.22 and 4.23 illustrate the photopic and melanopic light penetration for the view gazing toward the window under CCT sky conditions ranging from 5500 K to 25000 K.

In summer, both photopic and melanopic illuminance diminish progressively with increasing depth from the window, as expected. While the effectiveness of glare control remains constant, SSF(Blue) appears to perform the best in increasing the melanopic light penetration depth by over at least 10 ft in summer, followed by SSF(Purple) with about 5 ft. SSF(Orange), on the other hand, has decreased the melanopic light penetration by about 10 ft. In winter, there is a significant improvement in reducing the sudden drop of melanopic illuminance per depth. Additionally, SSF(Blue) performs the best in terms of retaining melanopic illuminance above 1100 EML, up to about 23 ft from the window, helping occupants to reach circadian entrainment within 1 hour. SSF(Purple) can also provide a similar effect but not as significantly. SSF(Orange), on the other hand, has decreased melanopic light penetration and introduces an under-entrainment space.

Overall, adjusting the material color shows promising improvement compared to Typ.SF, especially when it comes to smoothing the uneven melanopic light distribution in winter. Based on different circadian needs (such as people who live in high latitude areas with extreme long daytime), color adjustment can also reverse the melanopic impacts to help suppress unnecessary melanopic illuminance in the afternoon, helping occupants to regulate their circadian clock.

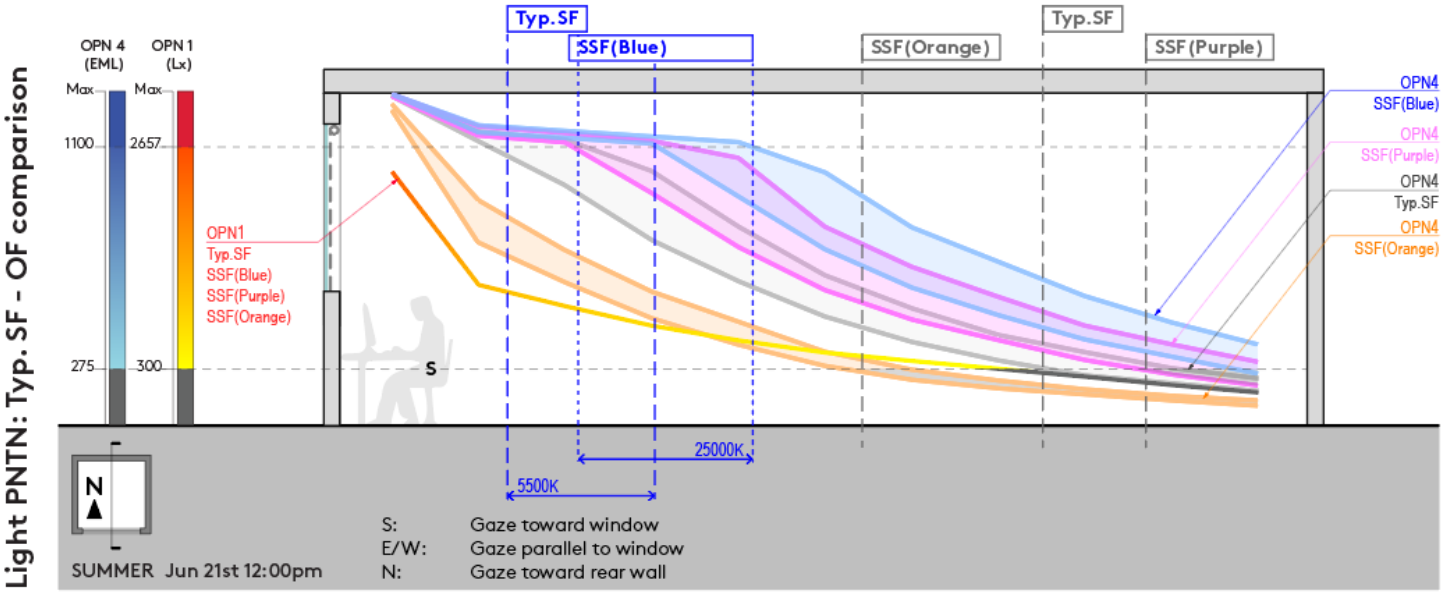

Fig 4.22: Photopic and melanopic light penetration with Typ.SF and SSFs (Blue, Purple, Orange) on summer solstice

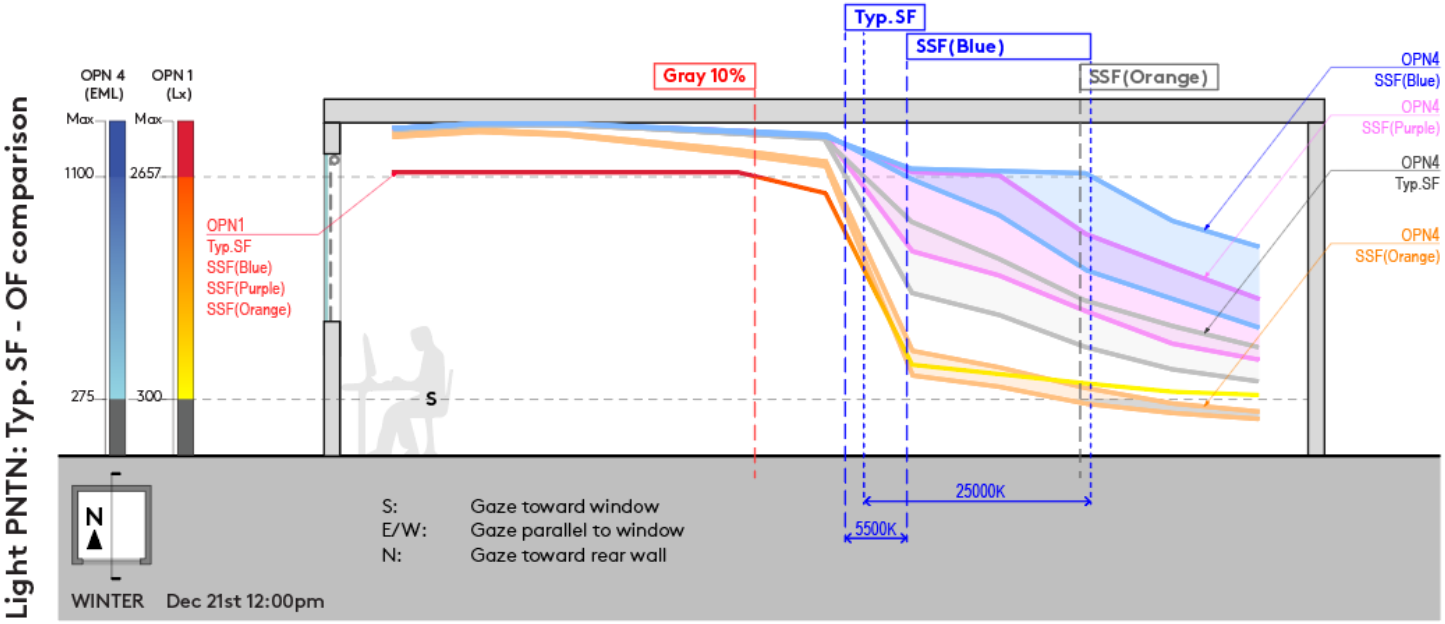

Fig 4.23: Photopic and melanopic light penetration with Typ.SF and SSFs (Blue, Purple, Orange) on winter solstice

Figures 4.24 and 4.25 present HDR image simulations and their false color mapping for various shade fabrics (SSFs) on the summer and winter solstices under 5500K CCT. Despite the perceptual differences between SSFs, the photopic luminance distribution remains consistent across all SF options, as anticipated from the glare-circadian balance and light penetration studies. However, there are notable differences in melanopic luminance distributions between SSFs.

In the summer, introducing the Typ.SF significantly reduces melanopic luminance levels. This reduction leads to under-entrainment issues near the rear wall, with a purple region appearing in the wall corner, indicating insufficient melanopic light. Deploying SSF(Blue) resolves this condition, as evidenced by a larger green region on the ceiling, suggesting a greater area illuminated by additional melanopic light and enhancing the overall distribution. SSF(Purple) also addresses the under-entrainment problem near the rear wall, but its overall melanopic luminance distribution is less significant compared to SSF(Blue). Conversely, SSF(Orange) suppresses melanopic luminance significantly, increasing the purple region and indicating a larger under-entrainment area. This SSF has a reverse effect, reducing the beneficial melanopic light.

In winter, the phenomenon is similar, but the overall changes in melanopic distribution are more even. More melanopic light is captured and reflected by the rear wall, indicating an improved distribution compared to summer. SSF(Blue) shows significant improvement, capturing and reflecting more melanopic light towards the rear wall, and providing a more uniform distribution. SSF(Purple) improves distribution near the rear wall but is less effective than SSF(Blue), with moderate overall enhancement. SSF(Orange) continues to suppress

melanopic luminance, increasing under-entrainment areas, and is less beneficial for maintaining adequate melanopic light.

Overall, SSF(Blue) significantly outperforms other options in retaining melanopic luminance, effectively resolving under-entrainment issues and providing a more uniform distribution of melanopic light. SSF(Purple) offers moderate improvement but is less effective than SSF(Blue). SSF(Orange), on the other hand, has a reverse effect, significantly suppressing melanopic luminance and increasing under-entrainment areas, although it may be useful in specific scenarios where reduced melanopic light is desired. While SSFs introduce different tints (blue, purple, orange), the color constancy of the human visual system enables chromatic adaptation, maintaining consistent color perception under varying lighting conditions. Therefore, the actual visual sensation may not be as prominent as depicted in HDR simulations. The analysis highlights the importance of selecting appropriate SSFs based on specific lighting and circadian requirements, with SSF(Blue) being the preferred option for maintaining circadian health.

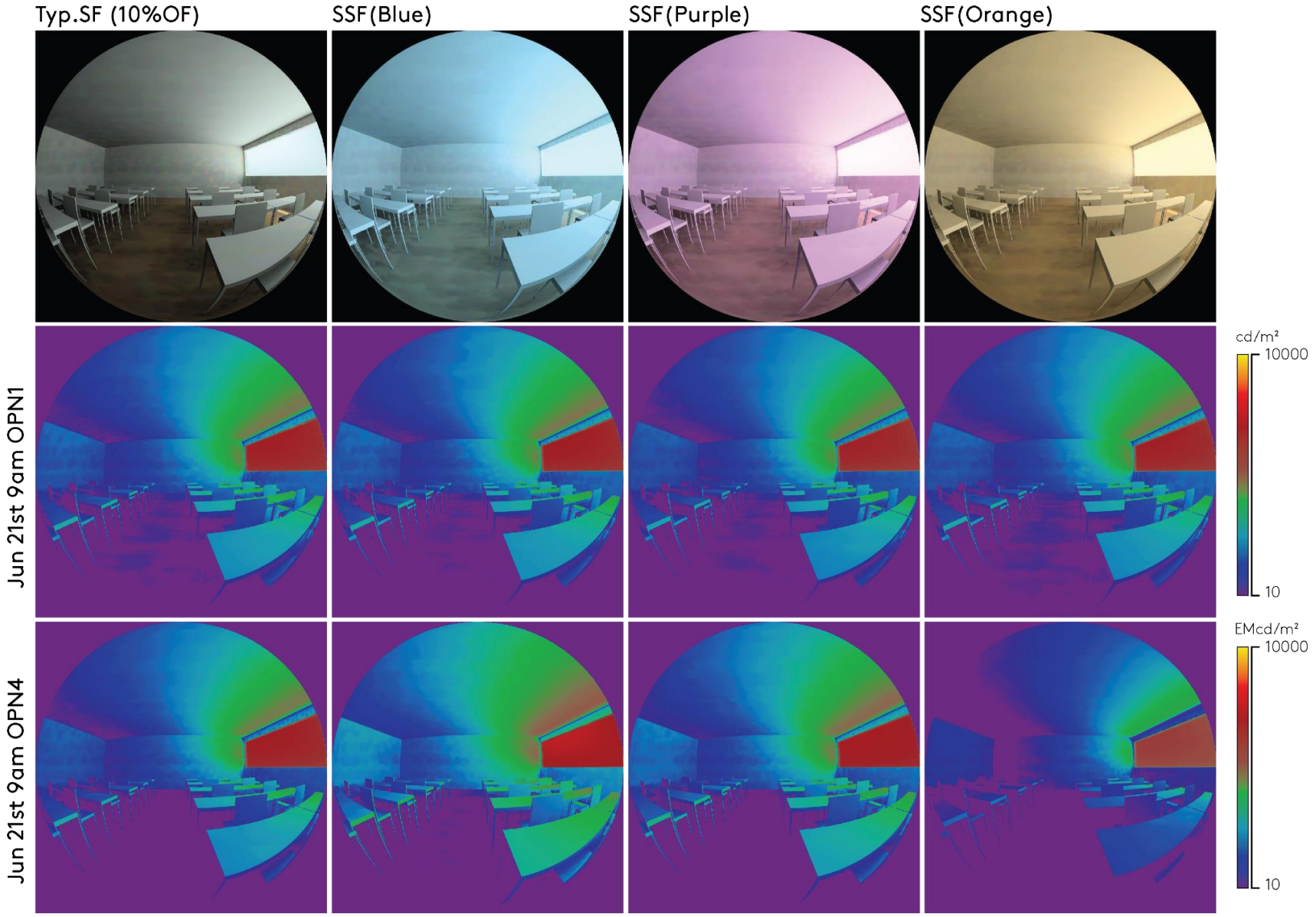

Fig.4.24: HDR image simulations of SSFs on summer solstice under 5500K CCT

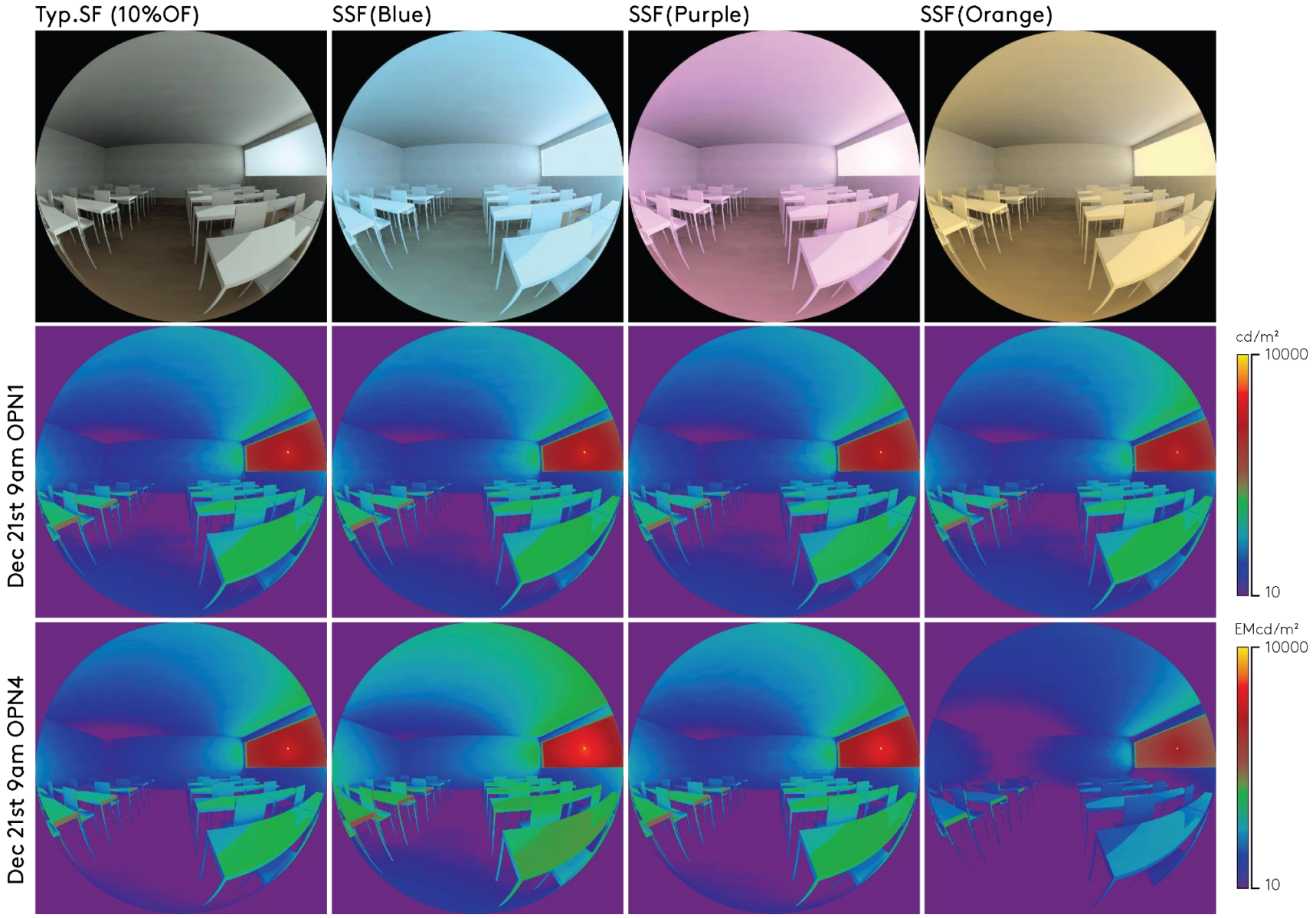

Fig.4.25: HDR image simulations of SSFs on winter solstice under 5500K CCT

4.4. — Shade Fabrics (SF) and Venetian Blinds (VB)

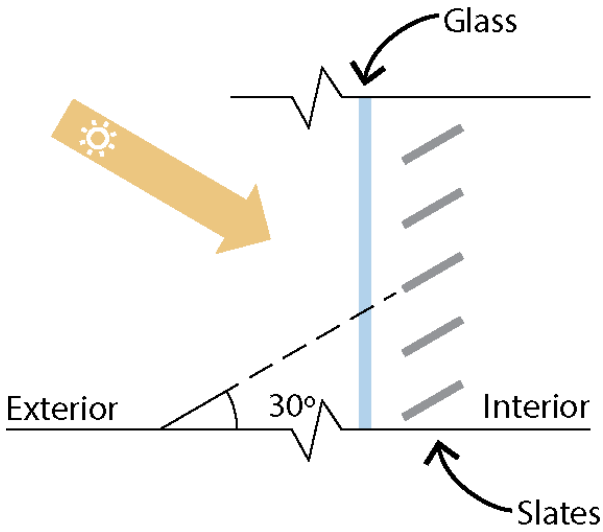

Fig.4.26: VB configuration

After comparing the performance of SSFs against Typ.SF, this research performs another set of simulations on venetian blinds (VBs) to see how they behave and can be used to provide glare-circadian balance differently. Similar to the SF simulation process, this research first simulates a typical VB product, named “VB(Gray) with the same color as Typ.SF and applies a color adjustment for further comparative analysis, named “VB(Blue/Red). Unlike SSF, VB(Blue/Red) is a spectrally-selective venetian blind which there are 2 different colors, blue and red, on the front and back side of the slats respectively, in order to investigate situations where people can rotate the slats based on their needs for either circadian entrainment or melanopic suppression. To mimic the situation realistically, slats face the exterior at a 30 degree angle as shown in Fig.4.26. Therefore, there are 2 derived simulations as VB(Blue) with blue facing the exterior, and VB(Red) with red facing the exterior accordingly.

After deploying VB(Blue) in summer, 59.66% of the classroom area has ideal photopic illuminance; 0% of the area has glare issues; 40.34% of the area has underlit problems with photopic illuminance under 300 lx; 61.74% of the area has ideal melanopic illuminance; 12.88%

of it has melanopic light higher 1100 EML; 38.26% of the area has under-entrainment problem. Overall, 59.66% of the area presents an ideal lighting balance; 2.08% of the area is dim; and 38.26% of the area is underlit. In winter, 63.83% of the classroom area has ideal photopic illuminance; 2.27% of the area has glare issues; and 33.9% of the area has underlit problems with photopic illuminance under 300 lx; 70.27% of the area has ideal melanopic illuminance; 19.51% of it has melanopic light higher 1100 EML; 29.73% of the area has under-entrainment problem. Overall, 63.45% of the area presents an ideal lighting balance; 2.27% of the area has glare issues; 0.38 of the area has enough photopic light but lacks melanopic illuminance; 4.36% of the area is dim; and 29.54% of the area is underlit (Fig.4.27).

After deploying VB(Blue) in summer, 59.85% of the classroom area has ideal photopic illuminance; 0% of the area has glare issues; 40.15% of the area has underlit problems with photopic illuminance under 300 lx; 62.31% of the area has ideal melanopic illuminance; 12.31% of it has melanopic light higher 1100 EML; 37.69% of the area has under-entrainment problem. Overall, 59.85% of the area presents an ideal lighting balance; 2.46% of the area is dim; and 37.69% of the area is underlit. In winter, 64.96% of the classroom area has ideal photopic illuminance; 2.27% of the area has glare issues; and 32.77% of the area has underlit problems with photopic illuminance under 300 lx; 71.21% of the area has ideal melanopic illuminance; 19.51% of it has melanopic light higher 1100 EML; 28.79% of the area has under-entrainment problem. Overall, 64.96% of the area presents an ideal lighting balance; 2.27% of the area has glare issues; 3.98 of the area is dim; and 28.79% of the area is underlit (Fig.4.28).

After deploying VB(Red) in summer, 59.85% of the classroom area has ideal photopic illuminance; 0% of the area has glare issues; 40.15% of the area has underlit problems with photopic illuminance under 300 lx; 61.93% of the area has ideal melanopic illuminance; 12.88%

of it has melanopic light higher 1100 EML; 38.07% of the area has under-entrainment problem. Overall, 59.85% of the area presents an ideal lighting balance; 1.89% of the area is dim; and 38.26% of the area is underlit. In winter, 63.83% of the classroom area has ideal photopic illuminance; 2.27% of the area has glare issues; and 33.9% of the area has underlit problems with photopic illuminance under 300 lx; 69.13% of the area has ideal melanopic illuminance; 19.7% of it has melanopic light higher 1100 EML; 30.87% of the area has under-entrainment problem. Overall, 63.64% of the area presents an ideal lighting balance; 2.27% of the area has glare issues; 3.03 of the area is dim; and 28.79% of the area is underlit (Fig.4.29).

After comparing the performance between Typ.SF 10% OF, SSFs, and VBs, it shows that, in general, VBs are 30% more effective in providing glare-circadian balance. However, the change of colors in VBs do not create a significant difference in adjusting photopic and melanopic illuminance compared to SSFs. For example, changing the color from VB(Gray) to VB(Blue) appears to improve melanopic illuminance by about 2%. Additionally, VBs' circadian performance throughout the year is relatively stable, with about 10% increased effectiveness in winter; whereas SSF(Blue) can be 16% more effective in winter. Yet, this performance does not consider slats' angle adjustment. Therefore, this increased effectiveness can fluctuate due to the change of slat angles.

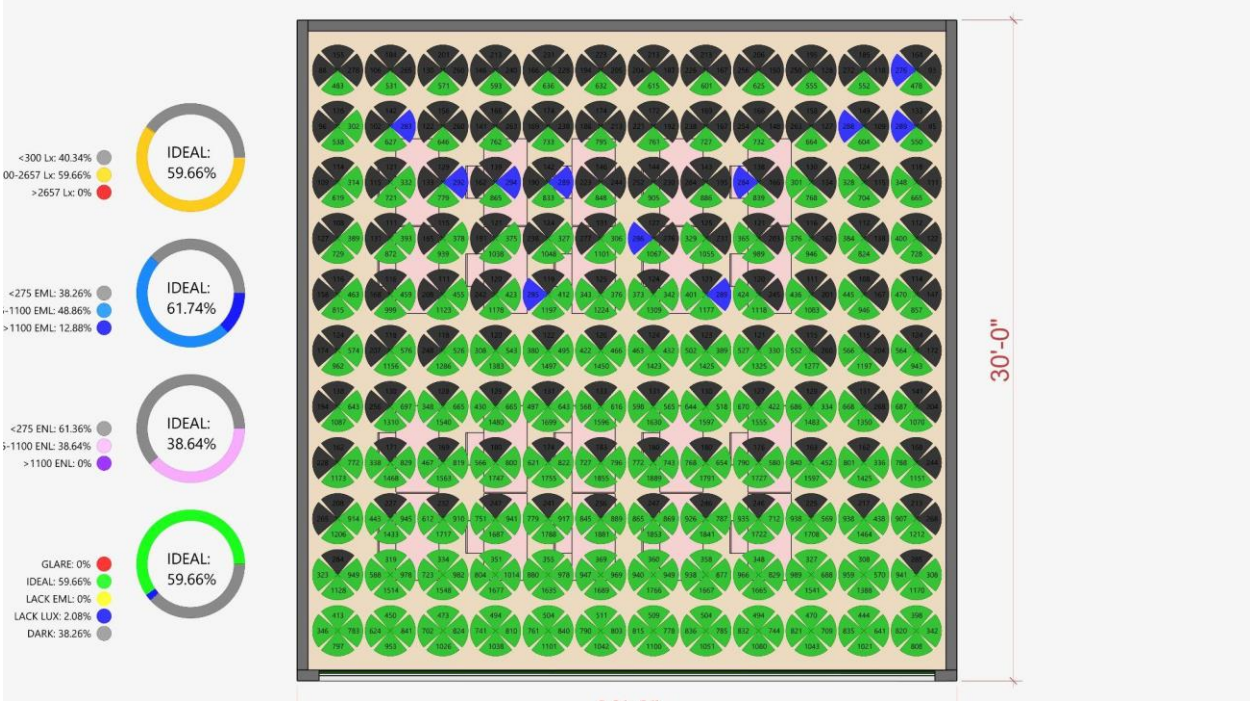

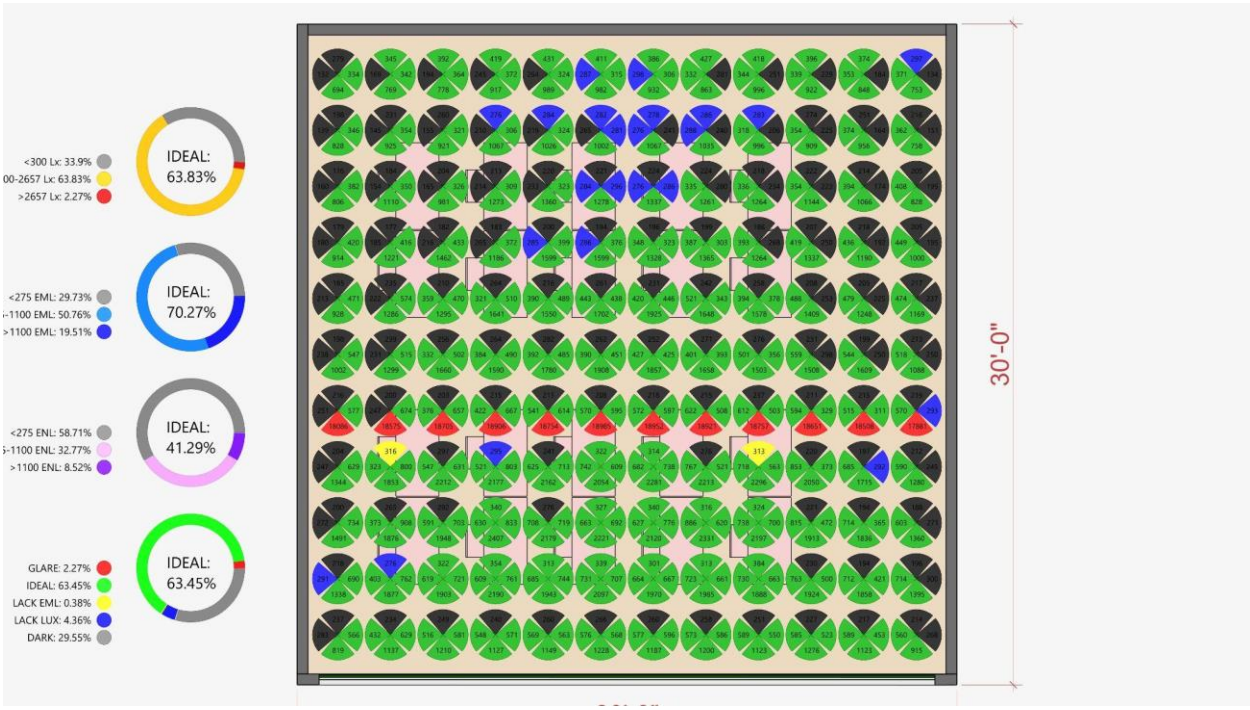

LUX	EML <275	EML >275
>2657	GLARE	
Enough	FAIR	IDEAL
< 300	UNDERLIT	DIM

Fig.4.27: Glare-Circadian Balance with VB(Gray) on Summer solstice and winter solstice

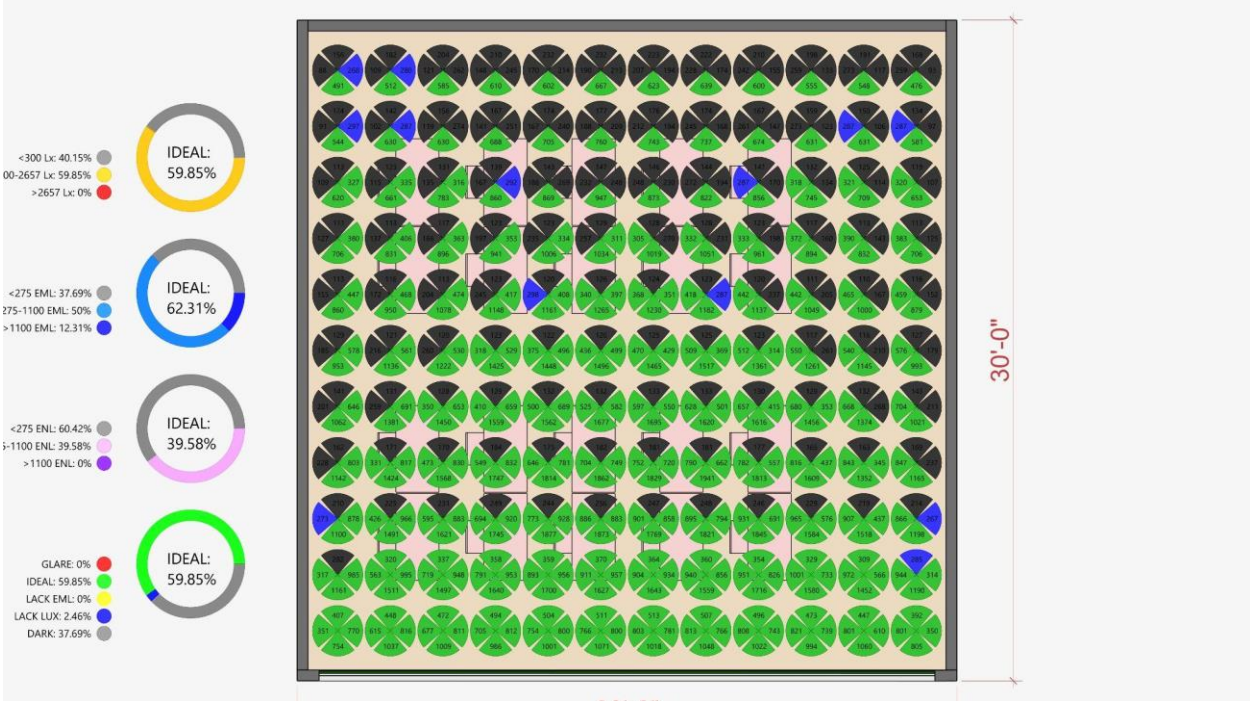

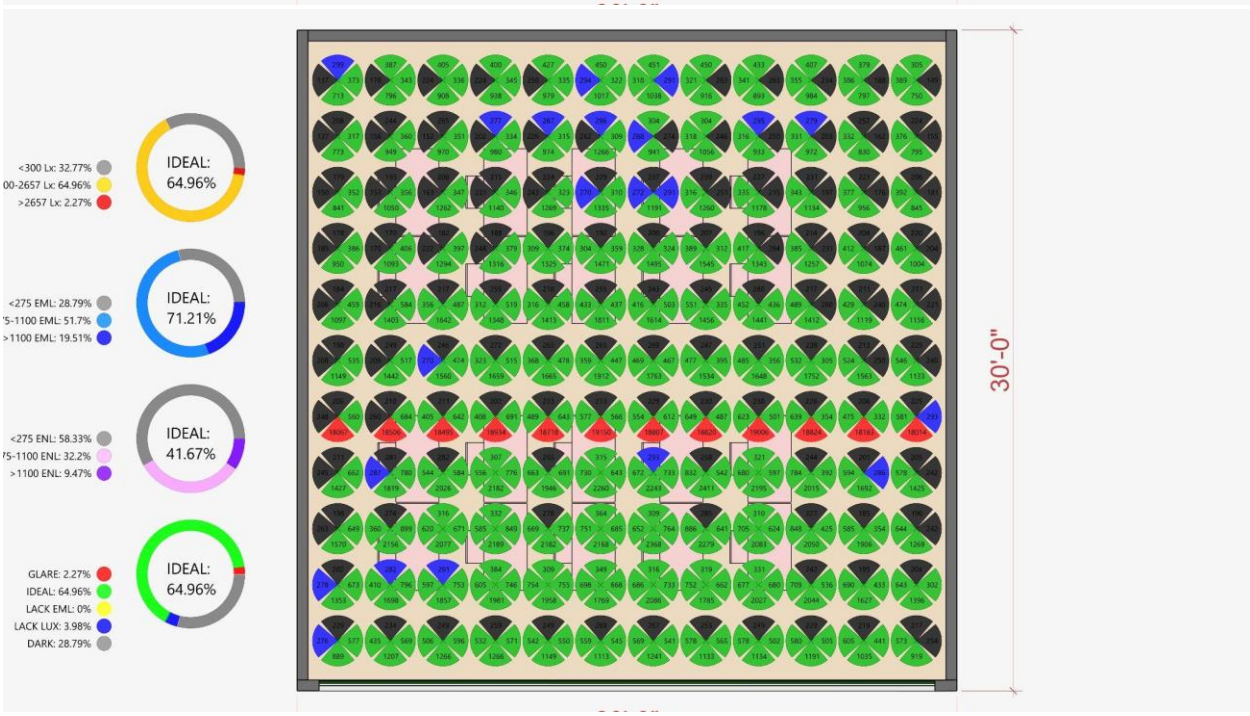

		EML	
		<275	>275
LUX	>2657	GLARE	
	Enough	FAIR	IDEAL
	< 300	UNDERLIT	DIM

Fig.4.28: Glare-Circadian Balance with VB(Blue) on Summer solstice and winter solstice

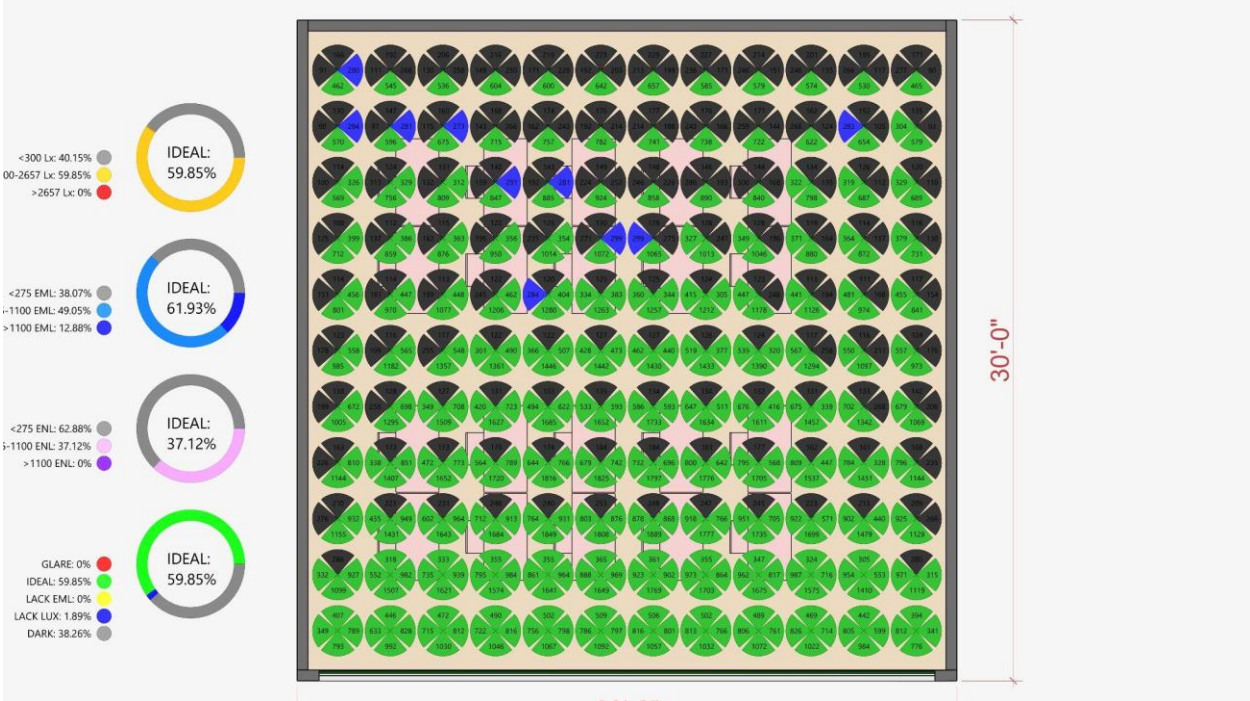

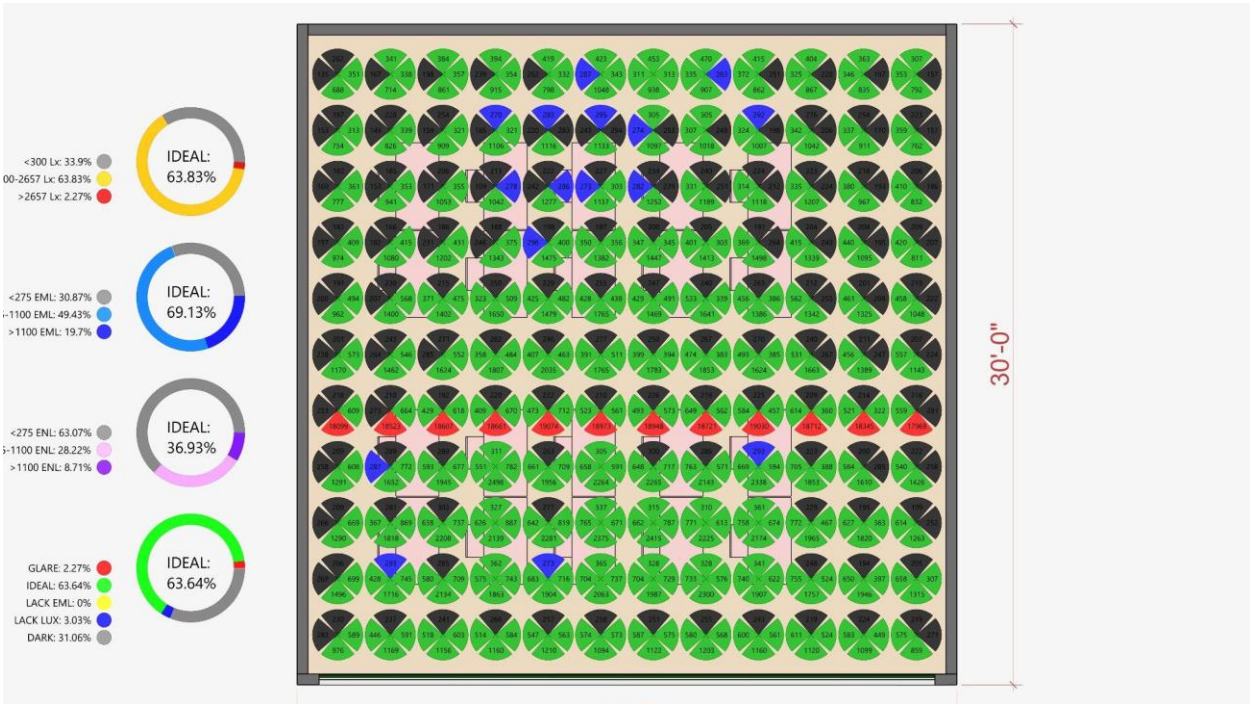

		EML	
		<275	>275
LUX	>2657	GLARE	
	Enough	FAIR	IDEAL
	< 300	UNDERLIT	DIM

Fig.4.29: Glare-Circadian Balance with VB(Red) on Summer solstice and winter solstice

Figures 4.30 and 4.31 illustrate the photopic and melanopic light penetration for views gazing toward the window under CCT sky conditions ranging from 5500 K to 25000 K.

In summer, VBs are not only more effective in promoting glare-circadian balance, but they also perform better at maintaining good illuminance over a longer distance. While the SFs mitigate photopic illuminance progressively and consistently per depth, VBs suppress more photopic light near the window, and help reflect more photopic light and maintain prominently higher illuminance levels to deeper space, in which no underlit problem emerges by the rear wall. Also, the VBs are better in maintaining optimal melanopic illuminance above the upper threshold for most of the area in the classroom, allowing circadian entrainment for occupants in 1 hour. In winter, the advantage of VBs comes into mitigating glare for space near the window, while retaining melanopic illuminance above optimal threshold for the entire classroom. However, VBs leave unpredictable glare issues at the central area of the classroom. This glary spike is likely to be caused by the direct daylight of the sun at a lower angle passing through the gap between the slats, which implies additional controls to fully resolve glare but it may also affect the light level of other locations.

Overall, unlike SFs' consistent and predictable impact on photopic illuminance, there is a sparsity when deploying VBs. Changing the color of VB is able to shape melanopic distribution slightly but not a noticeable improvement. This result is understandable as a substantial portion of the daylight may pass through the gaps between slats directly, hence not being affected by the colors of the slats.

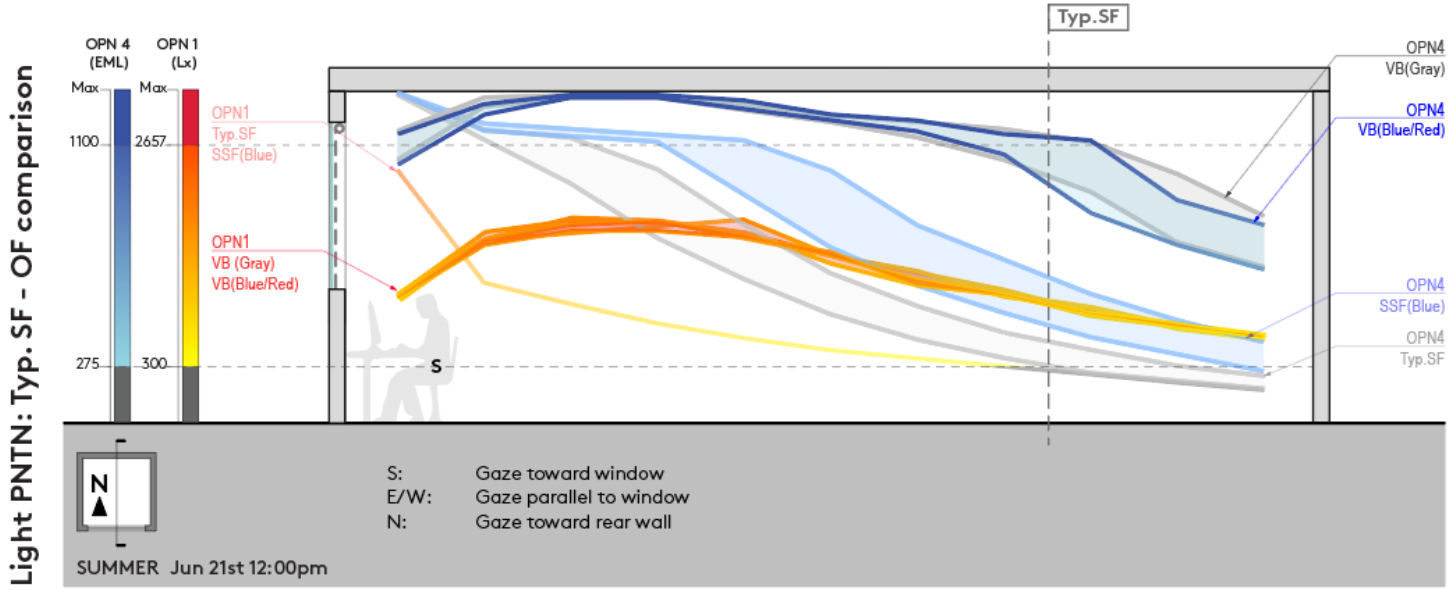

Fig 4.30: Photopic and melanopic light penetration with Typ.SF and SSFs (Blue, Purple, Orange) on summer solstice

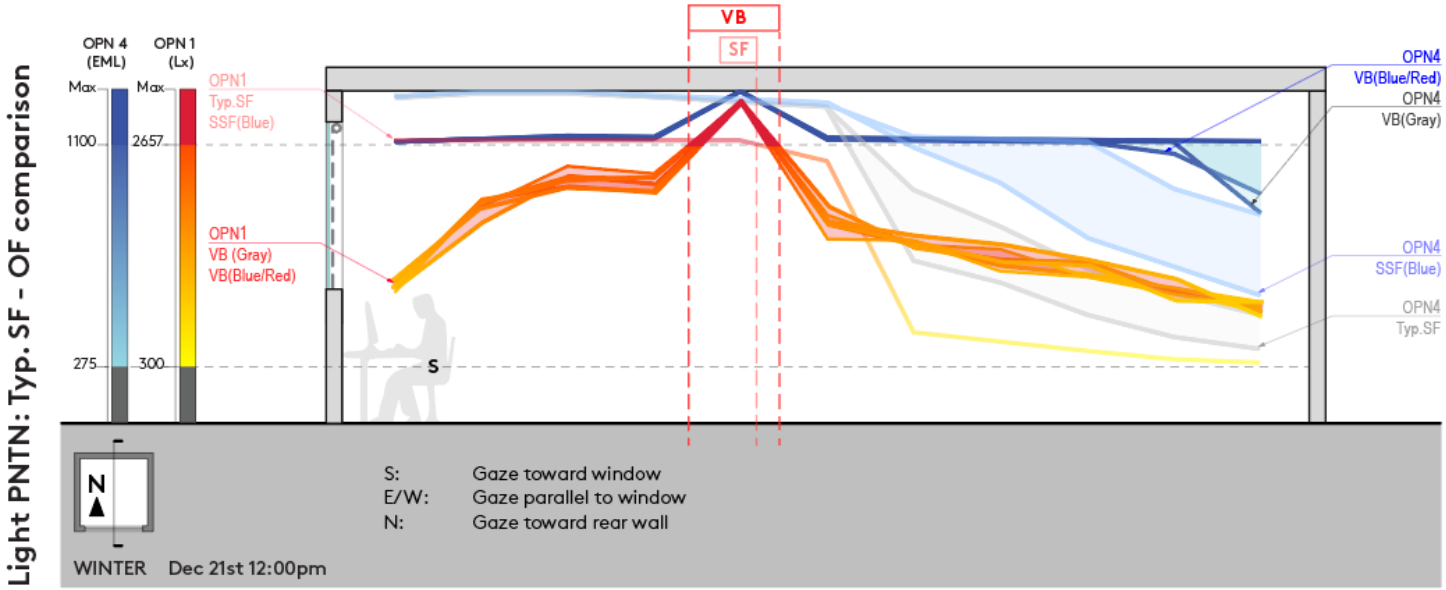

Fig 4.31: Photopic and melanopic light penetration with Typ.SF and SSFs (Blue, Purple, Orange) on winter solstice

Figures 4.32 and 4.33 display HDR image simulations for venetian blinds (VBs) compared to Typ.SF 10% OF and spectrally selective fabrics (SSF) in blue, under 5500K CCT on the summer and winter solstices. The human visual sensation differences among the colors of VBs are minor, with the main distinction being the blue or red tint of light reflected on the ceiling and the diffused reflection of the slats. Despite perceptual differences between shading options, the photopic luminance distribution remains consistent within shade fabrics (SFs) and VBs, as indicated by the glare-circadian balance and light penetration studies. However, notable differences arise when comparing photopic and melanopic luminance impacts between SFs and VBs.

In summer, a significant gradient change in false color implies that Typ.SF (10% OF) significantly reduces photopic luminance in deeper space, potentially leading to underlit areas as shown by the purple region. VBs maintain luminance levels throughout the entire space, with the rear wall remaining green, implying a more even distribution of photopic luminance. Regarding melanopic luminance distribution, SSF (Blue) mitigates the risk of under-entrainment but its overall melanopic luminance distribution is less significant compared to VBs. This is indicated by a larger red region on the ceiling and the green region extending to the rear wall. Changing the VB colors does not result in notable differences in melanopic light distribution compared to changing the SF colors.

In winter, the phenomena are similar, but the overall changes in melanopic distribution are more even. More melanopic light is captured and reflected by the rear wall, indicating an improved distribution compared to summer. SSF(Blue) shows significant melanopic distribution, it is outperformed by VBs. The melanin distribution lighting differences between the colors or VBs remain insignificant.

Overall, VBs significantly outperformed SFs options in providing glare control and retaining melanopic luminance, effectively providing glare-circadian balance. In addition, the visual sensation among all VBs closely aligns with the Typ.SF, unlike a noticeable blue tint given by SSF(Blue).

Overall, VBs significantly outperform Typ.SF and SSFs in providing a balanced combination of glare control and melanopic luminance retention. VBs maintain consistent luminance levels across the entire space, ensuring the rear wall remains adequately lit and contributing to a more uniform visual environment. They are superior in distributing melanopic light evenly, crucial for circadian rhythm regulation, especially during winter when natural light is lower. The visual sensation provided by VBs aligns closely with Typ.SF, avoiding the strong color tints seen with SSF(Blue), and creating a comfortable and visually appealing environment. Additionally, VBs effectively control glare without compromising light levels, ensuring both visual comfort and circadian health. In contrast, SSF(Blue) does not achieve the same level of performance, often introducing a noticeable blue tint. In conclusion, VBs offer a superior solution for balancing glare control, visual comfort, and circadian lighting needs, making them a more effective choice compared to Typ.SF and SSF options.

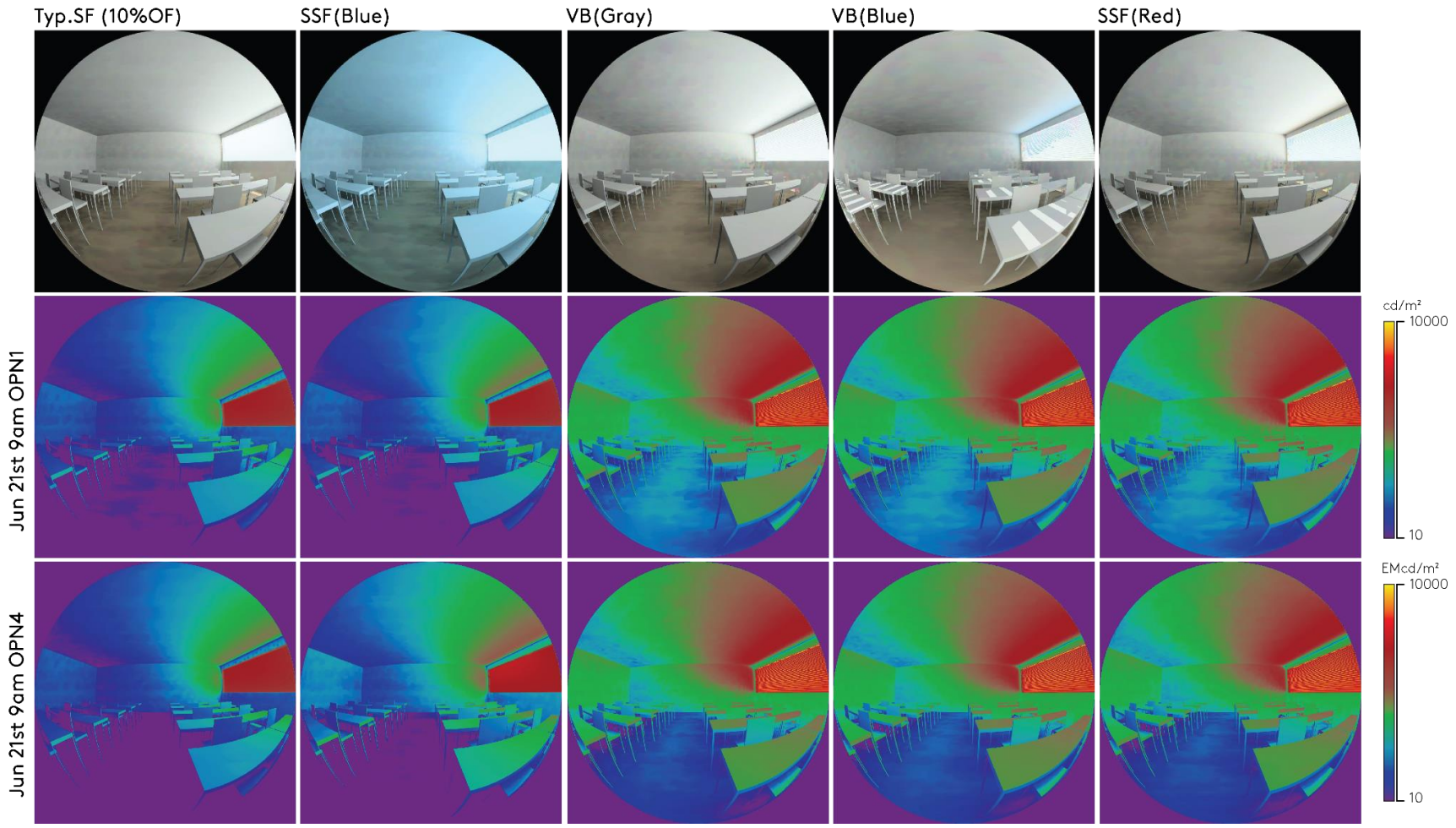

Fig.4.32: HDR image simulations of Typ.SF, SSF(Blue), and VBs on summer solstice under 5500K CCT

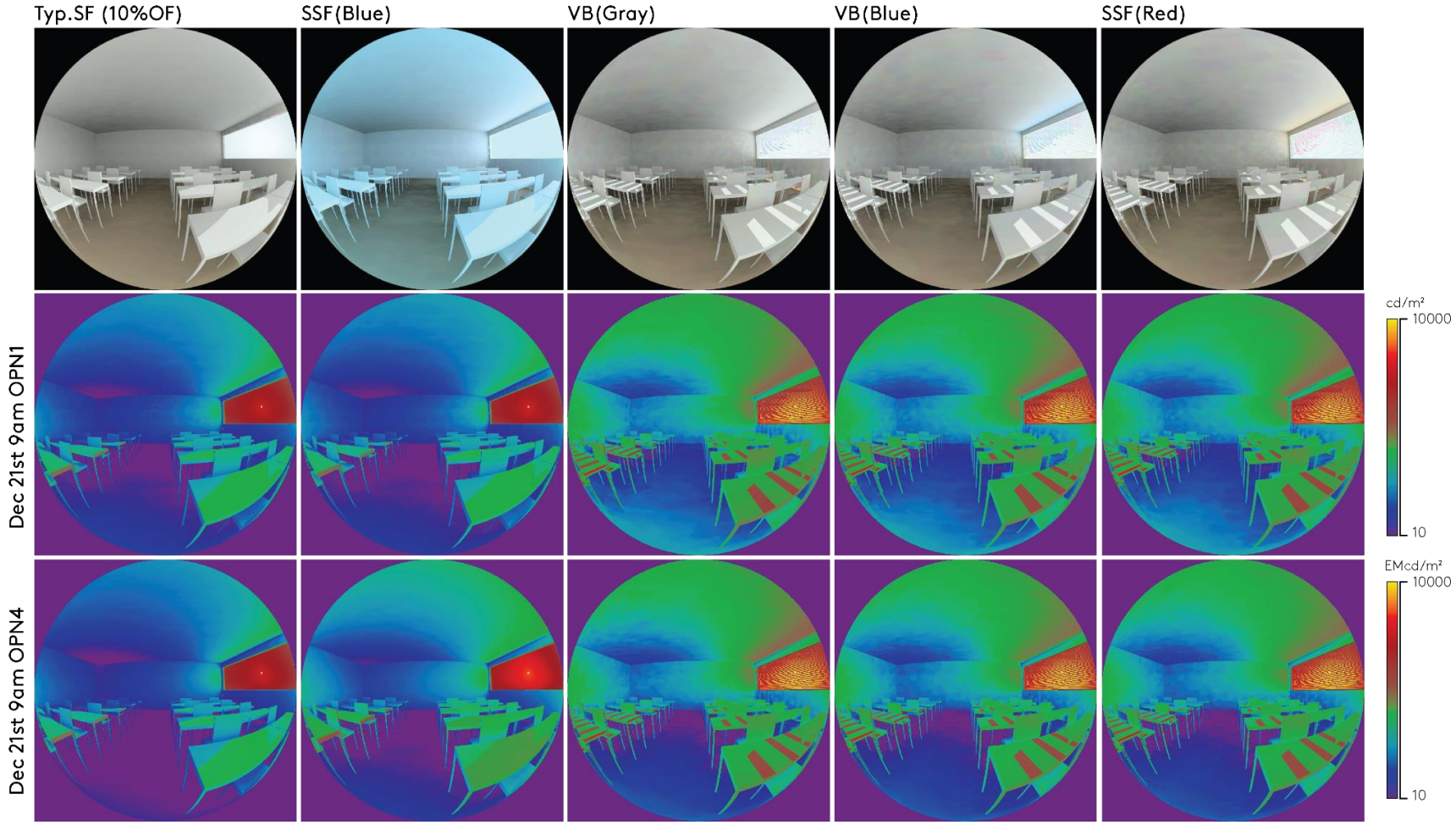

Fig.4.33: HDR image simulations of Typ.SF, SSF(Blue), and VBs on winter solstice under 5500K CCT

Summer-D65	OPN1 (%)			OPN4 (%)					Glare-Circadian Balance (%)				
Condition	Glare	Good	Underlit	Best	Good	Underlit	Ideal	Δ	Glare	Ideal	Fair	Dim	Underlit
Baseline	20.27	64.02	15.71	46.21	40.91	12.88	87.12	-	20.27	64.02	0	2.65	13.06
1% OF	0	6.82	93.18	0	7.58	92.42	7.58	-23.1	0	6.82	0	0.76	92.42
3% OF	0	13.26	86.74	0	14.02	85.98	14.02	-16.66	0	13.26	0	0.57	86.17
5% OF	0	18.94	81.06	2.27	17.61	80.12	19.88	-10.8	0	18.94	0	0.95	80.11
10% OF	0	27.46	72.54	3.79	26.89	69.32	30.68	-	0	27.46	0	3.22	69.32
SSF(Blue)	0	27.65	72.35	7.58	33.52	58.9	41.1	10.42	0	27.65	0	13.45	58.9
SSF(Purple)	0	25.95	74.05	5.3	29.55	65.15	34.85	4.17	0	25.95	0	8.71	65.34
SSF(Orange)	0	27.27	72.73	1.89	17.42	80.69	19.31	-11.37	0	19.32	7.95	0	72.73
VB(Gray)	0	59.66	40.34	12.88	48.86	38.26	61.74	31.06	0	59.66	0	2.08	38.26
VB(Blue)	0	59.85	40.15	12.31	50	37.69	62.31	31.63	0	59.85	0	2.46	37.69
VB(Red)	0	59.85	40.15	12.88	49.05	38.07	61.93	31.25	0	59.85	0	1.89	38.26
Winter-D65	OPN1 (%)			OPN4 (%)					Glare-Circadian Balance (%)				
Condition	Glare	Good	Underlit	Best	Good	Underlit	Ideal	Δ	Glare	Ideal	Fair	Dim	Underlit
Baseline	29.17	70.83	0	66.48	33.52	0	100	-	29.17	70.83	0	0	0
1% OF	0	13.64	86.36	0	13.64	86.36	13.64	-28.6	0	13.64	0	0	86.36
3% OF	0	13.64	86.36	4.92	13.45	81.63	18.37	-23.87	0	13.64	0	4.73	81.63
5% OF	0	23.86	76.14	13.64	13.45	72.91	27.09	-15.15	0	23.86	0	3.22	72.92
10% OF	7.2	33.14	59.66	13.64	28.6	57.76	42.24	-	7.2	33.14	0	1.7	57.96
SSF(Blue)	8.33	32.77	58.9	14.02	42.99	42.99	57.01	14.77	8.33	32.77	0	15.91	42.99
SSF(Purple)	2.65	36.36	60.99	13.64	34.85	51.51	48.49	6.25	2.65	36.36	0	9.47	51.52
SSF(Orange)	6.82	33.71	59.47	12.5	12.31	75.19	24.81	-17.43	6.82	17.99	15.72	0	59.47
VB(Gray)	2.27	63.83	33.9	19.51	50.76	29.73	70.27	28.03	2.27	63.45	0.38	4.36	29.54
VB(Blue)	2.27	64.96	32.77	19.51	51.7	28.79	71.21	28.97	2.27	64.96	0	3.98	28.79
VB(Red)	2.27	63.83	33.9	19.7	49.43	30.87	69.13	26.89	2.27	63.64	0	3.03	63.83

Fig.4.34: OP-1, OPN-4, Glare-Circadian Balance performance table

Chapter 5 — Conclusion

This thesis research attempts to explore how current shading devices can better establish the balance between visual comfort and circadian health in an indoor environment. This study focuses on comparing the performance of commercially typical shading devices, shade fabrics and venetian blinds, and their spectrally-selective color exploration, based on different photopic and melanopic sensitivities of the human eye, to identify optimal solutions that harmonize the demands of minimizing glare while maximizing the circadian stimulus, via LARK simulation under different CCT conditions of the sky. The results show that adjusting color of materials can significantly improve SFs' ability in retaining melanopic stimulus under the same photopic impact, but is rather ineffective when it comes to improving VBs. Key results indicate that VBs significantly outperform SFs in providing a balanced combination of glare glare control and melanopic light retention, essential for maintaining circadian health.

This research employs a simulation-based approach using LARK within the Rhino3D environment to perform detailed lighting simulations. The study first establishes a baseline environment by simulating a standard classroom without shading devices to understand the initial lighting conditions. It then simulates commercial typical shades with varying standardized OF (1%, 3%, 5%, 10%) to determine their impact on photopic and melanopic lighting. Next, the study develops spectrally selective fabrics tailored to enhance melanopic stimulation while maintaining photonic light levels, and explores the effects of different SSF colors. Additionally, the research includes simulations of VBs in various colors to assess their performance in balancing glare control and melanopic light retention. Data visualization techniques such as grid-based simulations, sectional graphs, and HDR renders with false color mapping are utilized to

analyze the visual and non-visual lighting responses under different sky conditions and times of the day.

The research findings reveal a comprehensive analysis of the effects of SFs and VBs on balancing glare and circadian stimulus. Given the existing OF value established as the commercial norm, 5% OF is the safe option in avoiding glare annually, at a cost of significant melanopic light suppression. With good layout design according to occupants' view orientations, 10% OF is a feasible solution for an additional 10% of ideal lighting area, and at least about 10-15 ft increase of light penetration, despite the potential risk of glare issues seasonally. Additionally, under the same photopic impact, applying spectrally-selective color can significantly change SFs performance in terms of its melanopic light retention, from about -17% by SSF(Orange) to +15% by SSF(Blue), under the same photopic impact. The improvement in melanopic retention is amplified under higher CCT of the sky and lower sun angles. While proven effective, the HDR image simulations show that the color adjustments can also substantially change the color of lighting in the interior environments; however, the actual human visual sensation may not be as prominent as depicted in HDR simulations due to the mechanism of color constancy in the human ocular system. Overall, VBs are generally 30% more effective than SFs in providing glare-circadian balance. The simulations show that not only VBs mitigate more photopic illuminance for the space near the window, but they also help maintain more light in a deeper area, due to the geometries of VBs allowing daylight passes through the gaps between slats without interference from the materials. However, the sparsity of light distribution shows VBs are relatively more unpredictable in preventing glare, also due to the gaps and the slat geometry; thereby resulting in an unpredicted glare spike which may require further manual adjustments. At the same time, while about 2% difference is recorded by

simulation, the change of colors on VBs do not yield a significant impact. In terms of seasonal impacts, SFs tend to reduce more photopic luminance in deeper spaces during summer, potentially causing underlit areas. VBs, on the other hand, maintain consistent luminance levels, ensuring even lighting distribution. During winter, the distribution of melanopic light is more even due to the solar angle, which the change in solar angle introduces a fluctuation in VBs' performance that is not found in SFs' performance.

The findings from this research have profound implications for architectural design and the selection of shading devices in indoor environments. The comprehensive analysis highlights the nuanced effect of SFs and VBs on balancing glaring and circadian stimulus, offering valuable insights for optimizing both visual comfort and circadian health. The research identifies that higher SFs with higher OF can be effectively used in specific design contexts to enhance daylight penetration and circadian lighting. It also demonstrates there is a room of color choices in designing SFs while maintaining their functional performance. And suppressing melanopic using color in material can also be beneficial in specific geographic regions where the day-night cycle is not balanced. This suggests that color adjustments in shade fabrics can be strategically used to enhance circadian stimulus without compromising visual comfort, particularly under higher correlated color temperatures (CCT) and lower sun angles. VBs are a versatile solution for ensuring even light distribution and supporting circadian health. The unpredictability of glare spikes due to the gaps between slats and their geometry suggests an opportunity to design in sophisticated geometry to maintain optimal lighting conditions. The color changes in VBs have minimal impact, reinforcing their robustness across different design scenarios. Moreover, the implications extend to sustainable building practices. By optimizing the use of natural daylight,

these shading strategies can reduce reliance on electric lighting, contributing to energy conservation and promoting healthier indoor environments. The ability to enhance visual and circadian comfort simultaneously aligns with contemporary green building standards, supporting occupant well-being and productivity.

The methodology employed in this research, while comprehensive, presents several limitations and challenges that should be considered when interpreting the findings. Firstly, the grid-based simulations were mainly constrained to the CIE D65 standard at 12:00 noon on the summer and winter solstices, which limits the understanding of lighting conditions at different times of the day. Although the dynamic changes in light quality and intensity throughout the day are partially captured in light penetration and HDR analysis, this temporal restriction in grid-base simulation may still potentially impact the accuracy of a thorough glare-circadian balance assessment. Additionally, actualizing the spectrally-selective color adjustments requires advancements in material science to develop shade fabrics that can achieve the desired spectral properties without compromising other functional attributes. The reliance on Greg Ward's generic material files in Radiance to calculate how light interacts with SFs may introduce another layer of limitation, as these files may not accurately reflect the specific texture and weave patterns of actual SFs samples, affecting the precision of the simulation results. Furthermore, the VBs were simulated at a fixed angle of 30 degrees, which does not capture the full range of lighting effects that different slat angles might produce. More simulations are needed to understand how varying the slat angle impacts light distribution and glare control. These limitations highlight the need for further research to address these gaps, including simulations at different times of the day, development of advanced spectrally-selective materials, more accurate

modeling of shade fabric properties, variable slat angle simulations for VBs, and the integration of dynamic daylighting controls.

Future research and development should build on the findings and limitations of this study to further enhance our understanding and optimization of shading devices for visual comfort and circadian health. One critical area for further investigation is conducting simulations with a broader range of colors for both shade fabrics (SFs) and venetian blinds (VBs). This would help identify the most effective color adjustments for maximizing melanopic light retention without compromising photopic performance. Additionally, a deeper dive into establishing more accurate calculation files for BRTDfunc material in Radiance is essential. Developing detailed and specific material files that accurately represent the texture, weave patterns, and spectral properties of actual shading materials will significantly improve the precision of simulation results. Exploring advanced geometries for blinds, such as curved slats, different textures, and adjustable angles, could provide new insights into optimizing light distribution and glare control. These advanced geometries could offer more flexible and effective daylighting solutions that adapt to changing environmental conditions. Furthermore, investigating the energy conservation potential of shading devices based on circadian health requirements is crucial. Understanding how these devices can reduce reliance on artificial lighting while supporting circadian rhythms will contribute to sustainable building practices and enhance occupant well-being. Overall, these areas of focus will advance the field by providing more nuanced and effective strategies for daylighting design, promoting both energy efficiency and human health in built environments.

In conclusion, this thesis explores how current shading devices can better balance visual comfort and circadian health in indoor environments. By comparing the performance of SFs and

VBs, and exploring spectrally selective color adjustments, the study identifies good directions that minimize glare while maximizing circadian stimulus. Using LARK simulations under various sky conditions, the research demonstrates that while color adjustments significantly improve SFs' melanopic light retention, VBs generally outperform SFs in balancing glare control and circadian health, by offering consistent luminance and support circadian rhythms more effectively. The study also underscores the importance of advanced material science, accurate modeling, and dynamic daylighting controls in future research. These findings provide valuable insights for designing shading devices that enhance both visual and circadian comfort, promoting energy efficiency and occupant well-being in sustainable building practices. The ongoing research and development in this field are essential to further refine these strategies, ensuring healthier and more productive indoor environments.

Bibliography

Aguilar-Carrasco, María Teresa, Ignacio Acosta, and Samuel Domínguez-Amarillo. "CircaLight, a New Circadian Light Assessment Tool for Grasshopper Environment: Development and Reliability Testing." *Journal of Building Engineering* 71 (July 2023): 106527. https://doi.org/10.1016/j.jobe.2023.106527.

Balakrishnan, Priji, and Alstan J.Jakubiec. "Spectral Rendering with Daylight: A Comparison of Two Spectral Daylight Simulation Platforms," 1191–98. Rome, Italy. Accessed June 6, 2024. https://doi.org/10.26868/25222708.2019.211158.

Blume, Christine, Corrado Garbazza, and Manuel Spitschan. "Effects of Light on Human Circadian Rhythms, Sleep and Mood." *Somnologie* 23, no. 3 (September 2019): 147–56. https://doi.org/10.1007/s11818-019-00215-x.

Boyce, P. R. (2021). *Human factors in lighting* (3rd ed.). CRC Press. https://doi.org/10.1201/9780429104763

Boyce, P. R. (2000). Is full-spectrum lighting special? *IRC Internal Report No. 659*. Lighting Research Center, Rensselaer Polytechnic Institute. Retrieved from https://www.researchgate.net/publication/2921975

Boyce, Peter R. "Lemmings, Light, and Health." *LEUKOS* 2, no. 3 (January 1, 2006): 175–84. https://doi.org/10.1582/LEUKOS.2006.02.03.002.

Boyce, Peter. "Editorial: Light Distribution – a Missing Variable." *Lighting Research & Technology* 46, no. 6 (December 2014): 617–617. https://doi.org/10.1177/1477153514556940.

Boyce, Peter. "Editorial: Lighting and Health." *Lighting Research & Technology* 53, no. 5 (August 2021): 375–375. https://doi.org/10.1177/14771535211028946.

Boyce, P. (2022). Light, lighting and human health. *Lighting Research & Technology*, 54(2), 101-144. https://doi.org/10.1177/14771535211010267

Blume, Christine, Corrado Garbazza, and Manuel Spitschan. "Effects of Light on Human Circadian Rhythms, Sleep and Mood." *Somnologie* 23, no. 3 (September 2019): 147–56. https://doi.org/10.1007/s11818-019-00215-x.

Boubekri, Mohamed, Jaewook Lee, Piers MacNaughton, May Woo, Lauren Schuyler, Brandon Tinianov, and Usha Satish. “The Impact of Optimized Daylight and Views on the Sleep Duration and Cognitive Performance of Office Workers.” *International Journal of Environmental Research and Public Health* 17, no. 9 (May 6, 2020): 3219. https://doi.org/10.3390/ijerph17093219.

Brainard, George C., John P. Hanifin, Jeffrey M. Greeson, Brenda Byrne, Gena Glickman, Edward Gerner, and Mark D. Rollag. “Action Spectrum for Melatonin Regulation in Humans: Evidence for a Novel Circadian Photoreceptor.” *The Journal of Neuroscience* 21, no. 16 (August 15, 2001): 6405–12. https://doi.org/10.1523/JNEUROSCI.21-16-06405.2001.

British Standards Institution. (2021). *BS EN 14501:2021 Blinds and shutters. Thermal and visual comfort. Performance characteristics and classification*. BSI Standards Limited.

Brown, Timothy M., George C. Brainard, Christian Cajochen, Charles A. Czeisler, John P. Hanifin, Steven W. Lockley, Robert J. Lucas, et al. “Recommendations for Daytime, Evening, and Nighttime Indoor Light Exposure to Best Support Physiology, Sleep, and Wakefulness in Healthy Adults.” *PLOS Biology* 20, no. 3 (March 17, 2022): e3001571. https://doi.org/10.1371/journal.pbio.3001571.

Brown, P. K., & Wald, G. (1964). Visual pigments in single rods and cones of the human retina. *Science, 144*(Whole No. 3614), 45–52. https://doi.org/10.1126/science.144.3614.45

Centers for Disease Control and Prevention (CDC). (2023, October 26). Ultraviolet (UV) radiation. *Centers for Disease Control and Prevention*. https://www.cdc.gov/niosh/topics/uvradiation/default.html

CIE. (1987). *International lighting vocabulary*. International Commission on Illumination.

CIE. (1924). *Commission Internationale de l'Éclairage: Proceedings of the 6th Session, Geneva, 1924*. Cambridge University Press.

CIE. (1995). *CIE publication 117: Discomfort glare in interior lighting*. International Commission on Illumination.

CIE. (2002). *Technical report: CIE TN 003:1998 methods for the calculation of the spectral luminous efficacy for photometry and colorimetry*. International Commission on Illumination.

CIE. (2010). *Guide for the measurement of daylight for the purpose of human health*. International Commission on Illumination.

CIE. (2013). *CIE publication 190: Lighting of indoor work places* (2nd ed.). International Commission on Illumination.

CIE. (2016). *Technical report: Discomfort glare in interior lighting* (CIE 171:2016). Vienna: CIE Central Bureau.

Clear, R. (2013). Discomfort glare: What do we actually know? *Lighting Research & Technology, 45*(2), 141-158. https://doi.org/10.1177/1477153512444527

Commission Internationale de l'Éclairage. (1932). *Commission internationale de l'Éclairage proceedings, 1931*. Cambridge University Press.

Commission Internationale de l'Éclairage. (1987). *CIE collection in photometry and radiometry* (CIE 114-1994). Division 2. ISBN 978 3 900734 58 9.

Commission Internationale de l'Éclairage. (2010). *Proceedings of CIE 2010 Lighting Quality & Energy Efficiency, March 2010, Vienna, Austria* (CIE x035:2010). Commission Internationale de l'Éclairage. ISBN 978 3 901906 83 1.

Commission Internationale de l'Éclairage. (2018). *Colorimetry* (4th ed.). CIE. ISBN 978-3-902842-13-8.

Crone, Simon. "RADIANCE USERS MANUAL," n.d.

Compagnon, Dr R. "A Simulation Tool for Daylighting Systems," n.d.

Ward, Greg. "Behavior of Materials in RADIANCE," 2022.

Duke-Elder, S., & Scott, G. I. (1971). *System of ophthalmology: Neuro-ophthalmology* (Vol. 12). Imprint Unknown. ISBN 9780853137597.

D'Souza, S. P., Swygart, D. I., Wienbar, S. R., Upton, B. A., Zhang, K. X., Mackin, R. D., Casasent, A. K., Samuel, M. A., Schwartz, G. W., & Lang, R. A. (2022). Retinal patterns and the cellular repertoire of neuropsin (Opn5) retinal ganglion cells. *Journal of Comparative Neurology, 530*(8), 1247-1262. https://doi.org/10.1002/cne.25272

EHS Works. (2011, November). Podcast focuses on vision during activities in dim light. *EHS Works*. https://ehsworks1.blogspot.com/2011/11/podcast-focuses-on-vision-during.html

Fotios, S., and M. Kent. "Measuring Discomfort from Glare: Recommendations for Good Practice." *LEUKOS* 17, no. 4 (October 2, 2021): 338–58. https://doi.org/10.1080/15502724.2020.1803082.

Gooley, J. J., Lu, J., Chou, T. C., Scammell, T. E., & Saper, C. B. (2001). Melanopsin in cells of origin of the retinohypothalamic tract. *Nature Neuroscience, 13*(1), 110-117.

Gou, Zhonghua, Stephen Siu-Yu Lau, and Feng Qian. "Comparison of Mood and Task Performance in Naturally-Lit and Artificially-Lit Environments." *Indoor and Built*

Environment 24, no. 1 (February 2015): 27–36. https://doi.org/10.1177/1420326X13507792.

Hattar, S., R. J. Lucas, N. Mrosovsky, S. Thompson, R. H. Douglas, M. W. Hankins, J. Lem, et al. "Melanopsin and Rod–Cone Photoreceptive Systems Account for All Major Accessory Visual Functions in Mice." *Nature* 424, no. 6944 (July 2003): 75–81. https://doi.org/10.1038/nature01761.

Helmholtz, H. v. (1948). Concerning the perceptions in general, 1867. In W. Dennis (Ed.), *Readings in the history of psychology* (pp. 214–230). Appleton-Century-Crofts. https://doi.org/10.1037/11304-027

Hernández-Andrés, Javier, Javier Romero, Juan L. Nieves, and Raymond L. Lee. "Color and Spectral Analysis of Daylight in Southern Europe." *Journal of the Optical Society of America A* 18, no. 6 (June 1, 2001): 1325. https://doi.org/10.1364/JOSAA.18.001325.

Hubel, D. H., and T. N. Wiesel. "Receptive Fields, Binocular Interaction and Functional Architecture in the Cat's Visual Cortex." *The Journal of Physiology* 160, no. 1 (January 1962): 106–54. https://doi.org/10.1113/jphysiol.1962.sp006837.

Ibrahim, M., & Elghali, L. (2023, July). Evaluating the accuracy of melanopic lighting simulation tools: A comparative study of DIALux and ALFA. *Applied Sciences, 13*(13), 6655.

IEA (2018), *World Energy Outlook 2018*. IEA, Paris https://www.iea.org/reports/world-energy-outlook-2018, License: CC BY 4.0

IEA (2021), *World Energy Outlook 2021*. IEA, Paris https://www.iea.org/reports/world-energy-outlook-2018.

Inanici, M., Brennan, M., & Clark, E. (2015, December 7-9). Spectral lighting simulations: Computing circadian light. In *Proceedings of International Building Performance Simulation Association Conference* (pp. 1245-1252), Hyderabad, India.

Inanici, M, B Abboushi, and S Safranek. "Evaluation of Sky Spectra and Sky Models in Daylighting Simulations." *Lighting Research & Technology* 55, no. 6 (October 2023): 502–29. https://doi.org/10.1177/14771535221103400.

International WELL Building Institute. (2020). *WELL building standard version 2* (WELL v2). International WELL Building Institute. Retrieved from https://www.wellcertified.com/

Iqbal, M. (1983) *An introduction to solar radiation*. Academic Press Canada.

Jackson, M. A., & Bollinger, M. (2022). Section 1: How blue light affects the eye and body; Chapter 4: Circadian rhythm. In *How to save your eyes in the digital age: The handbook on blue light, screen time, health, and electronics* (pp. 29–36). Eyesafe Inc.

Jalali, Mansoureh Sadat, James R. Jones, Elif Tural, and Ronald B. Gibbons. "Human-Centric Lighting Design: A Framework for Supporting Healthy Circadian Rhythm Grounded in Established Knowledge in Interior Spaces." *Buildings* 14, no. 4 (April 17, 2024): 1125. https://doi.org/10.3390/buildings14041125.

Jung B, Cheng Z, Brennan M, Inanici M. "Multispectral Lighting Simulation Approaches for Predicting Opsin-driven Metrics and their Application in a Neonatal Intensive Care Unit," International Building Performance Simulation Association (IBPSA) Conference, China, September 4-6, 2023

Jung, B, and M Inanici. "Measuring Circadian Lighting through High Dynamic Range Photography." *Lighting Research & Technology* 51, no. 5 (August 2019): 742–63. https://doi.org/10.1177/1477153518792597.

Kandel, E. R., & Squire, L. R. (2000). Neuroscience: Breaking down scientific barriers to the study of brain and mind. *Science, 290*(5494), 1113-1120. https://doi.org/10.1126/science.290.5494.1113

Kent, Mg, S Altomonte, Pr Tregenza, and R Wilson. "Temporal Variables and Personal Factors in Glare Sensation." *Lighting Research & Technology* 48, no. 6 (October 2016): 689–710. https://doi.org/10.1177/1477153515578310.

Kitsinelis, S., & Kitsinelis, S. (2017). *Light sources: Basics of lighting technologies and applications* (2nd ed.). CRC Press. ISBN 9781138034044.

Klepeis, N. E., W. C. Nelson, W. R. Ott, J. P. Robinson, A. M. Tsang, P. Switzer, J. V. Behar, S. C. Hern, and W. H. Engelmann. "The National Human Activity Pattern Survey (NHAPS): A Resource for Assessing Exposure to Environmental Pollutants." Journal of Exposure Science & Environmental Epidemiology 11, no. 3 (June 2001): 231–52. https://doi.org/10.1038/sj.jea.7500165.

Knoop, Martine, Kai Broszio, Aicha Diakite, Carolin Liedtke, Mathias Niedling, Inga Rothert, Frederic Rudawski, and Nils Weber. "Methods to Describe and Measure Lighting Conditions in Experiments on Non-Image-Forming Aspects." *LEUKOS* 15, no. 2–3 (July 3, 2019): 163–79. https://doi.org/10.1080/15502724.2018.1518716.

KU Leuven. (2017). *Lighting research at KU Leuven*. https://fhi.nl/app/uploads/sites/32/2017/09/KU-LEUVEN.pdf

Larson, G. W., & Shakespeare, R. A. (1998). *Rendering with Radiance: The art and science of lighting visualization*. Morgan Kaufmann Publishers. ISBN 1-55860-499-5.

L Jones, Nathaniel, and Christoph F Reinhart. "Fast Daylight Coefficient Calculation Using Graphics Hardware," 2015. https://doi.org/10.26868/25222708.2015.2462.

Lockley, S.W. (2009) *Circadian rhythms: Influence of light in humans*. In: Larry, R.S., Ed., *Encyclopedia of Neuroscience*, Academic Press, Oxford, 971-988.

Lucas, R. J., Douglas, R. H., & Foster, R. G. (2001). Characterization of an ocular photopigment capable of driving pupillary constriction in mice. *Nature Neuroscience, 4*(6), 621-626. https://doi.org/10.1038/88443

Lucas, R. J., Peirson, S. N., Berson, D. M., Brown, T. M., Cooper, H. M., Czeisler, C. A., Figueiro, M. G., Gamlin, P. D., Lockley, S. W., O'Hagan, J. B., Price, L. L., Provencio, I., Skene, D. J., & Brainard, G. C. (2014). Measuring and using light in the melanopsin age. *Trends in Neurosciences, 37*(1), 1-9. https://doi.org/10.1016/j.tins.2013.10.004

Mardaljevic, J, M Andersen, N Roy, and J Christoffersen. "DAYLIGHTING METRICS: IS THERE A RELATION BETWEEN USEFUL DAYLIGHT ILLUMINANCE AND DAYLIGHT GLARE PROBABILITY?," n.d.

Nabil, A., & Mardaljevic, J. (2005). Useful daylight illuminance: A new paradigm for assessing daylight in buildings. *Lighting Research & Technology, 37*(1), 41-57. https://doi.org/10.1191/1365782805li128oa

Panda, S., Sato, T. K., Castrucci, A. M., Rollag, M. D., DeGrip, W. J., Hogenesch, J. B., Provencio, I., & Kay, S. A. (2002). Melanopsin (Opn4) requirement for normal light-induced circadian phase shifting. *Science, 298*(5601), 2213-2216. https://doi.org/10.1126/science.1076848

Rea, M.S. (editor). 2000. *IESNA Lighting Handbook: Reference and Application*, 9th edition. New York: Illuminating Engineering Society.

Rea, Ms, and Mg Figueiro. "Light as a Circadian Stimulus for Architectural Lighting." *Lighting Research & Technology* 50, no. 4 (June 2018): 497–510. https://doi.org/10.1177/1477153516682368.

Rea, Mark S, Mariana G Figueiro, Andrew Bierman, and John D Bullough. "Circadian Light." *Journal of Circadian Rhythms* 8, no. 0 (February 13, 2010): 2. https://doi.org/10.1186/1740-3391-8-2.

Rea, Ms, Mg Figueiro, and Jd Bullough. "Circadian Photobiology: An Emerging Framework for Lighting Practice and Research." *Lighting Research & Technology* 34, no. 3 (September 2002): 177–87. https://doi.org/10.1191/1365782802lt057oa.

Schlangen, Luc J. M., and Luke L. A. Price. "The Lighting Environment, Its Metrology, and Non-Visual Responses." *Frontiers in Neurology* 12 (March 4, 2021): 624861. https://doi.org/10.3389/fneur.2021.624861.

Selkowitz, S, and E S Lee. "Advanced Fenestration Systems for Improved Daylight Performance," n.d.

Stockman, Andrew, and Lindsay T. Sharpe. “The Spectral Sensitivities of the Middle- and Long-Wavelength-Sensitive Cones Derived from Measurements in Observers of Known Genotype.” *Vision Research* 40, no. 13 (June 2000): 1711–37. https://doi.org/10.1016/S0042-6989(00)00021-3.

Sung, C. H., & Hattar, S. (2004). Neuropsin (Opn5): A novel opsin identified in mammalian neural tissue. *FEBS Letters, 554*(3-4), 410-416.

Tarttelin, E. E., Bellingham, J., Lucas, M. W., Hankins, M. W., & Foster, R. G. (2003). Neuropsin (Opn5): A novel opsin identified in mammalian neural tissue. *FEBS Letters, 554*(3-4), 410-416.

Wienold, Jan, and Jens Christoffersen. “Evaluation Methods and Development of a New Glare Prediction Model for Daylight Environments with the Use of CCD Cameras.” *Energy and Buildings* 38, no. 7 (July 2006): 743–57. https://doi.org/10.1016/j.enbuild.2006.03.017.

Wyszecki G. and Stiles W. S. *Color Science – Concepts and Methods, Quantitative Data and Formulae 2nd edition* (John Wiley and Sons, New York, 2000)

Dong, Yingjun, and Xin Zhang. “Study on the Effect of Awakening Daylight in Dormitories on Morning Alertness, Mood, Fatigue and Sleep Quality of College Students.” *Building and Environment* 203 (October 2021): 108060. https://doi.org/10.1016/j.buildenv.2021.108060.